Politecnico di Torino

Master of Science Degree in Civil Engineering

Structural Engineering

Motion magnification for vibration based damaged assessment of energy systems

Supervisors:

Prof. Marco CIVERA

Prof. Cecilia SURACE

Prof. Alessandro SABATO

Candidate:

Hussein ALI AHMAD

July 2025

Contents

List of Figure

List of Tables

I. Abstract

Hydropower plants are widely regarded as an effective and sustainable solution for electricity generation. They leverage water, a renewable resource, to produce energy, thereby promotion environmental sustainability. Their relatively low operational and maintenance costs contribute to their economic viability. The crucial water storage capacity in their reservoirs also enables the provision of auxiliary services, beyond solidifying their role as a versatile and reliable component in modern energy systems.

Optical Motion Magnification (OMM) is used for condition monitoring for hydropower turbines by enhancing small motions in video recordings, OMM is a non-contact, vision-based technique, allows for the detection and visualization of vibrations and displacements that would otherwise be hidden beneath the noise floor or invisible to the human eye. The technique approach is to track the mechanical characteristics of turbine components without the use of physical sensors by enhancing subtle movements in high-resolution video data.

The study explores OMM's potential as a substitute for conventional measurement tools including proximity probes and laser displacement sensors, which are frequently employed in defect detection and turbine vibration analysis. To evaluate OMM's sensitivity and accuracy against these well-known sensing technologies, several tests were carried out. Whether optical motion magnification can produce equivalent outcomes in detecting mechanical problems and describing the dynamic response of hydropower turbines is the goal.

By providing a more adaptable, non-invasive alternative that lessens the need for intricate installations and maintenance, the study's findings could make a substantial contribution to the field of condition monitoring. If successful, OMM might be a more affordable and secure option for keeping an eye on spinning equipment in extensive energy infrastructure.

II. Acknowledgments

I would like to express my greatest gratitude to Professor Alessandro Sabato for offering me this interesting topic, also providing me with the tools and software I need for the development of this thesis and for all his suggestions and help.

I would like to express my sincere gratitude to Professor Marco Civera and Professor Cecilia Surace for their support, trust and the invaluable opportunity they provided me to conduct my thesis research at the University of Massachusetts Lowell.

Many thanks also to all the other professors at the Politecnico di Turino who taught and instructed me during this last couple of years. This opportunity has helped me finish my academic training with new perspectives that I will carry with me.

I would also like to thank my family for their unconditional support for all the days of my life. They paved the path that brought me here.

Finally, thanks to all my friends who helped me by cheering me up. Without their emotional help, this would not be possible.

III. Structural Health Monitoring

1. Introduction

Condition Monitoring is a process to measure machine motion, temperature, and oil condition. Which allows us to notice any visible change that may cause an error or failure. Condition monitoring is collecting data over time, that shows us how the machine works now and how it worked in the past. By comparing these data, we can predict how the machine might behave in the future and do the maintenance before the failure happens [1]. By noticing this, it gives us the advantage to fix the problems before any series damage that lead to increase the machine service life [2].

2. Vibration Analysis

Unbalanced forces are frequently applied to rotational shafts in rotating machinery, which can result in a variety of defects and ultimately mechanical failure. These flaws are serious because they affect the appropriate operation of equipment used in both small and large-scale industrial settings. Vibration signals, which show amplitude variations and are regularly displayed as simple harmonic motion, can be analyzed to monitor these defects.

Monitoring vibration conditions is important for identifying and avoiding problems, which extends the life of rotating machinery. A few things can lead to bearing faults, such as cyclic loads, mistakes made by maintenance personnel, insufficient lubrication, and poor-quality component manufacturing. These problems frequently result in both localized and distributed faults.

The vibration spectrum's frequency characteristics can be used to identify each of these issues. This includes changes in energy levels and amplitude that reveal the kind and extent of the fault. The frequency characteristics of these bearing defects can be determined using a variety of techniques, including analytical, numerical simulations, and experimental approaches.

In addition to providing harmonic frequency data at different speeds and conditions, the frequency characteristics derived from these methods represent fundamental frequencies. Time, frequency, and time-frequency domain analyses are crucial factors to consider when comparing vibration analysis methods. These vibration signals lead to determine the machinery's overall health.[3]

3. Conditional Monitoring Techniques

As more data is gathered for condition monitoring, the system grows more complex and expensive. Full monitoring is therefore typically only employed when poor output, low availability, or poor quality could result in significant issues and warrant costs. Due to their strength, dependability, affordability, and efficiency, rotating motors are frequently employed in industries. These motors may experience issues while in operation, and if they exceed safe limits, they may fail, resulting in shutdowns and significant financial losses. Therefore, it's critical to keep an eye on them to identify problems early. Numerous techniques have been developed to identify issues with these motors.[4]

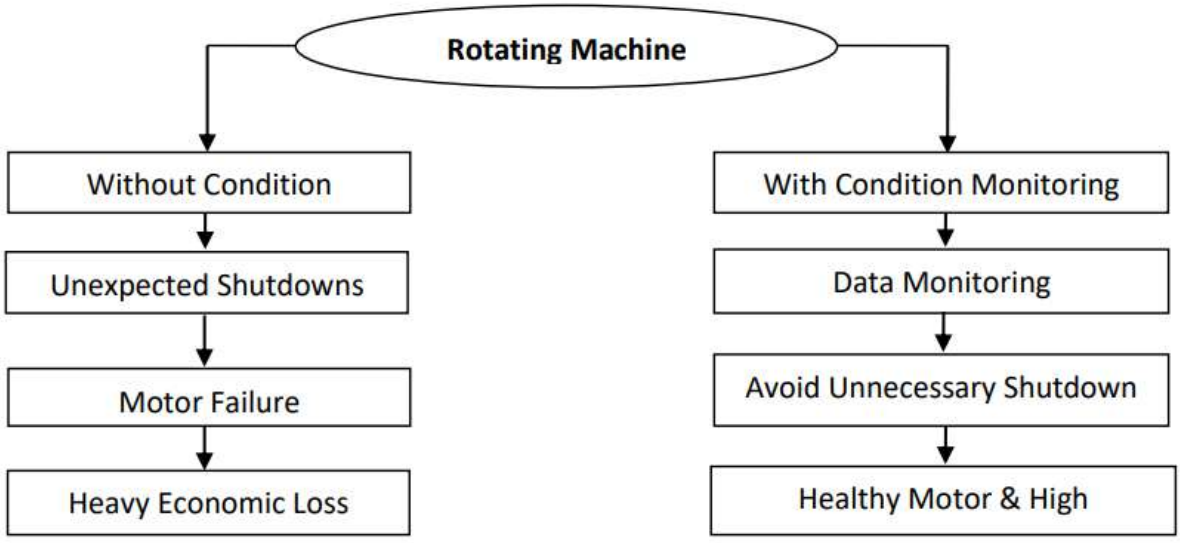

Figure 1:Need for Condition Monitoring

i.Infrared thermology

Non-destructive testing technique for predictive maintenance, infrared thermography tracks the temperature of equipment and operations. Infrared thermography tracks offer a remote, visible thermal view of the entire component or system, in contrast to conventional contact-based temperature measurement instruments like thermocouples and resistance temperature detectors. This makes it possible to identify irregular temperature distributions early on and perform preventative maintenance before possible malfunctions.

Civil infrastructure, electrical systems, machinery, aerospace, nuclear facilities, PCBs, food processing, and material fatigue studies are just a few of the many

diverse industries where infrared thermography tracks have been widely used for condition monitoring. It has demonstrated efficiency in assessing procedures such as chemical vapor deposition, tracking deformations, and examining welds. The method has also been utilized to detect high current densities in microwave circuits and in industries like the paper and wood sectors.[5]

ii.Ultrasound

Ultrasonic sensors are used to capture high-frequency waves produced by small cracks, scratches, or faults; ultrasound-based fault detection is a relatively new technique that is gaining attention across various industries for its ability to detect early-stage mechanical faults. Unless the crack becomes significantly large, the ultrasonic waves produced by these impulse shocks are often undetectable by traditional vibration analysis.

Ultrasound has limitations. It can find it difficult to distinguish between specific kinds of faults or detect false signals, including those brought on by frequent impacts from loose bolts. The location of the sensor has a significant impact on its efficiency, the closer the sensor is to the defect, the better the findings.

Ultrasound is used to determine bearing faults frequencies. However, vibration analysis is used to identify specific faults like unbalanced or misalignment.[6]

iii.Acoustic Emission

Acoustic emission is known as elastic stress waves within a material. This phenomenon is usually caused by deformation, sudden stress redistribution, or contact between rough surfaces. These signals have a broad frequency range, typically from 20 kHz to 1 MHz, and are naturally non-stationary. In addition to man-made processes like wear, slip, dislocation motion, plastic deformation, friction, fracture, phase changes, melting, leaks, matrix cracking, fiber breakage, and delamination in composite materials, acoustic emission can also result from natural events like earthquakes and rock bursts.

In rotating machinery, acoustic emission sources may include impacts, cyclic fatigue, material loss, turbulence, friction, cavitation, leakage, and contact between surface irregularities. Vibration analysis has been used by numerous researchers to study failure detection and prediction in such systems. However, compared to

traditional vibration sensors, acoustic emission sensors provide several clear advantages.

Firstly, surrounding noise and mechanical resonance can greatly change vibration signals, while acoustic emission signals are less vulnerable to these interferences. This makes it possible for acoustic emission sensors to deliver more accurate and clean data in noisy settings.

Secondly, mechanical surface flaws frequently produce a broad spectrum of frequencies that can be higher than vibration sensors' operational bandwidth. These signals are better captured by acoustic emission sensors, which can identify high-frequency stress waves.

Thirdly, small surface flaws might not have a noticeable impact on the overall structural vibration or cause noticeable variations in acceleration. However, acoustic emission sensing is more sensitive to early-stage or incipient errors since these minor flaws can still produce detectable acoustic emission activity.

Fourthly, flexible sensor placement is made possible by the spherical outward radiation of acoustic emission waves from a point source. Acoustic emission sensors can gather enough data from a single place or direction, in contrast to vibration sensors, which frequently need multi-axis measurements.

Finally, the precise location of the emission source can be determined thanks to acoustic emission technology. This feature is particularly useful for pinpointing the exact location of any damage and determining the underlying cause of malfunctions. Because of their better sensitivity and localization skills, acoustic emission-based diagnostics are becoming more and more popular in predictive maintenance applications.[7]

4. Condition Monitoring Types

Various formats and methods of monitoring the condition of machines each serve a specific purpose in terms of data collection.

The most popular formats are:

i.Offline Condition Monitoring

Offline condition monitoring involves assessing the performance and health of machinery or equipment by routine measurements, inspections, and sample testing. This usually takes place during planned maintenance or when the machinery is not in use. At some intervals, offline monitoring offers comprehensive insights into the state of the equipment. To enable preventive maintenance and a longer equipment lifespan, the major goal of offline condition monitoring is to identify possible defects, wear, or deterioration that could result in failures. It is a useful tool for companies where periodic downtime for inspections is possible and where equipment functions in stable, predictable conditions.

Numerous diagnostic methods, including vibration analysis, oil and fluid sampling, infrared thermography, ultrasonic testing, and insulation resistance testing, are employed in offline condition monitoring. Without interfering with regular operations, these techniques allow specialists to spot early warning indications of issues such imbalances, misalignments, wear, and material degradation.

This method is a cost-effective alternative for many companies since it can be planned during scheduled maintenance windows.

Although offline condition monitoring offers comprehensive and detailed data, inspections and analysis do take time. Regular and timely testing is essential to its efficiency since it guarantees that possible problems are identified before they become expensive failures.

An essential component of a proactive maintenance approach, offline condition monitoring helps businesses save maintenance expenses, increase equipment reliability, and prevent unscheduled downtime.

ii.Online Condition Monitoring

Online conditions monitoring is continuously monitoring the health of the machine by wirelessly attaching sensors connected to integrated software. These sensors track several factors, including vibration, acoustic emissions, ultrasound, and infrared thermal pictures, and they offer real-time alerts. It's crucial to consider the machine's form, bearing type, speed, parts, and components while choosing an online monitoring equipment.

The sensor wirelessly connects to a remote monitoring system that shows real-time data after it is positioned correctly on the machine. This enables operators to get a real-time picture of the machine's state. The system can monitor the asset and spot

possible problems using a variety of sensor data types, including vibration, thermal imaging, and acoustics.

Real-time notifications can be configured using online monitoring, which may notify operators via emails or remote devices when a problem is identified. Apart from the ongoing surveillance, data from sensors mounted on equipment can also be read by portable devices. We call this procedure "portable computer diagnostics."

The online condition monitoring tool offers proactive, ongoing insights into the state of the equipment, enabling prompt repair and lowering the possibility of unplanned breakdowns.[1]

5. Condition Monitoring Maintenance

Condition monitoring is a proactive maintenance strategy that involves routinely or periodically evaluating the functionality and state of machinery, equipment, or structural systems. Condition monitoring uses scheduled or real-time data collecting to find early indications of wear, degradation, or malfunction rather than waiting for a failure to happen. This makes it possible to plan maintenance tasks just when they are required, increasing dependability, decreasing downtime, and maximizing maintenance expenses.

This is accomplished by using a variety of sensor technologies to track important operating parameters that act as gauges of the equipment's health, such as temperature, vibration, pressure, or noise. To extract valuable information about the state of the system, the acquired raw data is processed and examined using sophisticated signal processing and decision-making algorithms.

In condition monitoring systems, a centralized diagnostic unit also known as a health control center is crucial. This section uses diagnostic techniques to identify and differentiate between various problem types, particularly in complex systems where fault identification can be difficult due to several interacting components.[1]

Maintenance strategies can be generally categorized into three stages of development:

i.Breakdown Maintenance

The run till failure maintenance approach involves keeping equipment in use until it totally fails, at which point it is replaced. This method is usually applied when a machine malfunction does not result in serious injury to humans or large financial losses.

This approach aims to prolong the equipment's operating life before resulting in increased expenses for extra personnel, increased machine downtime, and decreased production capacity.
However, due to the potential for safety hazards, equipment damage, and decreased overall efficiency, this approach is typically viewed as undesirable. Furthermore, a breakdown maintenance program frequently leads to higher expenditures, such as higher inventory management and spare part costs.[8]

ii.Preventive Maintenance

Time-based or periodic maintenance are common terms used to describe this kind of maintenance. Although it can lessen the likelihood of unforeseen failures, it is typically seen as economically wasteful. This method's fundamental principle is that a machine will continue to function well if it receives routine maintenance.
However, overall production is frequently reduced because of this strategy. Because it frequently relies solely on past data and experience, it also runs the danger of creating inaccuracies.
This maintenance approach's primary objective is to increase the equipment's useful life by controlling wear and tears before it becomes unacceptable. Over time, the rate of deterioration of certain equipment components is comparatively constant.
However, the wear patterns of some parts, such as rolling element bearings, vary greatly. This variance may result in forecasts where the average time before failure is two to three times longer than the bare minimum.[8]

iii.Condition-based Maintenance:

Condition-Based Maintenance is a traditional method based on fixed schedules. Condition-Based Maintenance is a modern approach to maintenance that assesses the current state of machines to determine when maintenance is necessary. Only when certain indicators indicate a decline in performance or a potential failure do Condition-Based Maintenance perform maintenance, extending machine lifespan, improving operational efficiency, lowering daily operating costs, improving system quality, minimizing maintenance workload, and lowering the risk of human error.
Condition-Based Maintenance is regarded as a demand-driven approach in which maintenance tasks are initiated based on the system's actual requirements rather than preset schedules. Condition Monitoring data is the main source of information used to inform these activities. By facilitating precise maintenance scheduling and

determining the best moments to step in, condition monitoring plays a critical role in making sure that parts are repaired before serious deterioration happens.
There are several crucial steps in the Condition-Based Maintenance process. First, information regarding the machine's working state is gathered by sensors and monitoring equipment. The data is then processed to identify irregularities and understand different signals. Lastly, to produce practical maintenance suggestions, decision-making procedures are used, such as diagnostic and prognostic algorithms. Analyzing real-time data to find functional changes and early warning indicators of failure is the process's ultimate objective.
Vibration analysis with non-contact sensors is one of the several condition monitoring approaches that has demonstrated significant potential in anticipating mechanical failures and determining maintenance requirements prior to breakdown. Reliability can be greatly increased and unexpected downtime can be decreased with these predictive capabilities.[8]

6. Conclusion

Vibration analysis is widely acknowledged as one of the most successful methods used in condition-based maintenance and is essential to many predictive maintenance programs. It provides a dependable, affordable, and useful method for keeping an eye on the condition of equipment and identifying problems early. The fundamental principle of vibration analysis is the presumption that modifications in the machine's vibration patterns accompany most mechanical breakdowns.
Vibration sensors, usually accelerometers, monitor the machine's vibration while it is operating to record these patterns. To increase accuracy, the gathered vibration signals go through pre-processing, which includes operations like data normalization and noise reduction. Depending on the type of fault being examined, the signals can be pre-processed and then evaluated in various domains, such as the frequency domain (spectrum analysis) or the time domain.

Organizations can minimize maintenance costs and production downtime, prevent unplanned equipment breakdowns, and execute timely repairs by identifying issues early. Additionally, this proactive approach maximizes revenue and operational efficiency. Predictive maintenance techniques are very beneficial to businesses because they minimize the need for expensive emergency repairs, reduce the demand for spare parts inventories, and prevent production delays brought on by equipment failure.

In addition to assisting in determining the sort of fault that exists, a thorough examination of vibration signals enables precise assessment of the machine's remaining usable life, necessary replacement parts, tools, available staff, and repair time. Vibration analysis therefore helps with better resource management and maintenance planning, which eventually results in significant cost savings and increased system reliability.

IV. Motion Magnification

1. Introduction

Monitoring the vibrating characteristics of structures and machines is crucial to their safe and efficient operation. This is true in cases where we don't fully understand how specific conditions or events are affecting the machine, as well as while performing routine inspections to evaluate if a machine or building is deteriorating over time. Vibration signals in these situations can serve as warning indicators, assisting us in identifying undesirable or hazardous alterations within the system or in the way it interacts with its environment. However, vibration isn't always an issue that can be resolved. Certain equipment, such as conveyor belts or vibrating tables, are designed to vibrate as part of their operation. We may modify the system to perform better under various loads or jobs by seeing how these vibrations behave.

Now, accelerometer sensors are the most used method of measuring vibrations. These are often affixed straight to the machine and can be either piezoelectric or Micro-Electro-Mechanical Systems varieties. At the location where the sensor is installed, they gauge how much the machine is speeding up or slowing down. Other techniques, such as sensors that use magnetic fields (eddy current), lasers that measure distance, or devices that use the Doppler effect to determine speed, can be used if we need to take measurements without encountering the machine. The data we obtain from these sensors can be utilized independently or transformed into various practical formats, such as changes in speed, location, or shape. We now have versatile methods to comprehend and characterize vibrations in considerably greater depth thanks to contemporary hardware and software.

Traditional approaches do have a drawback, though, in that they only provide data from spots. This implies that humans may overlook important information, particularly in complicated constructions or machines with numerous moving parts or complex stress patterns. Adding extra sensors is one approach to address this, but doing so complicates and increases the cost of the system. Using computer models based on our understanding of the structure, we occasionally attempt to fill in the blanks by estimating how the entire system will react based on a single measurement or two. However, these assumptions may not be entirely correct. People frequently simply follow typical testing methods without thinking of quicker or more efficient ways to complete them. For example, picking the right location for a sensor or modifying its settings may call for additional effort or perhaps several tests, which slows down the process overall.

Using conventional sensors has additional drawbacks. Certain conditions, such as extremely hot, damp, or unclean surroundings, can harm the sensors or prevent them

from functioning correctly. Even connecting a sensor to the machine can be challenging in certain situations. Additionally, adding the sensor can occasionally alter the machine's normal operation, particularly if the sensor weighs more than the element it is measuring. To explain these kinds of problems, a table (Table 1) contrasts conventional accelerometers with camera-based measurement devices. There are new ways to observe how objects vibrate thanks to computer vision techniques that use cameras and intelligent software. One example is measuring a structure's movement or deformation under both stationary and moving conditions by employing triangulation and tracking points.

Table 1: Comparison of base constrains of accelerometer and visual motion sensor.

Accelerometer	Video Camera
Contact	Simultaneous multi point location (quasi continuous)
Close neighborhood impact in assembly point (sensitivity to temperature, chemical, etc.)	Line of sight disturbance sensitivity (sensitivity to lighting, fog, smoke, etc.)
Measurement of absolute values	Measurement of relative values (relative to camera base)
Direct acquisition	In plane 3d to 2d projection (in case of single camera)

Motion magnification is a particularly helpful category of visual aids. Without encountering the item, these techniques can track several points simultaneously and determine their locations, accelerations, and speeds. For example, they have shown great utility in verifying the motions of robotic arms and contrasting the outcomes with those obtained from conventional sensors.

When measuring vibrations, we typically don't really see them; instead, we receive data from the sensors, process them, and display the results as numbers, graphs, or charts. These devices enable us to see things that are ordinarily invisible to the naked eye, such as minute motions. This is altered by motion magnification, which allows us to directly perceive these tiny motions by making them visible. It is important to realize that when we use the term small in this context, we are referring to motions that are not typically visible to the human eye, not because they are not significant or meaningful. The outcomes of these methods are typically displayed in easily interpreted visual representations, such as waveforms, graphs, or animated plots.

However, even watching a video of a machine in action can also be beneficial but only if the movements are visible. Making a graph out of raw measurement data is

frequently insufficient to identify the problem. Making decisions quickly can sometimes be greatly aided by experiencing the movement immediately, even if only visually. Sailors judging the wind based on the appearance of the sea is a basic example. They simply observe the waves without the usage of sensors.
Instead of going through hard measurement methods, users can make better and faster decisions for many devices when they can see clearly how something is vibrating. Advances in camera technology and computational power have made it feasible to record and analyze machine video to identify vibrations. This implies that by employing cameras as a sort of eye between the machine and the observer, we might investigate novel approaches to vibration observation. Over time, the camera takes a few pictures. Each image depicts the object's 3D shape as seen from a single viewpoint at that precise instant.
These techniques magnify the slight variations between video frames until they are large enough for us to see. This is referred to as motion microscopy or motion magnification. It functions by adding motion to the video, which makes it simpler for the human eye to pick up on minute movements.[9]

2. Motion Magnification Methods

Applications for motion magnification are quite diverse and span a wide range of domains, such as medical diagnostics (mostly because they are non-invasive) and the observation of different technological items.
When information about motion in an image is recorded as optical flow, we can intentionally distort it to highlight displacements that allow us to draw conclusions about processes at the objects that are not visible to the unaided eye when watching the video recording directly.

i.Lagrangian Motion Magnification Method:

Lagrangian motion analysis, a method from fluid dynamics, was the first known way to amplify motion in videos. This strategy needs monitoring the motion of individual particles over time, frequently with the aid of techniques such as optical flow. Defined motion perception as the outcome of variations in patterns of brightness brought about by the relative movement of the visual sensor (such as the CMOS sensor in a camera or the retina in human eyes) and the scene being examined. By estimating motion as vector fields, optical flow techniques measure these changes, frequently with a very fine (even sub-pixel) level of detail. The assumptions that support these estimations, such as object structural consistency and movement

smoothness, are mathematically expressed in what are referred to as the optical flow constraint equations (OFCE).

$$\partial_t I(x,t) + \partial_x I(x,t)u = 0 \qquad (1)$$

Where $I(x,t)$ is the brightness intensity at 1-D spatial location x, temporal index t, and u is a spatial displacement assuming that temporal displacement is 1. The equations basically mean finding vector fields in the local area with respect to minimal variation of total brightness. Assumed the hard constraint zero change in image brightness between local patch patches of two different timepoints choose a soft constraint a minimize of constraint violation:

$$u = \underset{u}{\operatorname{argmin}} \int_N \left((\partial_x I(x,t)x + \partial_t I(x,t))^2 + \mu \|\nabla u(x,t)\|_2{}^2 \right) dx \qquad (2)$$

Where N is the considered local area, u is an optical flow field, and μ is the regularization parameter for smoothness of optical flow. Suitable assumptions and implementations are made for specific types of tracked motions.

To preserve object structure over time, they track periodic feature points as they travel through video frames and then cluster these motion courses according to comparable movement patterns. Since it is assumed that only global affine motion affects these stable sites, it is possible to reconstruct their locations from predicted flow vectors with an acceptable degree of inaccuracy.

Changes in perspective, such as the camera's movement or adjustments to the position or shape of objects, frequently cause the perception of motion in videos. To analyze and comprehend physical entities, the latter object-related motion is the main emphasis of this study. Several techniques that reduce the impact of unimportant motion sources have been put forth to isolate significant motion. A popular method involves using feature points to register successive frames, then calculating warp matrices to align frames depending on shifts that are identified. After then, motion magnification is used while maintaining the video sequence's texture and object shape consistency.

The motion trajectories of feature points are tracked across frames and their motion trajectories are clustered based on correlation, so that each group corresponds to a common motion source. For example, objects traveling along the same path, like those carried by a current, may have different speeds, but are still grouped based on their directional similarity. Since multiple motion patterns may overlap in the same spatial area, additional visual cues, such as texture, are used to assign pixels to the most likely motion layer (the background usually forms the largest cluster, which is

characterized by minimal movement, while smaller clusters represent regions with more significant motion).
This method is not regarded as biologically plausible, even if it successfully stabilizes and segments motion layers using conventional video processing techniques. Instead of using global operations like full-scene segmentation or clustering to analyze the entire visual field, human visual processing depends on selective attention and concentrates on regions of interest.
This has led to the development of a motion magnification technique that is more biologically inspired. It makes use of principal component analysis for unsupervised motion layer separation and sophisticated motion estimates based on a multi-channel Gaussian model. This method is inspired by research in visual neuroscience that indicates the brain recognizes complicated motion patterns using higher-order directional cells. To create meaningful motion clusters that correlate to moving objects, these neural properties are combined over time and location.
This approach utilizes a combination of first and second order filters over many spatial temporal dimensions rather than depending just on fundamental horizontal and vertical derivatives. This improves motion estimation in difficult areas like sharp corners or even surfaces. Projecting motion data into orthogonal subspaces, each of which represents an uncorrelated motion pattern allows for the separation of various motions. These subspaces can be independently amplified and are found without supervision. This approach removes the requirement for direct feature point tracking and creates denser, smoother motion fields, although requiring more computing power.
Another method uses a parametric scaling function to define a scale space for motion magnification, which is a heuristic approach. The highest expected motion magnitude and the desired magnification factor are used to model this function exponentially. Each target frame is aligned to a reference frame and then to the last frame in the sequence using a two-step registration procedure. This approach emphasizes acceleration more precisely, the change in motion magnitude between successive frames rather than velocity amplification. Forward warping is then applied to the motion field to produce magnified frames. This method highlights the benefits of using Lagrangian-based techniques to capture subtle yet important motions that are otherwise included into large-scale motion patterns.[10]

ii.Eulerian Motion Magnification Method

A standard video input is first broken down into spatial components, followed by the application of temporal filtering. Then, using a selected magnification factor, this filtered signal is increased to help reveal minute or subtle motions that are often

invisible to the naked eye. This method is based on the Eulerian methodology, which was first applied to the study of fluid dynamics and involves tracking changes in parameters such as velocity and pressure over time at fixed points in space.
When applied to videos, the Eulerian approach accentuates oscillate within a certain frequency range of interest by analyzing how pixel values vary over time at each point. Temporal filtering, for instance, can be used to identify low-frequency signals like a baby's breathing or a person's heartbeat. Even if these weak signals are otherwise obscured by digital noise, they can be made visible by boosting them.
This technique can highlight slight color shifts in addition to revealing small motions. It works effectively for minor displacements and motions with little spatial information because the same temporal filter is applied uniformly across all spatial levels and pixels. Other techniques stress higher-frequency filtering to highlight significant movements or provide exaggerated, unrealistic visual effects, but this method is most effective for subtle, low-frequency changes.
The Eulerian method increases motion by improving temporal changes at specified pixel places, in contrast to techniques that directly estimate object motion (such as the Lagrangian approach). It is based on the same mathematical ideas as optical flow approaches, which use variations in pixel intensity over time to infer motion. In the past, temporal filtering has also been employed for a variety of reasons, including highlighting otherwise undetectable information or smoothing out motion. Measuring a person's pulse from a basic facial video captured with a normal webcam in natural illumination is one useful application of this technique. Other studies have demonstrated that ordinary digital cameras may be used to extract cardiovascular signals, demonstrating that minute variations in skin tone brought on by blood flow can be identified for medical purposes such as remote health monitoring, fitness tracking, or skin condition examination.
By converting high frame-rate videos into regular playback speeds and using filters to lessen problems like motion artifacts or temporal aliasing, some systems also provide real-time processing capabilities. These filters can be tailored to do a variety of functions, such minimizing blur, smoothing motion, or creatively altering the way motion appears in the video. To further manage how motion is emphasized or muted, data in the frequency domain are also analyzed using certain filter sets.
Overall, Eulerian video magnification is an effective method for identifying and amplifying increase changes in video, particularly those that are not visible to the human eye. Newer techniques have enhanced the original method, which relied on linear approximations, by providing more sophisticated image processing tools and more effective methods for handling phase-based motion magnification. To further improve the output and lessen visual artifacts, post-processing procedures have also been suggested.[11]

a) Linear Approximation Method

The Eulerian based linear approximation method combines spatial and temporal processing to explore the imperceptible motion, temporal variations in video. This process is illustrated in figure 2.

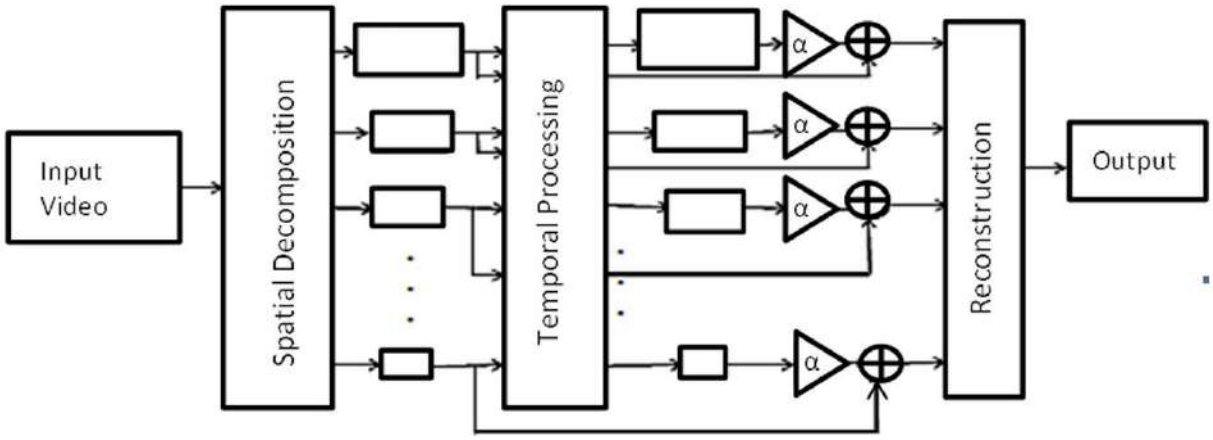

Figure 2: Video magnification framework

1. The input is a regular video sequence. To find the necessary frequency band, it is then divided into several bands using a three to four level Gaussian pyramid. To create a Laplacian pyramid, each video frame is down-sampled after being filtered using a low-pass filter (LPF). Different frequency bands may be amplified to differing degrees because their signal to noise ratios vary.
2. Band-pass filtering is used to isolate the frequency range of interest by applying temporal filtering to each spatial frequency band. To do this, the time series data for every spatial pixel in the selected frequency range must be examined. For example, increasing a baby's pulse rate can be achieved by applying a narrow band filter around a frequency range of 0.4–4 Hz, or 24–240 beats per minute.
3. An amplification factor (α) is used to increase the signals. The following is the definition of the acceptable range for α:

$$(1+\alpha)\delta(t) < {}^{\lambda}/_{8} \qquad (3)$$

Where:

- δ(t) = spatial displacement function

- Spatial wavelength (λ) = $\frac{2\pi}{\omega}$
- ω = spatial frequency

The motion magnification in temporals relies on the first order-Taylor series expansions.

4. By collapsing the spatial pyramid and integrating the amplified signal with the original signal, the final output video is recreated.

The frequency of color changes in the extracted band-pass signal can be used to estimate heart rate. A bandpass filter is constructed using two first order lowpass filters with cutoff frequencies ωl and ωh. For example, a temporal window size of 10 to 15 frames is typically used for videos recorded at 30 frames per second. The choice of temporal filter depends on the application, for instance, a narrow bandpass filter is preferred for color amplification to minimize noise, but a broader bandpass filter is better suited for motion magnification.[11]

b) Phase-Based Video Processing Using Complex Steerable Pyramid

Another solution inside the Eulerian framework that overcomes the drawbacks of linear approaches is phase-based video motion processing. This method concentrates on the phase information in the video signal, as opposed to linear alternatives, which assume motion changes in a straight-line fashion. Because of this, it can manage greater motion amplification across all spatial frequencies, which means it performs well at various image detail levels. In comparison to linear approaches, it also tends to generate less visual noise because it just processes the phase component.

The foundation of this method is complex-valued steerable pyramids, which are modeled after phase-based optical flow, a methodology for motion estimation in video. In this case, phase shifts indicate slight movements within several picture regions, or sub-bands. Reducing noise in these phase signals and amplifying tiny motions are the primary objectives. To do this, the image is divided into several layers according to position, orientation, and spatial scale the size of the features.

The technique extends the sophisticated steerable pyramids to include sub-octave bandwidth filters to enhance motion detection and amplification even more. These more precisely adjusted filters provide superior spatial coverage and aid in precisely identifying and enhancing minute movements. Even the smallest motions in a movie can be made more noticeable while maintaining low noise levels because of this method is layered breakdown and filtering procedure.

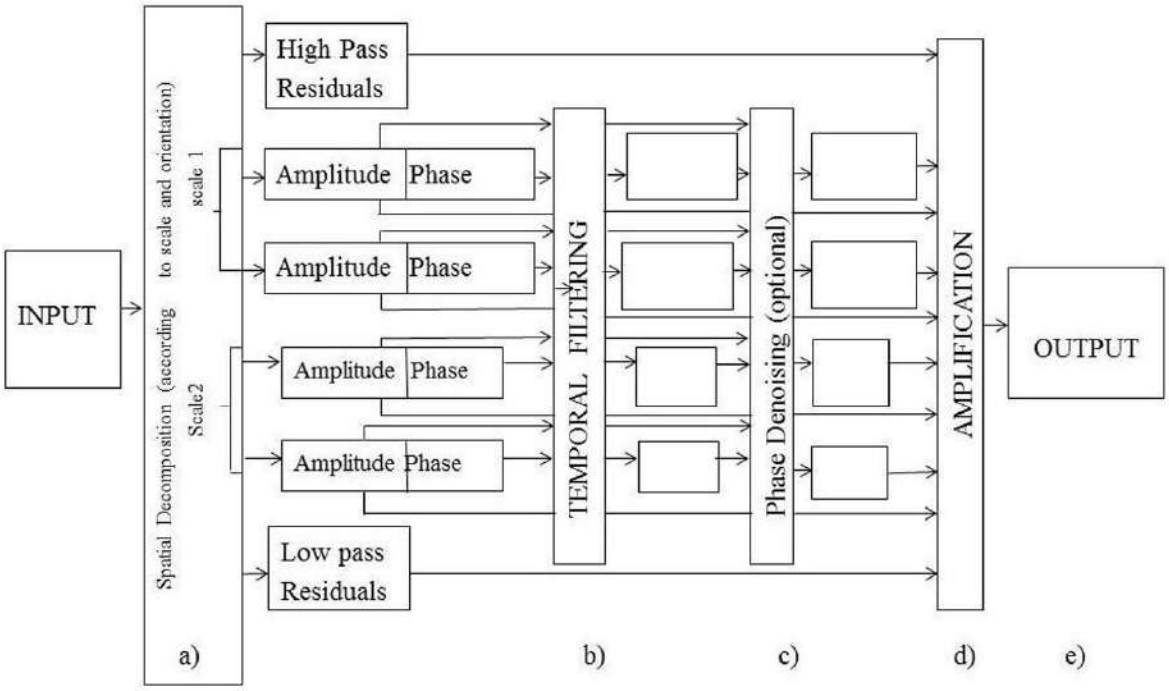

Figure 3: Process for Phased-Based Video Motion Magnification

Where:

a) Decomposition of video and separation of amplitude from phase.
b) Temporal filtering at each location, orientation and scale.
c) Phase denoising to increase phase SNR (Signal-to-Noise Ratio).
d) Amplify or attenuate temporally band pass phase.
e) Reconstruction of video.

This method uses a steerable pyramid to calculate the local phase of the video over time at each level of detail (spatial scale) and direction (orientation). These phase values are then subjected to temporal bandpass filters. Only particular motion frequency ranges are permitted to flow through these filters, which eliminate any constant motion (DC component). The filtered phases are amplified by an amplification factor α, to increase the visibility of the motion since they describe real motion in the film. A magnified motion effect is then produced by adjusting each video frame using these amplified phase alterations.[11]

The limits of α for octave-bandwidth (for 4 orientation) steerable pyramid is:

$$\alpha\delta(t) < \frac{\lambda}{4} \quad (4)$$

- δ(t) = spatial displacement function
- Spatial wavelength (λ) = $\frac{2\pi}{\omega}$
- ω = spatial frequency

The limits of α for half octave (for 8 orientation) steerable pyramids are:

$$\alpha\delta(t) < \frac{\lambda}{2} \quad (5)$$

- δ(t) = spatial displacement function
- Spatial wavelength (λ) = $\frac{2\pi}{\omega}$
- ω = spatial frequency

c) Fast Phase-Based Video Processing Using Riesz Pyramid

The Eulerian technique to phase-based video motion magnification works well with a more recent image representation known as the Riesz pyramid. The motion magnified films it generates are comparable in quality to those made with the complex steerable pyramid, but it processes information far more quickly, roughly four times faster. The Riesz pyramid operates fully in the spatial domain, avoiding visual distortions known as wrapping around artifacts that can be introduced by some earlier techniques that operate in the frequency domain.
Using the Riesz transform, the technique applies phase analysis to the input image at all scales. An effective, self-invertible image pyramid (like the Laplacian pyramid) is used to first divide the image into non-oriented sub-bands before constructing the Riesz pyramid. Each of these sub-bands is then subjected to the Riesz transform.

A two-dimensional extension of the one-dimensional Hilbert transform is the Riesz transform (RT). Two basic filters called three-tap finite difference filters are used in its construction. Each pixel is main feature is aligned with a quadrature pair, which is a pair of signals that are 90 degrees out of phase, thanks to this transformation. The block diagram in Figure 4 illustrates how this configuration enables efficient motion analysis and magnification.

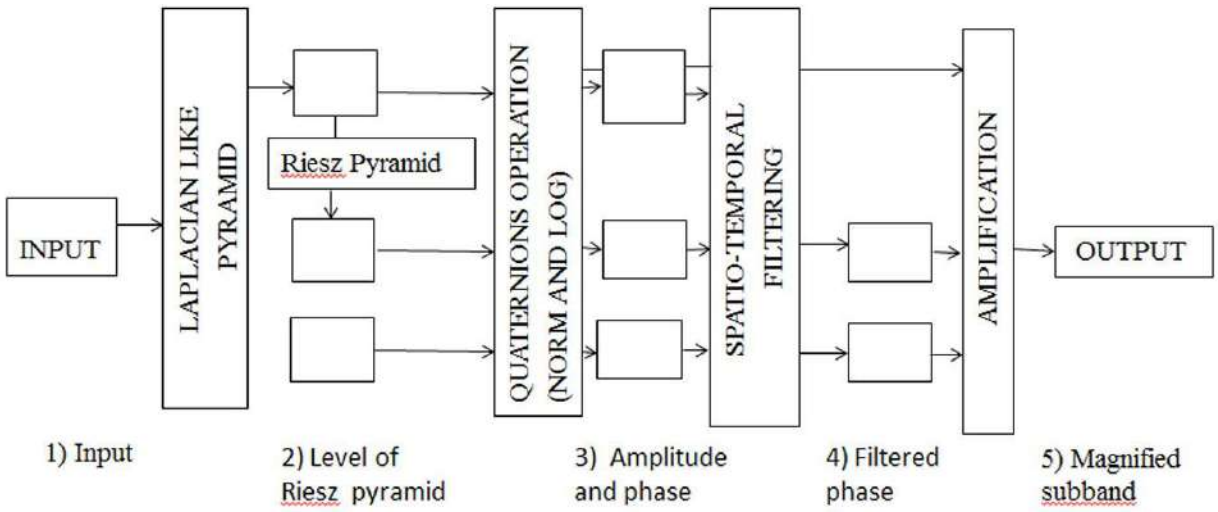

Figure 4: Stages for motion magnification using Riesz pyramid

Where:

1) Input video.
2) Decomposition using a Laplacian-like pyramid (only one level is shown). The Riesz transform is taken to produce the Riesz pyramid.
3) The quaternion norm is used to compute the amplitude (top row) and the quaternion logarithm is used to produce the quaternionic phase (bottom rows).
4) The quaternionic phase is spatial temporally filtered to isolate motions of interest and then this quantity is used to phase-shift the input Riesz pyramid level to produce a motion magnified sub-band
5) These sub-bands can then collapse to produce a motion magnified video.

The fastest phase-based method is obtained by using the Riesz pyramid in the spatial domain. According to the results, this approach is four to five times quicker than the sophisticated steerable pyramid with eight orientations. In addition, it is less costly to install than a sophisticated steerable pyramid.
The only limitation is unlike the ideal Riesz transform, the approximate Riesz transform may not preserve the power of an input signal, which may result in slight artifacts.[11]

d) Enhanced Eulerian Video Magnification

To enhance the conventional Eulerian Video Magnification, a new post-processing technique has been put forth. This method enables pixel-level motion mapping by first using values directly, in contrast to regular Eulerian Video Magnification. It can therefore withstand more motion amplification and be less impacted by noise. This increases its stability and efficacy, particularly when handling delicate or intricate motion Eulerian Video Magnification as a tool to assess motion in a video across time and location. The Enhanced Eulerian Video Magnification method does not, however, adapt the video's pixel. The block diagram in Figure 5 depicts the entire procedure.

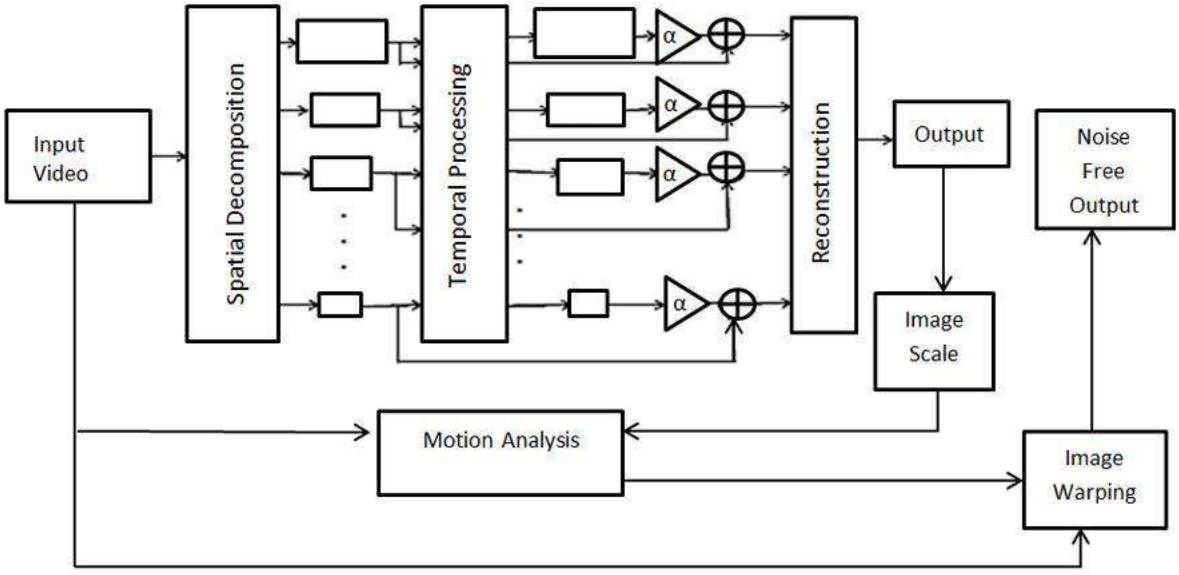

Figure 5: Overview of the Enhance Eulerian Video Magnifications Framework

Pixel-level motion mapping is computed in the Enhanced Eulerian Video Magnification method by comparing the output of conventional Eulerian Video Magnification processing with the original input video. Every pixel in the video may be seen moving over time in this motion map. Using a technique known as picture warping, which involves shifting certain frame pixels in the direction suggested by the motion map, motion in the video is amplified. The motion map is sub-sampled to speed up processing, resulting in a sparse grid that requires fewer calculations.

The noise problems that are frequently present in ordinary Eulerian Video Magnification can be more successfully addressed using the Enhanced Eulerian Video Magnification approach. It doesn't considerably lengthen processing time because it merely employs sparse grid warping and low-resolution image disparities.

Regardless of this, it has important advantages including allowing for more motion amplification with less noise and distortions.

Furthermore, the Enhanced Eulerian Video Magnification technique can also be used to eliminate or reduce minor, undesired movements in films by flipping the motion mapping (also known as negative motion mapping). This makes it especially helpful for tasks like video stabilization, motion de-noising, and the removal of minor movements.[11]

iii. Advancements and/or Variations to the Main Motion Magnification Techniques

In addition to the main motion magnification technique proposed above, there has been subsequent work recently to advance and/or vary these fundamental techniques.

a) Spatial Decomposition

This type of transformation primarily makes use of Gaussian derivatives, which are frequently employed in image processing due to their resemblance to the way the human eye perceives objects. The Riesz transforms and other comparable filters have unique characteristics, such as remaining constant when the image's size or location changes. The earliest stages of human eyesight likewise exhibit these characteristics. By phase, energy, and frequency at each instant, these transforms provide a means of characterizing pictures and 2D signals.

This allows the signal to be rebuilt with little distortion or noise while applying further mathematical procedures. The way the Riesz transforms the handles phase is one of its primary distinctions from other filters. The Riesz transform discovers the phase in two dimensions since it operates with one more dimension than the input signal, whereas normal filters only take the phase in one direction.

Additionally, this technique eliminates the necessity of precisely aligning the filter direction with the image feature direction, which is typically challenging. An intelligent and practical method for picture analysis is the Riesz transform, which is a sophisticated variant of the Hilbert transform for signals with multiple dimensions.

To speed up the procedure, it is suggested to employ the Laplacian pyramid once more rather than the self-inverting pyramid. This alteration would, however, result in a smaller impulse response, lowering the maximum motion magnification. To minimize grid noise around the edges of moving objects, it is also advised to apply a median filter after reconstructing the image from the pyramid.

Some methods use wavelet decomposition to construct the picture pyramid rather than Laplacian or steerable filters, as the original MIT researchers did. This approach provides data in both the frequency and time domains. A Chebyshev Type I band-pass filter was employed for filtering over time.

Using filters that break down the image using the dual-tree complex wavelet transform (DT-CWT) is an additional choice. These filters have benefits including maintaining crisp edges and are easier to use than steerable pyramids. Additionally, DT-CWT does not require time-based filtering, hence it can be applied even in cases where the motion's frequency is unknown. Motion is magnified by multiplying the phase discrepancies between frames by a factor after the image has been decomposed using DT-CWT.

One method substituted a fast local Laplacian filter during the spatial breakdown step for the standard Laplacian filter in Eulerian motion amplification. This adjustment preserves the image's edges while smoothing out minor textures. Motion magnification can thereby highlight edges without significantly distorting other areas of the image.[12]

b) Extraction of the Emphasis of Motion Signals

After spatial decomposition, principal component analysis (PCA) was applied to the sub-bands to enhance the amplitude-based Eulerian (linear) motion magnification approach.
They broke down the image geographically and then concentrated on clearly isolating the motion-related components of the signal.

More specifically, they believed that motion was depicted in the video as minor adjustments to a still image. Thus, a single frame can be defined as follows:

$$I_r(x, y, t) = I_0(x, y, t) + \Psi(x, y, t) + n(x, y, t) \quad (6)$$

Where:

- $I_0(x, y, t)$ is represents the mean observed image intensity.
- $\Psi(x, y, t)$ denotes the motion signal component.
- $n(x, y, t)$ denotes the video acquisition noise.

Subtracting the meaning gives the residual signal:

$$I_r(x, y, t) = \Psi(x, y, t) + n(x, y, t) \quad (7)$$

- $\Psi(x, y, t)$ denotes the motion signal component.
- $n(x, y, t)$ denotes the video acquisition noise.

The residual frames Ir (x, y, t) of the movie are then subjected to Principal Component Analysis (PCA) to identify the primary, unrelated directions of variation. This aids in separating noise from motion signals. Every frame is handled as a distinct sample. Therefore, for numerous frames, a vector is made for each pixel position (x,y), and these vectors are analyzed using PCA.

Similarly, another approach used Empirical Mode Decomposition (EMD) to break down the data before applying motion magnification. This was done to isolate and eliminate background information that is deemed noisy and is not significant.

In addition to background information, repeated motions are deemed superfluous or extraneous when describing motion. To ensure that only the most significant motions are retained, a sparsity constraint was introduced into the dynamic mode decomposition procedure, as detailed below:

$$I(x, y, t) \approx argmin\ (\phi DV_{and}) \quad (8)$$

Where:

- Φ and V represent spatial and temporal components of motion.
- D is their respective coefficients.

Before employing the Laplacian pyramid, an additional step was added to the phase-based motion magnification procedure. They began by dissecting the video frame and extracting the motion-related phase information using a Fourier transform. A Butterworth low-pass filter is then utilized for temporal filtering once this phase

information has been transferred into the phase-based motion magnification procedure.[12]

c) Motion Representation

Rather than use manually designed filters to depict motion in video frames, this approach automatically learns the filters using deep convolutional neural networks (CNNs). The appropriate motion representations are produced with the use of these filters and subsequently enlarged.
Three neural networks are used in the process: an encoder, a manipulator, and a decoder. The encoder first distinguishes between shapes and textures in the video frames. The manipulator then gains knowledge of the non-linear changes in these forms between frames. The video frame is then reconstructed by the decoder using magnified motion, and the results are compared to the original frame (ground-truth). An L1 loss function that contrasts textures, forms, and brightness (intensity) is used to quantify the difference.

The objective is to use a complete encoder-manipulator-decoder network to learn and magnify subtle form changes. However, the quality of the synthetic training data has a significant impact on the method's performance. As a result, biases in the training samples may affect the encoder and decoder, even when the test results seem realistic.

In another section of their study, they suggested an alternative method to the standard Riesz transform approximation for calculating local phase, which is used to describe motion. Atomic functions, or mathematical functions with simple derivatives, served as the foundation for their approach. It is possible to estimate the Riesz transform and determine the local phase using these derivatives, particularly the first-order one.[12]

d) Small Motion Vs Large Motion

First, they examined the challenge of distinguishing between small and large motions. This is crucial because motion magnification functions best when the camera or objects remain largely still. Only the motions that are important to us should be magnified, not the entire scenario.

By segregating the regions with meaningful motion from the backdrop, early systems attempted to address this issue. In one technique, the target area was manually selected by segmentation in a layer-based manner, ensuring that just that portion would be amplified.

Using an additional depth sensor, another approach sought to address the same issue. This would allow a depth-weighted bilateral filter to automatically pick out areas of the image that were at the same depth and magnify them as a single layer.

A third approach employed a similar concept, but it identified significant areas by using saliency the degree to which a portion of the image sticks out based on structure matrix decomposition. After that, these areas were divided for motion magnification.

Lastly, kernel k-means segmentation was employed in another method. To better distinguish the crucial region, this technique projected the first video frame into a higher-dimensional space. After that, it employed picture matting to give the chosen area more precise and organic borders. This step models the pixel intensity as a combination of background (B) and foreground (F) values.

$$I(x,y) = \alpha(x,y)F(x,y) + (1\alpha(x,y)B(x,y)) \tag{9}$$

For some foreground opacity α(x,y). Rewriting this, we get:

$$\alpha(x,y) \approx aI(x,y) + b, \forall\ (x,y)\ \varepsilon\ w \tag{10}$$

Where a=$\frac{1}{F-B}$, b=$\frac{B}{B-F}$ for small window w. Then a cost function J is minimized for parameters:

$$J(\alpha,a,b) = \sum_{(p,q)\in I}\left(\sum_{(x,y)\in w}\left(\alpha(x,y) - a(p,q)I(x,y) - b(p,q)\right)^2 + \varepsilon a(p,q)^2\right) \tag{11}$$

They observed that while large motions, like those from camera shake or facial movements, tend to be linear, little motions are typically non-linear. To make minor, non-linear motions easier to notice, they presented a novel idea: rather than amplifying all motion equally throughout time, they advised increasing the changes in motion (called acceleration).

The second derivative of a signal I (x, t) over time is its acceleration. They employed a temporal acceleration filter, which adds a second-order derivative to $I(x,t)$, to obtain this acceleration. A Laplacian filter, the second derivative of a Gaussian smoothing filter, was used for this.

The following formula explains the relationship between the Laplacian filter and the second derivative due to the mathematical principles of linearity:

$$C(x,t) = I(x,t) \otimes \frac{\partial^2 G_\sigma(t)}{\partial t^2} = \frac{\partial^2 I(x,t)}{\partial t^2} \otimes G_\sigma(t) \qquad (12)$$

Where:

- G_σ(t) is a Gaussian filter.
- σ its variance.
- $\frac{d^2 G_\sigma(t)}{dt^2}$ is the Laplacian

This acceleration is amplified by a factor α reincorporated in the signal I(x,t) resulting in the acceleration magnified signal. For instance, for the amplitude based Eulearian motion magnification technique of reference.

$$\hat{I}(x,t) = I(x,t) + \alpha C(x,t) \qquad (13)$$

For the case of phase based Eulerian motion magnification, the temporal filtering is applied to the phase ϕ instead, by convolving with a Laplacian:

$$C(x,y,t) = \phi(x,y,t) \times \frac{d^2 G_\sigma(x,y,t)}{dt^2} = \frac{d^2 \phi(x,y,t)}{dt^2} \times G_\sigma(x,y,t) \qquad (14)$$

And this is then amplified with α and added to the phase:

$$\hat{\phi}(x,y,t) = \phi(x,y,t) + \alpha C(x,y,t) \qquad (15)$$

There are certain drawbacks to this approach, particularly when big motions change rapidly. In those situations, even though they are not the intended little motions, these rapidly changing huge motions are also captured by the second-order derivative filter and ultimately magnified.

They proposed using a smoothness filter based on jerk the third derivative of motion over time to address this. Jerk helps to lessen the impact of sudden, undesired big motions by measuring the rate at which acceleration changes.

More specifically, they applied a third-order derivative to the phase signal $\phi(x,y,t)$ to obtain the jerk-filtered signal for phase based Eulerian motion magnification. They then used convolution to smooth it using a Gaussian filter:

$$D(x,y,t) = \frac{d^3\phi(x,y,t)}{dt^3} \times G_\sigma(x,y,t) = \phi(x,y,t) \times \frac{d^3 G_\sigma(x,y,t)}{dt^3} \qquad (16)$$

A jerk based smoothness function f(·), is then constructed using this result. It provides a value near 0 for abrupt or irregular motion and near 1 for smooth motion. Before the acceleration signal is magnified by a factor α, it is smoothed out using this function. The result is then obtained by adding the smoothed and amplified signal to the original signal's phase:

$$\hat{\phi}(x,y,t) = \phi(x,y,t) + \alpha(C(x,y,t) \times f(D(x,y,t)) \qquad (17)$$

Crucially, a third-order Gaussian filter was used to compute the third-order term $D(x,y,t)$, which denotes jerk. The ultimate outcome was obtained by magnifying this value and then adding it back to the image's local phase:

$$\hat{\phi}(x,y,t) = \phi(x,y,t) + \alpha D(x,y,t) \qquad (18)$$

The premise behind the video acceleration magnification technique is that little changes are non-linear, but large motions are linear. This assumption, however, fails to consider the possibility that some huge motions may potentially be non-linear.

To make this better, the approach uses the input motion signal $I(x,t)$ as a composite displacement function. This means that the movement is derived from a combination function $\theta(t)$, which shows how the displacement varies over time:

$$I(x,t) = f(x + \theta(t)) \qquad (19)$$

Where the composite function:

$$\theta(t) = \delta(t) + \zeta(t) \qquad (20)$$

Composes the translation motion (small change) δ(t) and ζ(t) denotes the large motion. The aim is then to obtain the amplified signal:

$$\hat{I}(x,y,t) = f(x + (1+\alpha)\delta(t) + \zeta(t) \quad (21)$$

They estimate the equation as follows in the case of amplitude based Eulerian motion magnification using the first-order Taylor series expansion around point x:

$$I(x,t) = f\big(x + \theta(t)\big) \approx f(x) + \frac{df(x)}{dx}\theta(t)$$
$$= f(x) + \frac{df(x)}{dx}(\delta(t) + \zeta(t)) \quad (22)$$

Let B(x,t) denote the deviation between the signal I(x,t) at time t, and the initial signal I(x,0) =f(x), then:

$$B(x,t) = \frac{df(x)}{dx}(\delta(t) + \zeta(t)) \quad (23)$$

After that, frequency domain filters are applied to $B\ (x,\ t)$ to extract only the portion pertaining to $\frac{df(x)}{dx}\delta(t)$ The basic idea is to apply a Fourier transform to translate $B(x,t)$ into the frequency domain. Then, spectral amplitude thresholding is used to exclude the large motions, leaving only the small, significant ones.

Then $\frac{df(x)}{dx}\delta(t)$ is amplified by α and reincorporated into the signal I(x,t), obtaining:

$$\hat{I}(x,t) = I(x,t) + \alpha\frac{df(x)}{dx}\delta(t)$$
$$= f(x) + (1+\alpha)\delta(t)\frac{df(x)}{dx} + \zeta(t)\frac{df(x)}{dx}$$

$$\approx f(x + (1+\alpha)\delta(t) + \zeta(t)) \quad (24)$$

Where the last line is due to approximation by the first order Taylor series, indicating that only the small motion, spatial displacement δ(t), has been magnified by the amount (1+α).[12]

e) Distinguishing or Manipulating the Target Motion

The difficulty lies not only in distinguishing between small and large motions, but also in identifying the target's particular movement amid numerous irrelevant ones. Even in the presence of additional distracting motions, resolving this would assist in concentration on and improve only the crucial movement.
More specifically, this technique can be applied to any type of motion data, including frame difference and optical flow. The main concept is that the motion data comes from a variety of sources. Previous approaches attempt to distinguish between different motions in the frequency domain by utilizing their existing knowledge of the target motion's frequency, or how frequently it occurs.

Researchers discovered a limit on the amount of phase change in a different field of study known as phase-based frame interpolation. When attempting to comprehend motion, this limit helps prevent confusion, but if it is exceeded, the new frames may appear incorrect.

One issue with the frequency-based method is that it cannot separate the target motion from other movements that occur at the same or similar frequency.

To comprehend the relationship between the motion data and the desired motion, the primary technique is to employ a deep convolutional neural network (CNN). In particular, the CNN receives the motion data as input and outputs the target motion signal's first-order derivative. At time t, an image I (x, t) is composed of many frequencies sub-bands, each of which takes the following form:

$$A(s,\theta,t)e^{i\phi(s,\theta,t)} \tag{25}$$

For specific scale s and orientation θ.

Taking the first order temporal derivative of the local phase ϕ(s,θ,t):

$$X_1(s,\theta,t) = \phi(s,\theta,t+1) - \phi(s,\theta,t) \tag{26}$$

Motion at scales and orientations can be inferred from the phase fluctuation over time (between successive image frames). The CNN model, Deep Mag, learns the first-order time derivative from existing datasets of paired films and real motion signals rather than directly computing the target motion X1. The target motion is magnified or approximated with a factor γ after the estimated gradients are

normalized using the L1-norm across a few time steps (N). In this machine learning technique, N and γ are both programmable settings (hyper-parameters).

Conventional motion removal techniques operate globally, processing the full video frame and are typically employed for video noise reduction. Some techniques, on the other hand, concentrate on eliminating motion at the level of specific objects within any frame. For instance, video de-animation preserves only small, intricate motions while separating and eliminating massive movements in user-selected places.

One prevalent belief is that high-frequency variations are seen as noise, while the intended motion signals occur at low frequencies. In time-lapse videos, this concept is utilized to eliminate tiny, fast motion hiccups.

In addition to increasing motion visibility, motion attenuation is the opposing technique. This is accomplished by setting the magnification factor α to -1, which eliminates motion in a specific frequency band and cancels out phase shifts over time. Motion attenuation has been used to minimize minor facial movements so that color-based motion magnification does not also magnify them, as well as to eliminate atmospheric turbulence, which creates low-to-mid frequency jitters in videos.

Motion component magnification was presented as a solution to the problem of selectively eliminating motion. Principal component analysis (PCA) is used in place of the conventional linear temporal filtering in motion magnification. The output images are separated into 8x8 pieces after the image has been spatially broken down. PCA is applied to the aggregated data of all 64 series, with each pixel in a block being regarded as a time series channel. Using power spectral density, the top four primary components are selected and examined. The power in a certain frequency band divided by the overall power is known as the normalized band power. The motion of interest can be eliminated by multiplying the component with the highest value (Q) by zero.[12]

iv. Amplitude-Based Filtering for Video Magnification in Presence of Large Motion

Techniques for video magnification assist in displaying minute changes in videos that are difficult for the human eye to detect. These consist of motions such as breathing, heartbeat, or item vibrations. But when there is a lot of motion in the video, conventional techniques frequently falter, leading to noise and blurring.
Older techniques, such as Eulerian video magnification, work well for little movements but poorly for large ones. To address this problem, more recent methods have been developed. Some use special depth cameras or need human selection of specific video segments, however they might be slow, imprecise, or condition specific.

A new amplitude filtering technique that performs better in huge motion. It can vividly display even the smallest changes without the need for additional data or human input. It demonstrates that their approach improves outcomes and lessens blurring by testing it on both genuine and false videos. They also go over its limitations and how it operates.[13]

a) Amplitude Based Filtering

It is recommended to use a pre-filter in conjunction with a conventional band-pass filter to concentrate on the tiny signals because the video contains big movements. The suggested technique lessens the impact of large motion by using amplitude-based filtering. When there are large movements in the video, this easy method helps to increase the magnification. Strong motion distortions have bigger amplitudes than the slight changes we are looking for, which is the basis for the concept. A Fourier transform is used to convert the brightness variations over time into the frequency domain for signal analysis. To distinguish between small and big motions, the complex signal is divided into two components in this form.

$$S_D(x, w) = S_{\rho a}(x, w) + S_{\rho}(x, w) \quad (27)$$

Where:

- $S_{\rho a}(x, w)$ stands for the signal's component with spectral amplitude above the threshold ρ.

- $S_{pb}(x, w)$ stand for the signal's component with spectral amplitude below the threshold ρ.

Selecting the appropriate threshold for spectral amplitude control is crucial for eliminating significant motion from the time series. When the amplitudes of the major motions are greater than those of the minor changes, this works well. The amplitude-based filtering separates the massive movements from the little signals we wish to retain using a unique weighting function, much like an ideal band-pass filter.

$$W_{A,w} = \begin{cases} 1 & A\epsilon\,[\rho 1, \rho 2] \\ 0 & otherwise \end{cases} \quad (28)$$

Where:

- $[\rho 1, \rho 2]$ denotes the amplitude range of interest.
- ρ1 is the minimum amplitude bound, which is not critical because small noise can be negligible after selecting the frequency band of interest.

Alternatively, we set the value to 0.0001 which is an empirical value. h is the maximum amplitude threshold used for removing the large motion, which can be set using the mean or median of amplitude. Specifically, we first compute the meaning and median of amplitude. Then, the smaller of them is selected as the value of h.[13]

b) Modified Phase Based Motion Magnification

When it comes to video motion magnification, the phase based Eulerian method outperforms the standard linear method with less noise. Amplitude-based filtering is used to phase changes in videos with a lot of motion to eliminate interference and draw attention to the minor motions. For instance, the image brightness can be expressed as a function of the steady motion of an item in a one-dimensional signal. Fourier series can then be used to evaluate and amplify the subtle variations in this image by breaking it down into a few wave-like components.

$$I(x,t) = f(x - \theta(t)) = \sum_{w=-\infty}^{\infty} A_w e^{i\omega(x-\theta(t))}$$

$$= \sum_{w=-\infty}^{\infty} A_w e^{i\omega x}\, e^{-i\omega\theta(t)} \quad (29)$$

The amount that an object moves over time is correlated with the global phase of a signal in the video. We can quantify this movement by comparing the phase at time with a reference frame. Small movements can be made more noticeable by multiplying this phase difference by a magnification factor if the motion is straightforward and steady. However, this straightforward approach may produce hazy results if there is also a lot of motion. The smaller movements are separated and focused on using amplitude and frequency-based filters since large motions typically have greater signals in the frequency domain.

Most videos have local motion rather than global motion, which means that various areas of the image move in different ways. The image is divided into local wave-like signals to address this, and local phase changes are monitored throughout time. Small motions are then highlighted using these local modifications. Phase unwrapping is a technique that fixes wrapping problems caused by phase signals repeating in a cycle.[13]

3. Conclusion

For mechanical systems and structures to be safe, long-lasting, and functional, vibrations must be studied and analyzed. Contact-based sensors, such piezoelectric and MEMS accelerometers, which offer precise, localized acceleration readings, have historically been used to do this. These gadgets work well in a variety of settings and provide accurate information for identifying wear, malfunction, or anomalies. Nevertheless, they have several drawbacks, including the need for physical contact, sensitivity to environmental variables like temperature, humidity, or contamination, and the potential for intrusive placement or disruption of the system dynamics. Furthermore, traditional sensor configurations usually only record information at locations, making it difficult to see dispersed or intricately spaced vibrations throughout a surface or building.

Camera-based techniques have emerged in response to the need for sophisticated, non-invasive, and scalable vibration measurement methods as systems become more

complex and reliability needs rise. High-resolution video and computational techniques for visual sensing create new ways for a more comprehensive and intuitive knowledge of mechanical action. Even accurate movements can be identified and examined, frequently in real time, by recording the motion of a whole object or structure across time and using signal processing techniques.

Motion magnification, which attempts to magnify minute vibrations in video recordings, so they are visible to the human eye, is one of the most potent of these visual approaches. This facilitates interpretation and helps close the gap between visual comprehension and raw numerical sensor data. There are two primary methodological approaches utilized in motion magnification: Eulerian and Lagrangian.

The Lagrangian approach tracks individual feature points over video frames and analyzes their motions. It is based on concepts from fluid dynamics. By clustering trajectories, this technique may separate distinct motion layers within a film and is efficient in handling complex, multi-source motions. It estimates motion with sub-pixel accuracy using complex mathematical models such as optical flow constraint equations. To better differentiate overlapping motion patterns, more biologically inspired versions have been created that use PCA and multichannel Gaussian models to simulate the selective attention of the human visual system. Despite being precise and adaptable, Lagrangian techniques can be computationally taxing since they require motion layer stabilization, feature tracking, and clustering.

To infer motion, the Eulerian method uses a fixed spatial perspective and examines how pixel intensity values vary over time. This technique amplifies minute frequency variations at each pixel position by using temporal filtering. Even when low-amplitude, periodic actions like breathing or heartbeat are not visually noticeable in the original film, it is excellent at amplifying them. To increase stability, lower noise, and enable higher amplification without appreciable distortion, improved versions of this approach employ post-processing techniques such as pixel-level motion mapping. Accuracy and speed have been further enhanced by innovations like phase-based video magnification employing intricate steerable or Riesz pyramids. By using phase changes in sub bands of image data to analyze motion, these methods minimize visual artifacts and enable high-fidelity magnification across a variety of spatial scales and orientations.

High sensitivity and spatial detail are provided by phase-based techniques, especially those that employ steerable pyramids, which makes them appropriate for examining intricate motions in biological tissues or mechanical components. With a notable speedup and smaller memory footprint, the more modern Riesz pyramid offers comparable visual quality while increasing computational efficiency. For real-time or near-real-time applications in robotics, medical diagnostics, industrial monitoring, and infrastructure evaluation, phase-based magnification is therefore feasible.

Camera-based systems provide non-contact, high-resolution, and spatially continuous measurements, but accelerometers record absolute values and function well in harsh environments. Despite their sensitivity to visual disturbances like sunlight, fog, or occlusion, cameras offer a great deal of versatility in settings where traditional sensors are unfeasible or physical access is limited.

The transition from physical to visual sensors is indicative of a larger change in engineering diagnostics, moving away from hardware-centric, localized solutions and toward software-augmented, comprehensive systems that make use of computer vision and machine learning. These techniques should become more precise, widely available, and be integrated into standard monitoring systems as cameras and processing units become more sensitive and powerful. In addition to research and diagnosis, the ability to visually and intuitively watch, measure, and even interact with vibrational behaviors holds great promise for quality assurance, preventive maintenance, and even real-time system control.

Motion magnification methods, whether Eulerian or Lagrangian, linear or phase-based, constitute a revolutionary advancement in vibration analysis. They make it possible for a new paradigm of high-resolution, non-invasive motion recording by getting around the environmental and spatial constraints of conventional sensors. By bridging the gap between measurement and observation, these techniques enable quicker, better-informed decision-making in a wide range of applications and bring invisible phenomena into the visible realm. Further development of these methods will solidify their position as vital resources in contemporary engineering, medicine, and other fields, particularly regarding computing speed, noise resilience, and conditional flexibility.

V. Lab Experiment

1. Introduction

Several monitored laboratory tests are carried out in this chapter to assess the motion magnification technique's viability and accuracy. In particular, the study uses phase-based RDI software to magnify small movements to verify its accuracy by comparing its results with measurements from a high-precision laser sensor.
Two important research questions are intended to be addressed by the study:

1. How reliable are the results generated by the RDI software?
2. How does the camera's working distance from the target affect the noise floor?

These initial assessments are necessary to guarantee a thorough comprehension of the system's strengths and weaknesses before it is implemented in actual field settings, where operational and environmental factors may be erratic or uncontrollable.

2. RDI Software

Machines are meant to move, excessive motion and unplanned vibrations can cause structural damage, equipment wear, and unanticipated breakdowns. These problems lead to expensive downtime and higher maintenance requirements in addition to reducing the lifespan of vital assets. Vibration is a common early sign of mechanical issues in industrial environments. Oscillations from motors, pumps, bearings, shafts, gears, and other parts can deteriorate performance and jeopardize safety over time.
Although some vibration is inevitable when a machine is operating, excessive or erratic movement may indicate more serious mechanical problems such imbalance, misalignment, looseness, or structural instability. Reliability and operating efficiency of the equipment depend on determining the underlying cause of these issues early on. However, when working with complicated systems or low-frequency movements, traditional vibration monitoring techniques may not be able to give a complete picture.

Motion Amplification from RDI Technologies provides a revolutionary answer to these problems. This method turns the entire field of view into a vast array of non-contact vibration sensors by converting each pixel into a data point using a high-speed camera and sophisticated video processing algorithms. This makes it possible

to see motion that would otherwise be imperceptible to the human eye, giving engineers and maintenance specialists the ability to precisely detect, measure, and diagnose movement and vibration.

Motion Amplification has been demonstrated in real-world applications to enhance worker safety, lower maintenance costs, and avoid unscheduled downtime. The method improved component life in a power plant by detecting excessive movement in a turbine coupling that was missed by conventional sensors. It discovered that rolling equipment alignment problems were being caused by flexing in structural supports at a steel factory. The system's visualization of resonance in overhead crane supports at a manufacturing facility resulted in targeted upgrades that improved dependability and safety.

Motion Amplification facilitates quicker diagnosis, more efficient maintenance plans, and long-term performance enhancements in a variety of sectors by offering concise, actionable insights regarding machine behavior.

Modal Amplified offers a quick, camera-based solution that replaces time-consuming, conventional procedures, introducing a revolutionary way to modal testing and analysis. To evaluate structural dynamics, conventional modal testing usually entails thorough sensor mapping, accurate physical sensor placement and fixation, and sophisticated animation modeling. Much of this setup is removed by Modal Amplified, allowing for immediate data collection, real-time visualization, and in-depth study of actual structures.

With the use of high-speed video, this method synchronizes the measurement of input forces with the structural response. By converting every camera frame into a dense grid of virtual sensors, users can create an infinite number of zones of interest within a structure. This eliminates the need for time-consuming physical instrumentation and allows for the instant visualization of mode shapes and modal outcomes within minutes of data capture.

Modal Amplified produces actionable data more quickly and clearly by streamlining the procedure and boosting measurement density. Previously time-consuming test setups that took hours or even days to complete can now be finished in a fraction of the time. Because of its portability, the device may be easily repositioned to capture numerous viewpoints, guaranteeing a more thorough comprehension of the

structural behavior seen in real life. This lowers the total cost and complexity of modal analysis in addition to streamlining procedures.

Building on the revolutionary capabilities of the original Iris M, RDI Technologies' all-new Iris MX extends Motion Amplification's power to high-speed applications. The Iris MX enables users to see and measure motion over a wide frequency range, including motions well above 5,000 Hz, by capturing video at up to 1,400 frames per second in high definition (HD) and even surpassing 10,000 fps at lower resolutions. This capability level offers unmatched insight into the behavior of equipment, structures, and supporting environments by enabling the detection and analysis of almost every displacement within a scene.

Figure 6: Iris MX High Resolution Camera

The Iris MX was created with portability in mind, allowing for quicker and more adaptable field data collecting. By capturing the complete system in motion rather than simply individual parts, it gives users a comprehensive view and facilitates the identification of the underlying causes of mechanical problems. Technology facilitates communication between technical and non-technical staff by producing clear and understandable visual outputs, which speeds up and improves decision-making. An important development in motion diagnostics and structural health monitoring is the Iris MX, which combines high-level analysis with an easy-to-use interface.

3. Laser Displacement Sensor

Non-contact measurement capabilities, the best option will rely on the particulars of the target material and application environment. Keyence's 1D laser displacement sensors offer a highly accurate, non-contact solution for measuring the height, position, or distance of a target, when multiple sensors are combined, additional measurements such as thickness and width can also be performed.
Light is sent and received along the same axis in confocal displacement sensors. This idea is strengthened by multi-color confocal sensors, which project several wavelengths with distinct focal points. The color that is clearly concentrated on the target is used by the sensor to calculate distance. Regardless of surface reflectance, stable measurement is possible with this technique. With the help of a high-intensity light source and small, light sensor heads that are simple to mount on machinery, Keyence's CL-3000 Series ensures precise distance measuring even in difficult or constrained configurations. This series is perfect for high-precision positioning in automated industrial settings because it reduces measurement mistakes brought on by heat or electrical noise.

Laser triangulation sensors use the angle of reflected laser light to determine displacement. The sensor determines displacement by sensing the shift in the angle of reflection caused by changes in the distance to the object. High-resolution sensors are used in the LK-G5000 Series to provide consistent readings of even the smallest displacements, especially in dynamic or fast-moving applications. Laser triangulation sensors are often speedier, which makes them ideal for high-speed production lines. However, their sensitivity to surface properties like gloss or transparency can limit performance.

Figure 7:Keyence LK-G5000

For more complex applications, surface scanning confocal sensors, like those in the Keyence LT-9000 Series, quickly sweep across the measurement range using a dual-axis scanning mechanism and a vibrating objective lens. This makes it possible to employ a focused laser beam as narrow as 2 µm in diameter to make extremely accurate and steady observations. This technique is very effective on a range of surface types, including clear, glossy, or uneven surfaces, because it depends on detecting when light is strongly concentrated through a pinhole and is not impacted by changes in light intensity.

Figure 8:Keyence LT-9000

These sensors are used in a variety of materials and applications. Conventional contact-based techniques like calipers or Linear Variable Differential Transformers can harm or introduce measurement inaccuracies for fragile surfaces like silicon wafers, thin films, or polished metals. Non-contact laser displacement sensors, on the other hand, provide precise, repeatable findings without influencing the target. These sensors guarantee accuracy and dependability whether they are utilized for position control in robotic applications, real-time feedback in coating or welding procedures, or quality inspection.

Confocal sensors can perform better than conventional laser displacement systems in specific situations, such as measuring the thickness of glass, particularly when surfaces have distinct reflectance characteristics because of coatings or patterns. For instance, by identifying the exact focus point of the reflected wavelength, the CL-3000 Series removes tracking mistakes brought on by fluctuating reflectivity. This increases the speed and uniformity of inspections by guaranteeing extremely precise and reproducible measures.

Figure 9:Keyence CL-3000

Confocal sensors can be installed next to the nozzle in automatic dispensing systems to measure and regulate height in real time. This configuration reduces errors brought on by vibrations or residual movement and guarantees precise coating, even on translucent or uneven surfaces. A greater range of materials and surface geometries can be measured using the confocal method's coaxial nature without sacrificing accuracy.

The capacity of this technology to precisely measure challenging objects, including semi-transparent solder masks on Printed Circuit Boards or even delicate surfaces, like soap bubbles, is among its most remarkable features. The instability typical of measurements affected by diffuse reflections is avoided by Keyence's confocal sensors, which analyze only the targeted wavelength band. Even for intricate or light-sensitive materials like silicon wafers, glass, or micro lenses, this capacity allows for accurate measurements.

Several crucial elements, such as measuring range, resolution, speed, and the target's material characteristics, influence the choice of displacement sensor. While laser triangulation sensors offer faster measurements and are therefore well-suited for high-speed industrial operations, confocal sensors often offer superior stability and are best suited for surfaces with variable reflectance. Comprehending these principles facilitates the selection of the best sensors, allowing for more precise monitoring, control, and inspection in modern production settings.

4. Proximity Probe

An apparatus that can identify the existence of an object in proximity without requiring physical contact is known as a proximity sensor. Numerous pieces of equipment and electronic systems frequently employ this kind of sensor. Its unique ability to perceive items by invisible signals, that is, without the sensor and the object it detects coming into physical contact makes it unique.
Typically, proximity sensors emit an electromagnetic field or a beam of electromagnetic radiation, like infrared light, to detect their surroundings. The sensor then keeps an eye out for any modifications to that signal or field. The sensor can identify the presence of something if it approaches closely enough to disrupt the field or reflect the light. The target of the sensor is frequently the object being detected.

Different sorts of sensors are needed for different kinds of targets. For instance, a photoelectric sensor or a capacitive proximity sensor may be used to identify a plastic object. Non-metal materials can be detected by these sensors. However, as an inductive proximity sensor is built especially to detect metal targets, it would be the ideal option if the object is made of metal. Since not all sensors are compatible with all materials, this is crucial.

The long working life and high reliability of proximity sensors are two major benefits. This is because they don't require contact with the object they are sensing and don't have any moving parts. The sensor can function correctly for a long time without breaking or requiring much maintenance because of reduced wear and tear.

Another popular application for proximity sensors is the monitoring of machine vibration. Engineers must monitor the amount that the shaft a spinning component of the machine moves inside its support in huge machines like electric motors, compressors, and steam turbines. Sleeve-type bearings are frequently used in these devices, and it's critical to determine whether the shaft is moving excessively or insufficiently. The tiny variations in distance between the shaft and the bearing can be measured by a proximity sensor, which aids in the early detection of issues.

Proximity sensors are sometimes employed at very close ranges. They can function as a touch switch when positioned in this manner. This is typical of contemporary touch-sensitive gadgets, where a function can be activated by merely bringing your finger near the surface.

Figure 10: Proximity Probe

5. Experiment 1

In this experiment, varying amounts of imbalanced mass were introduced to measure the vertical displacement of a rotor motor under various beginning conditions. The RDI software (used IRIS MX camera), which was placed at a predetermined working distance of 0.5 meters from the region of interest, was used to assess the measurement accuracy. These outcomes were contrasted with the reference standard, which was a laser displacement sensor (Keyence LK-G5000).
Five different initial conditions were used for the experiment: a balanced state and four imbalanced states produced by gradually adding 2g, 4g, 6g, and 8g of mass. To guarantee consistency in the data and to make statistical analysis easier, each condition was tested three times.

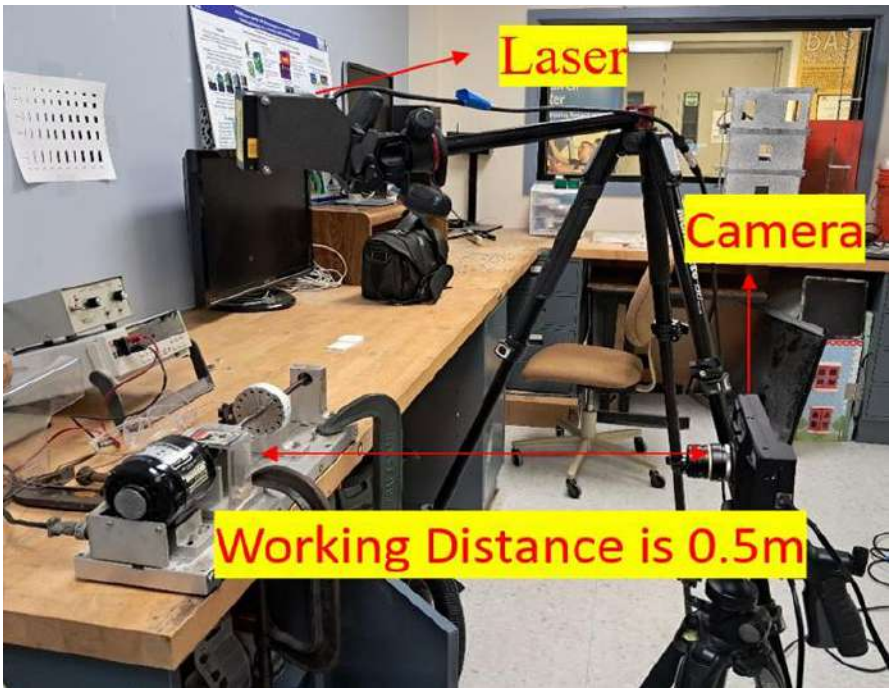

Figure 11: Experiment Setup 1

- Rotor motor is clamped to the table.
- The shaft rotation speed is 40 Hz.
- The camera frame is 1,000 frames per second.
- The laser frame is 1,000 data per second.

My Region of interest, where the camera is focused and the laser dot is positioned, is shown in the picture below. Motion magnification requires an edge to magnify the

video and provide findings, and the laser displacement sensor requires a clean, flat surface, which is why this area was chosen.

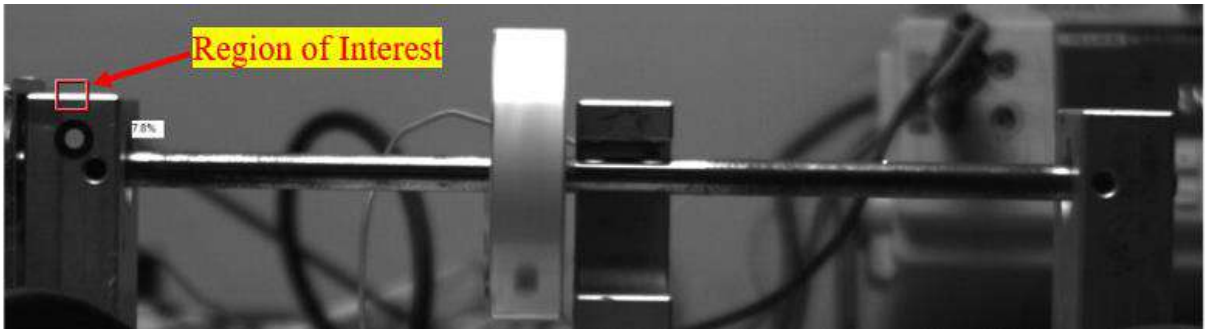

Figure 12:Region of Interest for Experiment 1

a) Balanced (No mass added)

For every case, we collect data, plot the time-history signals, and then transform them into the frequency domain using a Fourier Transform. Then, we compute the RMS values in the time domain and compare the laser displacement sensor's and the RDI system's RMS and peak amplitude values.

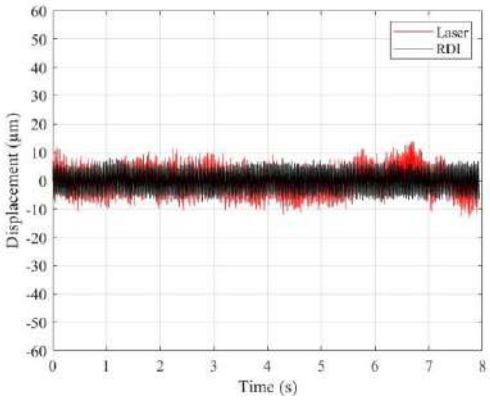

Figure 13: Time Domain for Sample 1

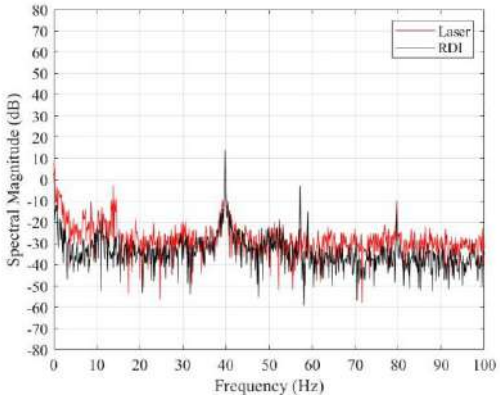

Figure 14:Frequency Domain for Sample 1

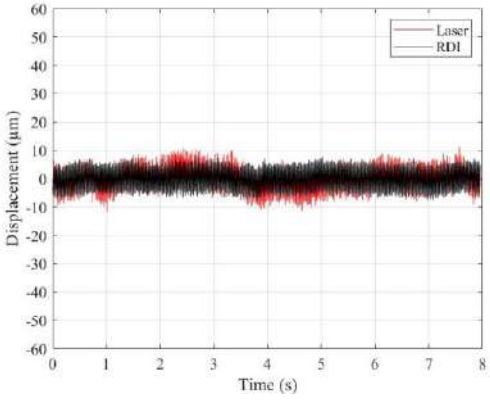

Figure 15:Time Domain for Sample 2

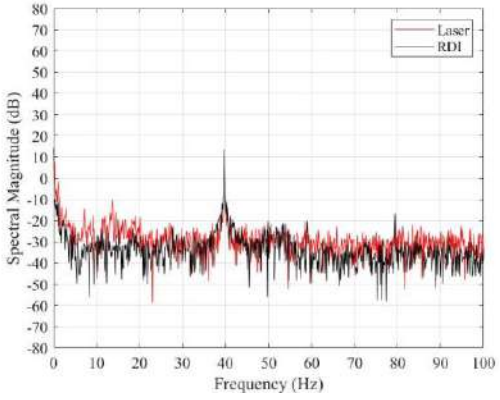

Figure 16: Frequency Domain for Sample 2

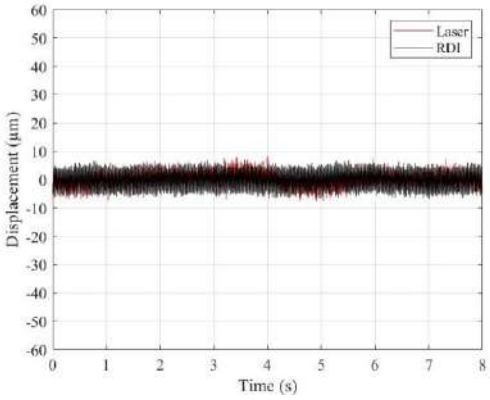

Figure 17: Time Domain for Sample 3

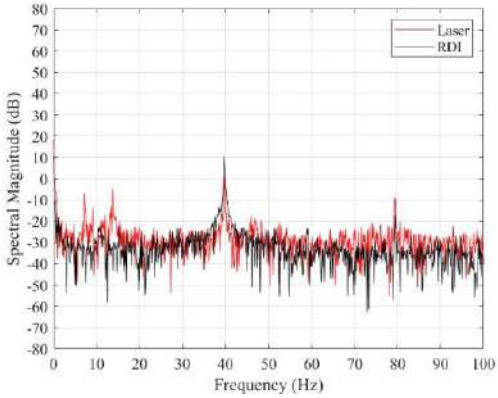

Figure 18: Frequency Domain for Sample 3

Finally, we compute the mean and standard deviation for the three samples.

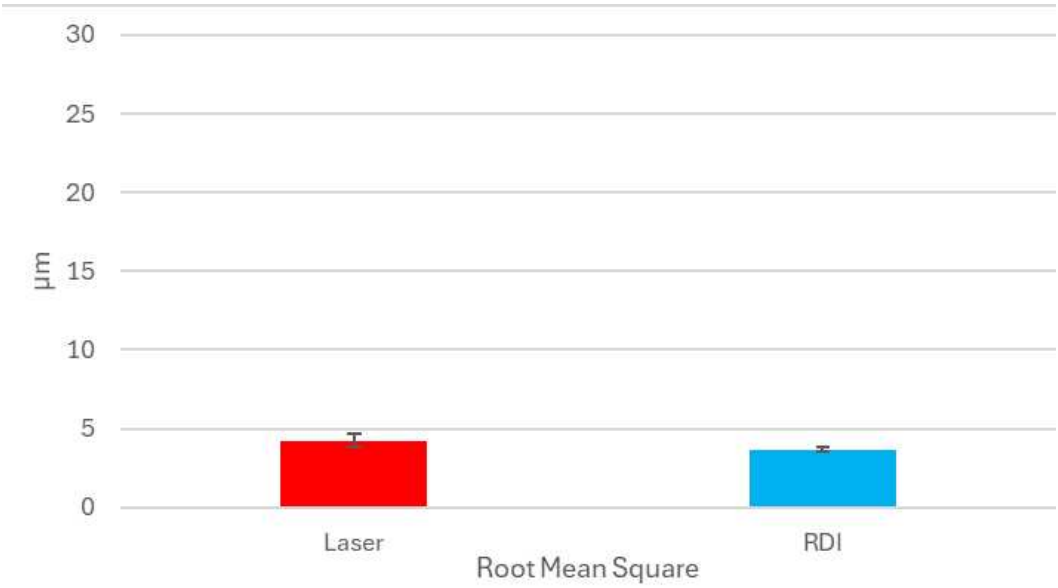

Figure 13: Compared Results of RMS

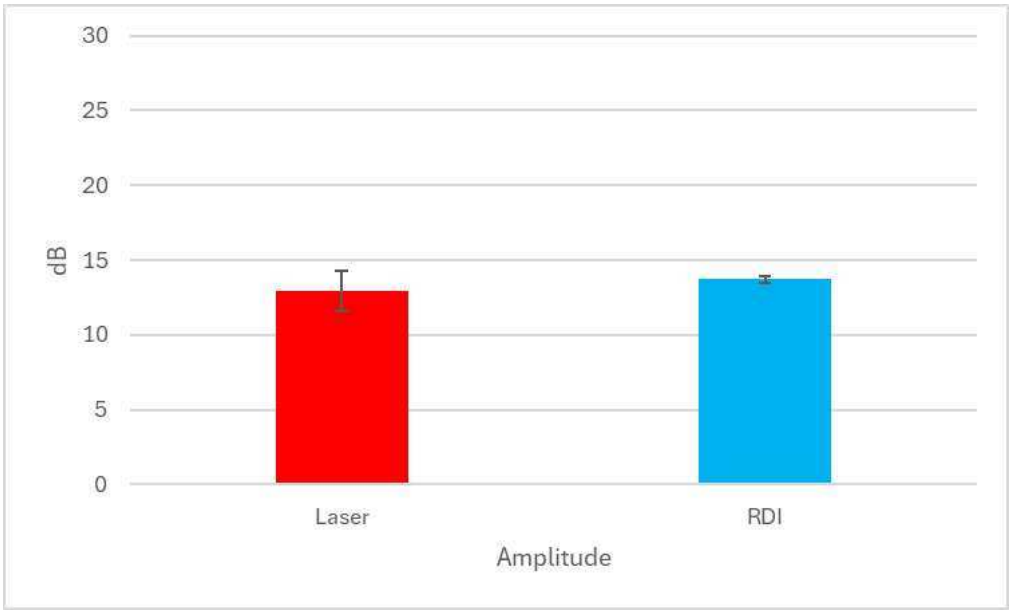

Figure 14: Compared Results of Amplitude

b) Unbalanced (2g Added)

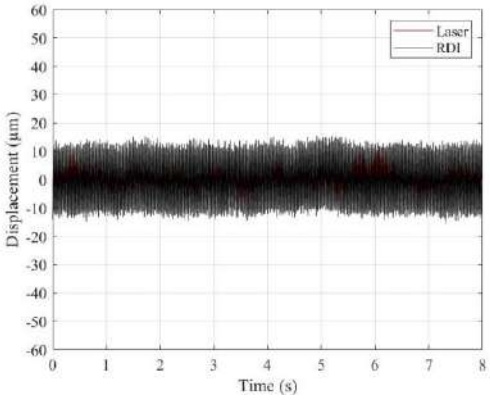

Figure 21: Time domain of Sample 1

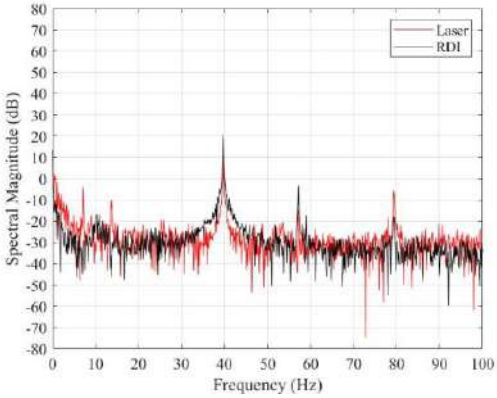

Figure 22: Frequency Domain of Sample 1

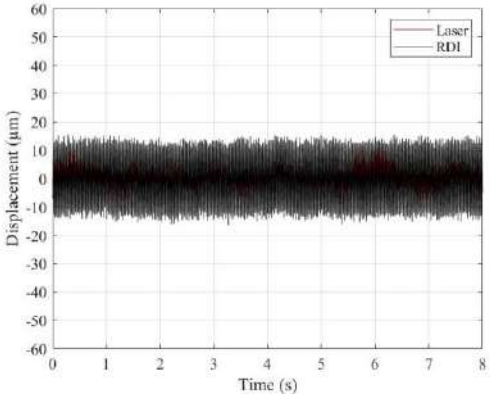

Figure 23: Time Domain of Sample 2

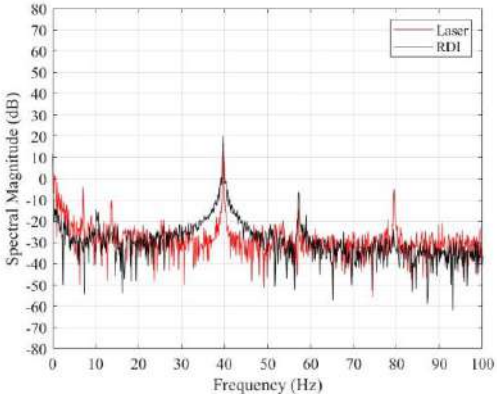

Figure 24: Frequency Domain of Sample 2

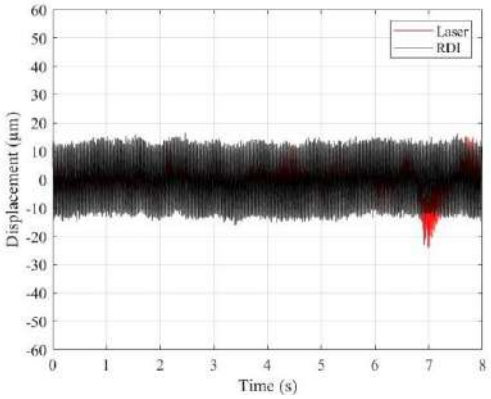

Figure 16: Time Domain of Sample 3

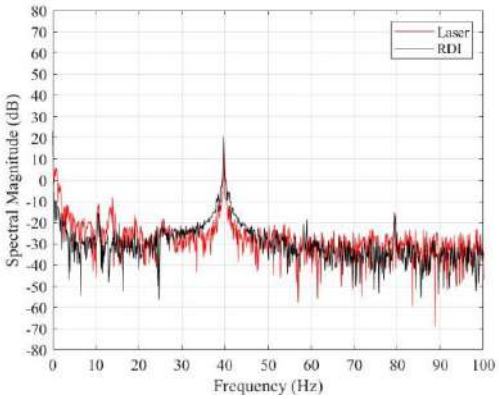

Figure 17: Frequency Domain sample 3

Finally, we compute the mean and standard deviation for the three samples.

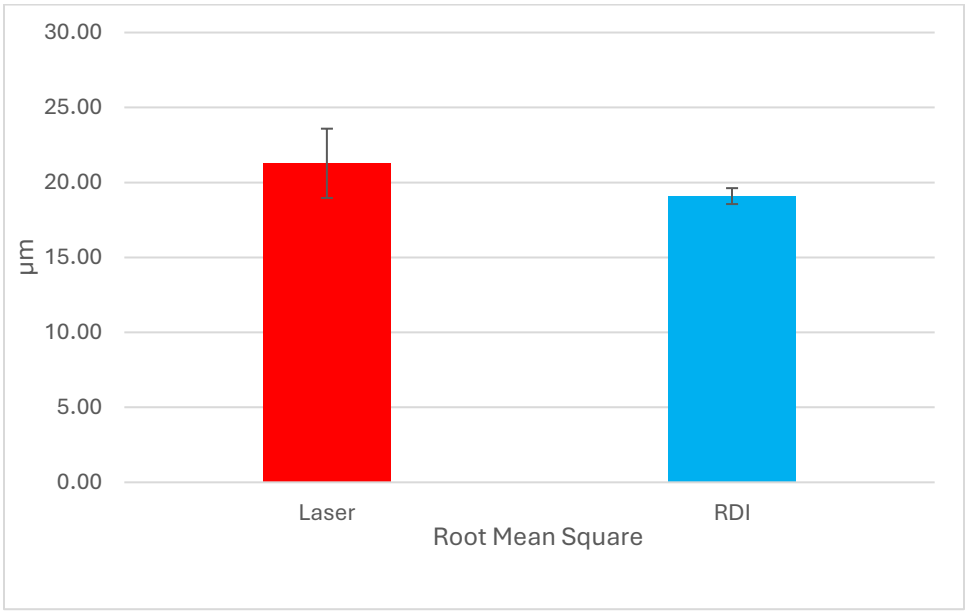

Figure 18: Compared Results of RMS

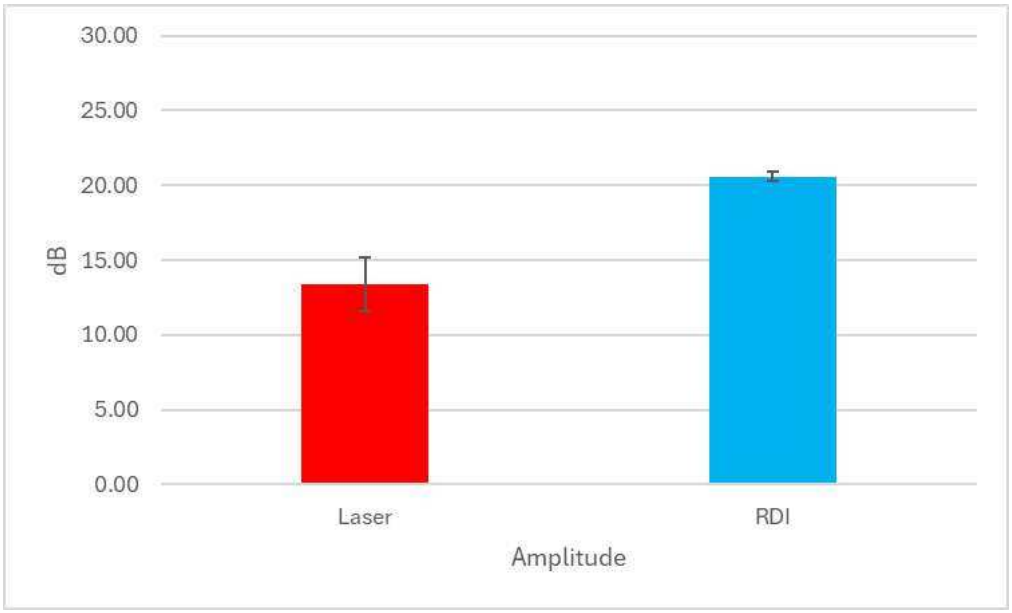

Figure 19: Compared Results of Amplitude

c) Unbalanced (4g added)

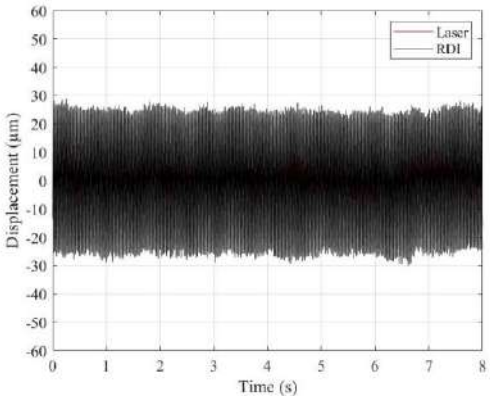

Figure 30: Time Domain of Sample 1

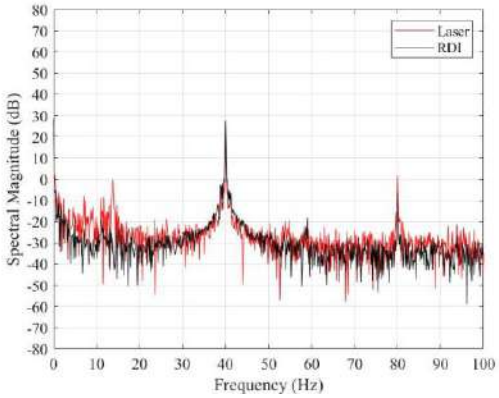

Figure 31: Frequency Domain of Sampe 1

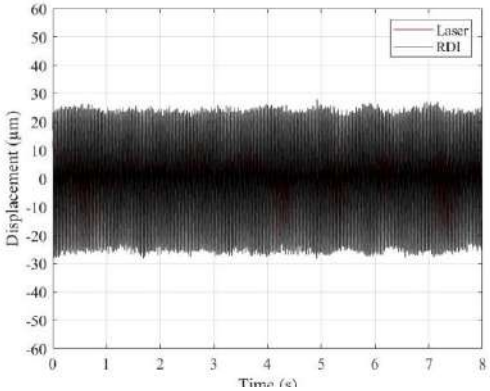

Figure 20: Time Domain of Sample 2

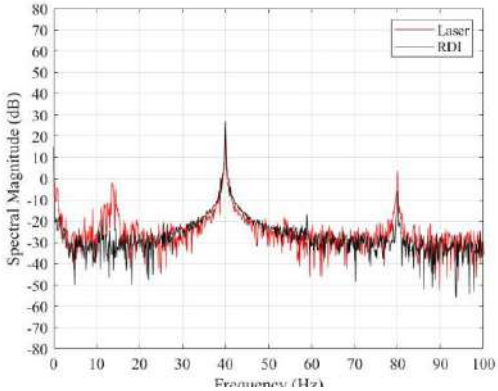

Figure 21: Frequency Domain of Sample 2

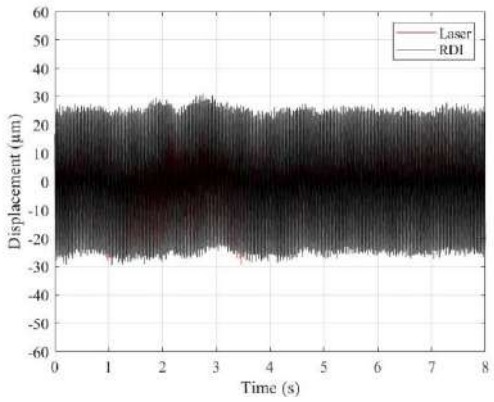

Figure 36: Time Domain Sample 3

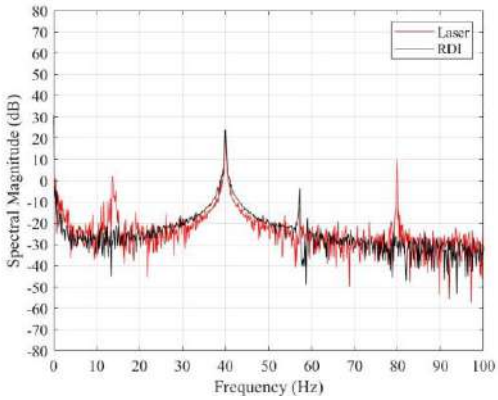

Figure 37: Frequency Domain Sample 3

Finally, we compute the mean and standard deviation for the three samples.

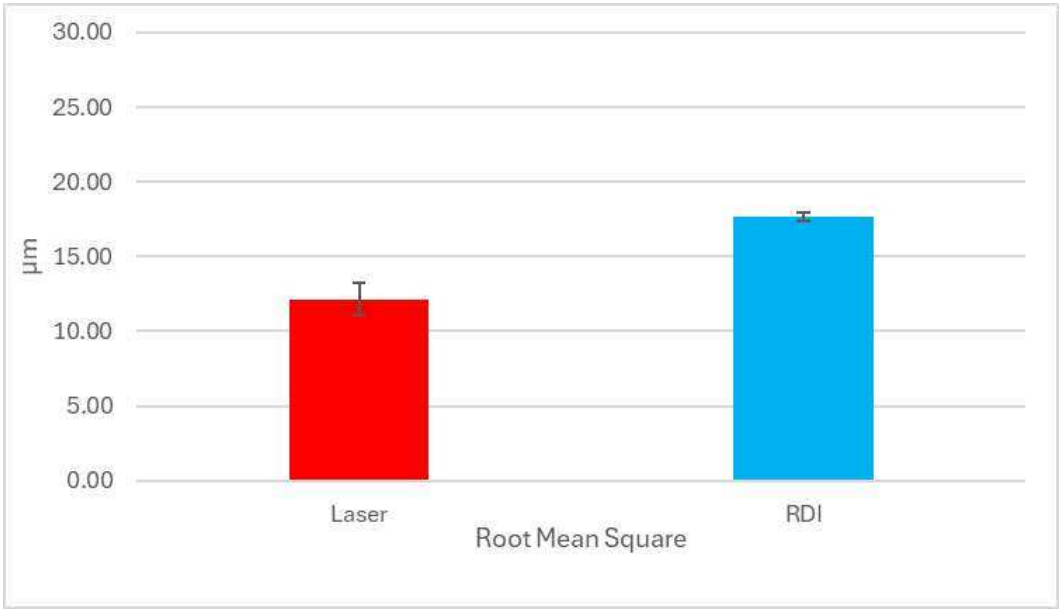

Figure 24: Compared Results of RMS

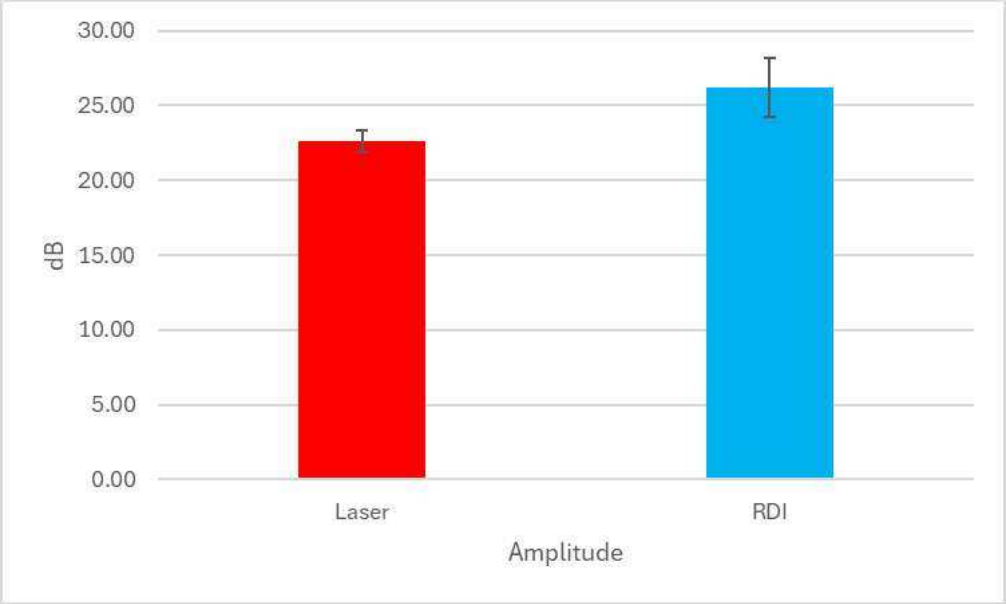

Figure 25: Compared Results of Amplitude

d) Unbalanced (6g added)

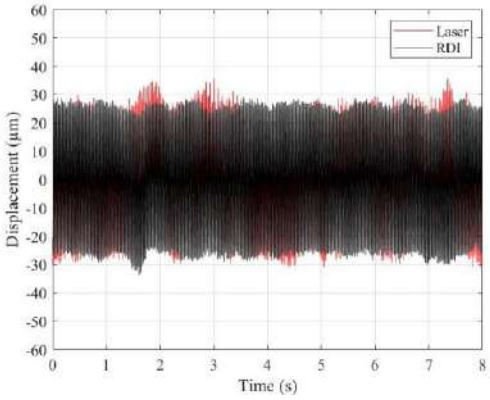

Figure 40: Time Domain of Sample 1

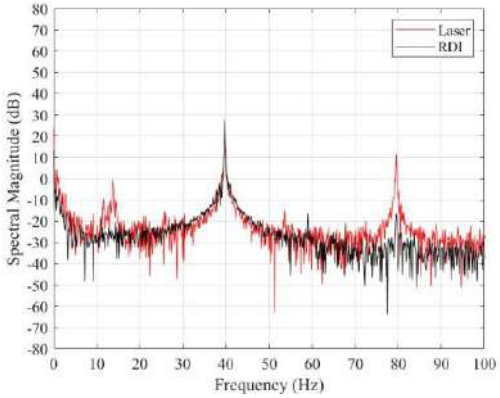

Figure 41: Frequency Domain of Sample 1

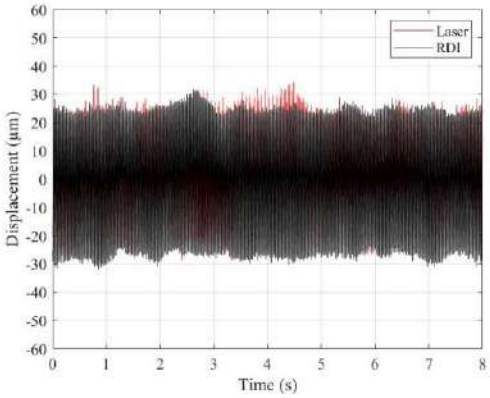

Figure 42: Time Domain of Sample 2

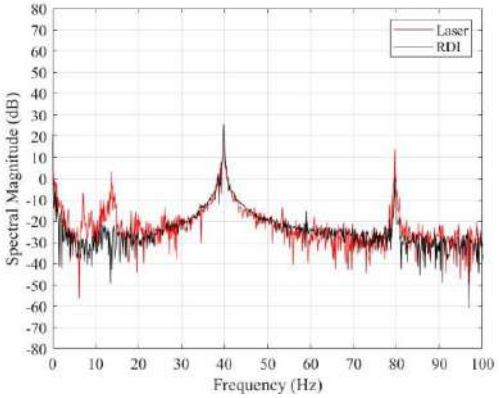

Figure 43: Frequency Domain of Sample 2

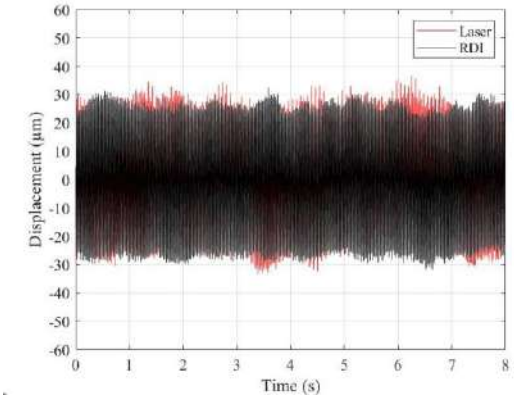

Figure 44:Time Domain of Sample 3

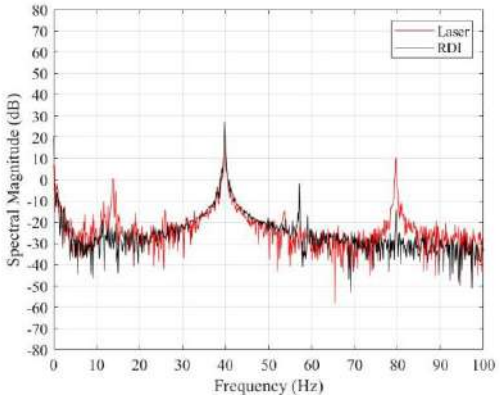

Figure 45: Frequency Domain at Sample 3

Finally, we compute the mean and standard deviation for the three samples.

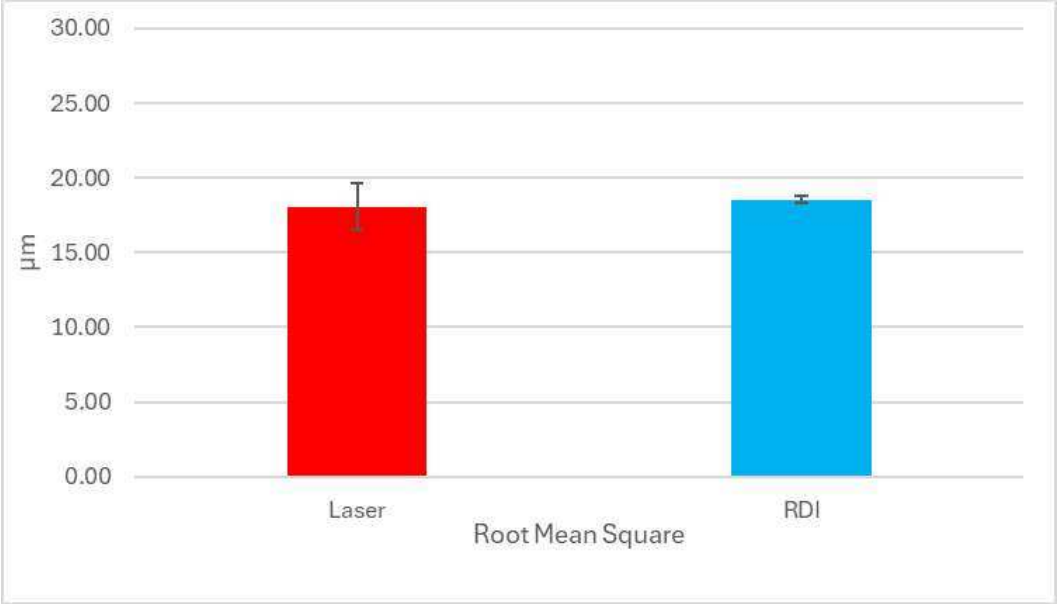

Figure 26: Compared Results of RMS

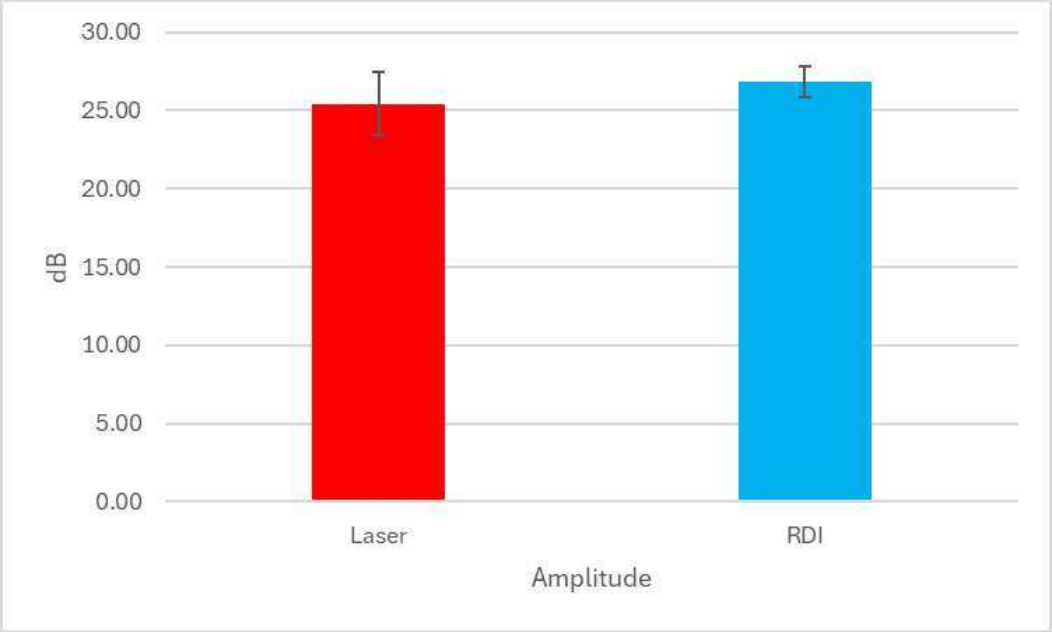

Figure 27: Compared Results of Amplitude

e) Unbalance (8g added)

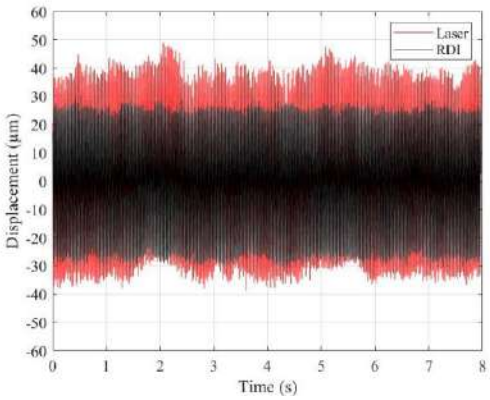

Figure 48: Time Domain od sample 1

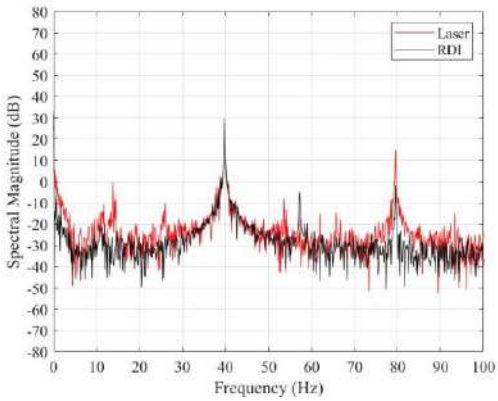

Figure 49: Frequency Domain of Sample 1

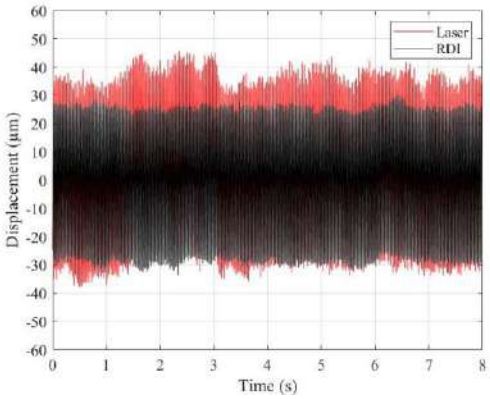

Figure 50: Time Domain of Sample 2

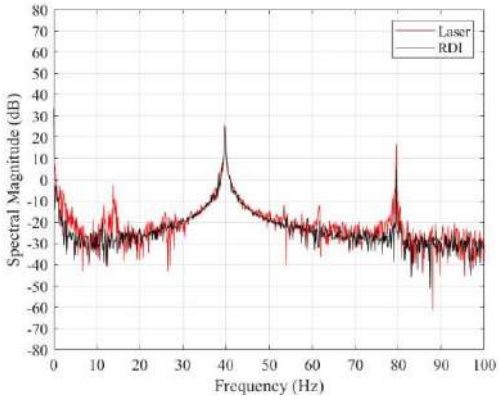

Figure 51: Frequency Domain of Sample 2

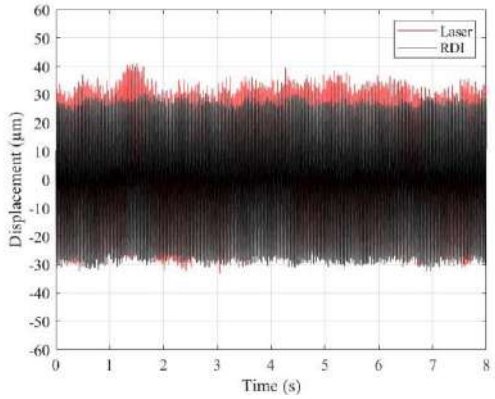

Figure 52: Time Domain of Sample 3

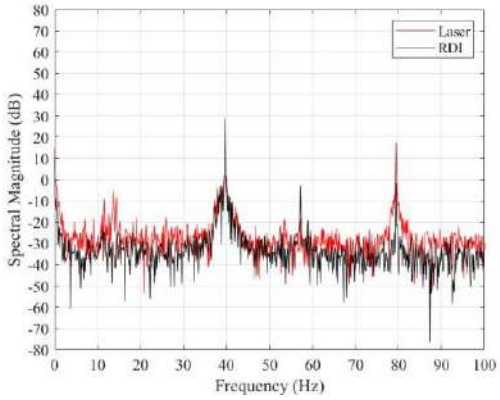

Figure 53: Frequency Domain of Sample 3

Finally, we compute the mean and standard deviation for the three samples.

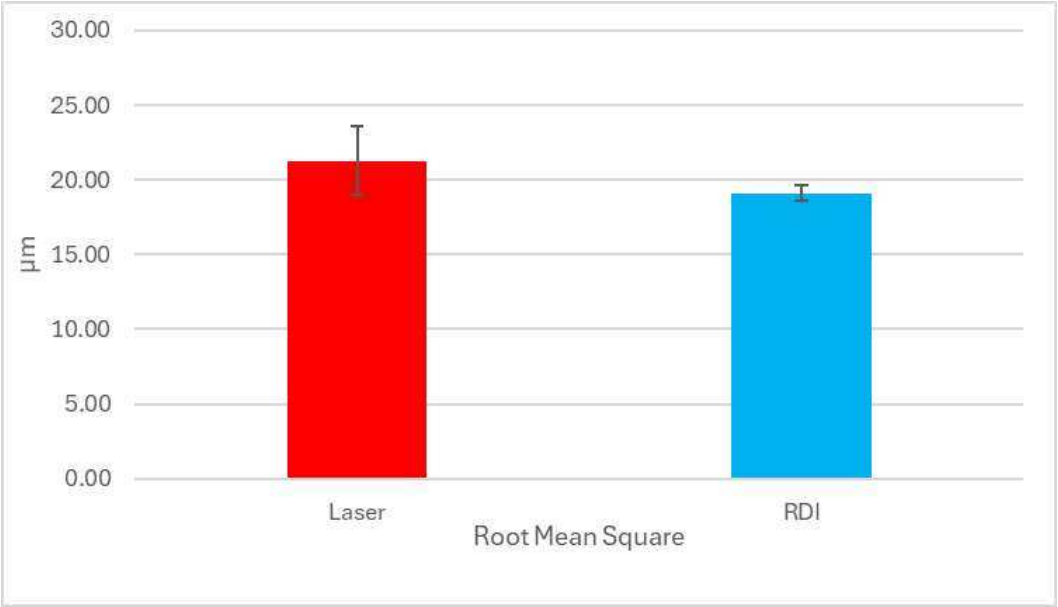

Figure 28: Compared Results of RMS

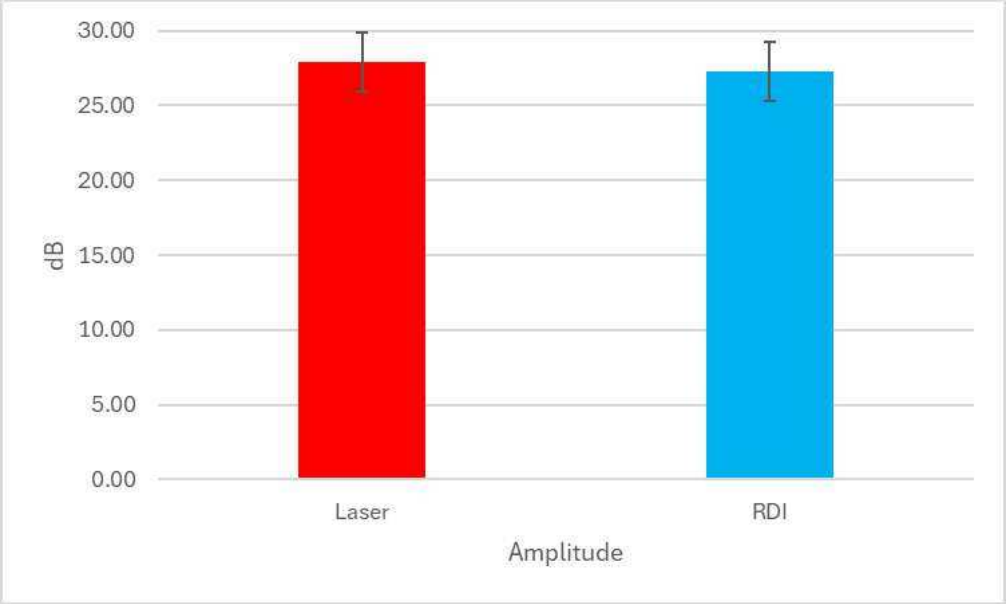

Figure 29: Compared Results of Amplitude

f) Conclusion

To evaluate measurement accuracy and consistency, the mean and standard deviation of the data were calculated after all experimental experiments were finished. After that, a comparison of the outcomes produced by the RDI software and the laser displacement sensor was carried out. The results show a high degree of agreement and validate the accuracy and dependability of the RDI software with respect to the reference sensor (Laser), with all data points from both measurement systems falling within one standard deviation from the mean.

6. Experiment 2

In this experiment, a bar was firmly attached to a table so that a regulated impact could be applied and the dynamic response could be recorded. Both a laser displacement sensor and the RDI software were used to gather data at the same time. Plotting of the time-domain and frequency-domain signals was then done for comparison. To assess the accuracy and consistency of the two approaches, the experiment's main goal was to align the signals from the two measuring devices and produce the Time Response Amplitude Curve (TRAC) and Frequency Response

Amplitude Curve (FRAC). The test was repeated four times to allow statistical measurements.

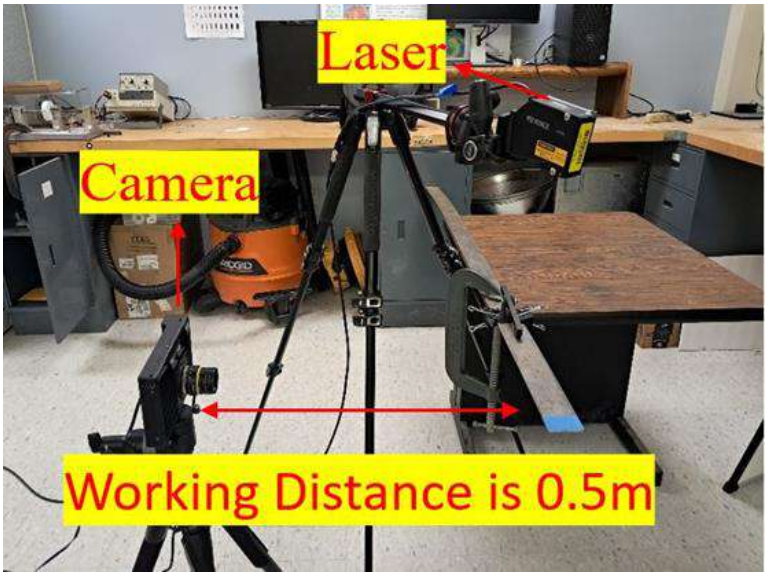

Figure 30: Experimental Setup 2

- Bar is clamped on the table.
- The camera frame is 1,000 frames per second.
- The laser frame is 1,000 data per second.

The Figure below shows my region of interest.

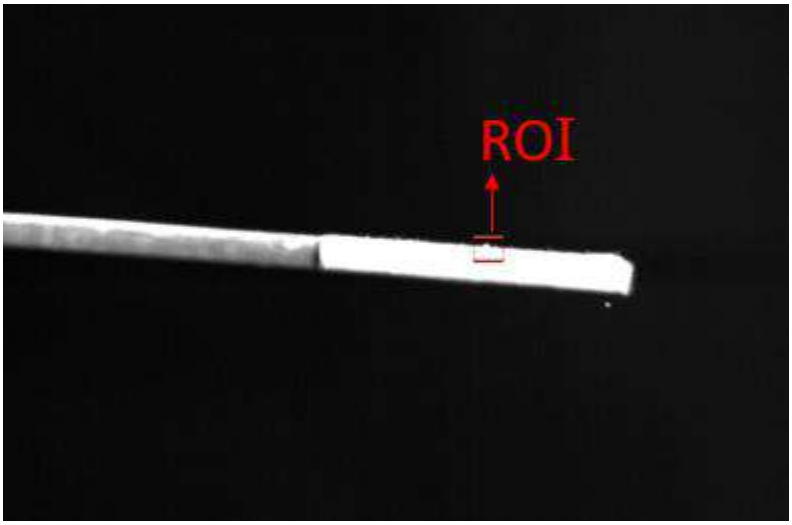

Figure 31: Region of Interest

This test is repeated four times to allow statistical measurements.

a) Sample 1

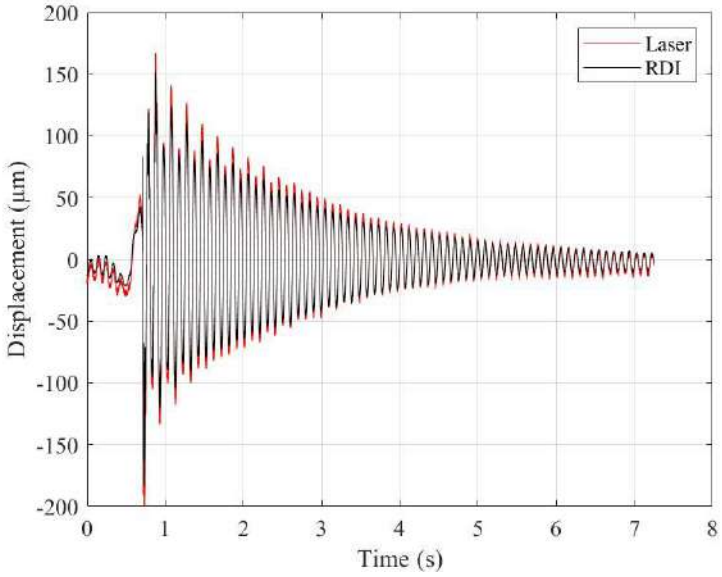

Figure 32: Time Domain Sample 1

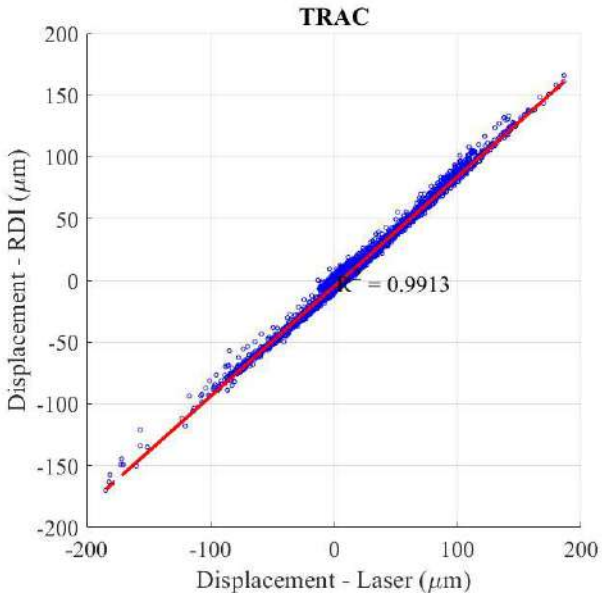

Figure 33: Time Response Amplitude Curve Sample 1

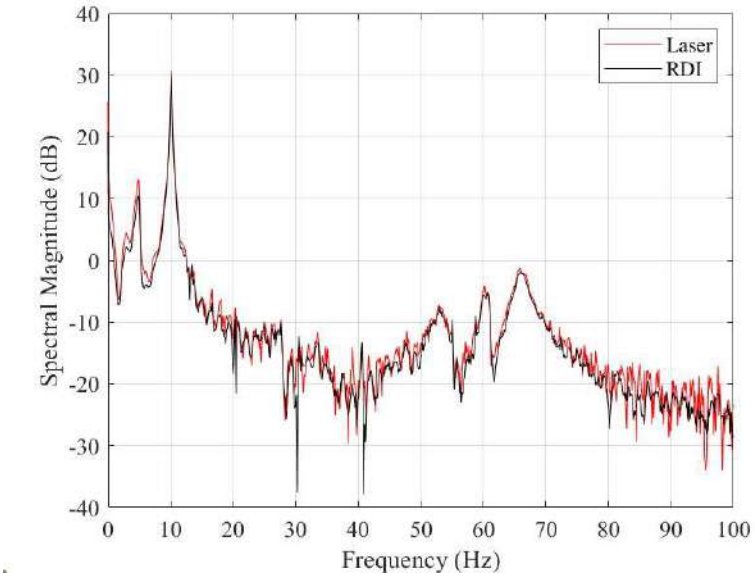

Figure 34: Frequency Domain Sample 1

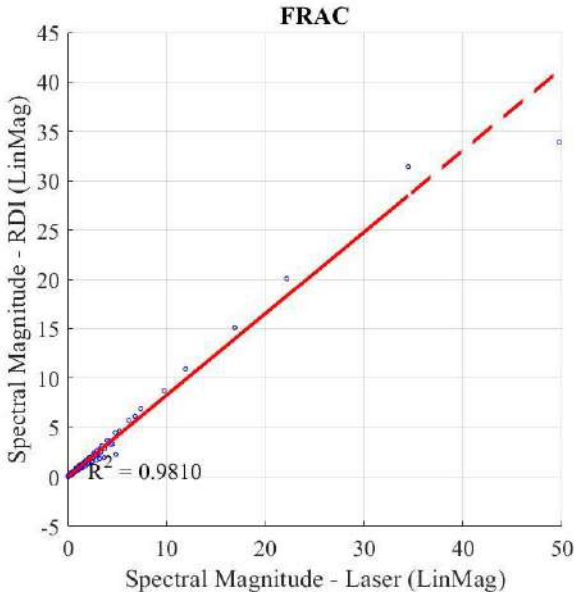

Figure 35: Frequency Response Amplitude Curve Sample 1

b) Sample 2

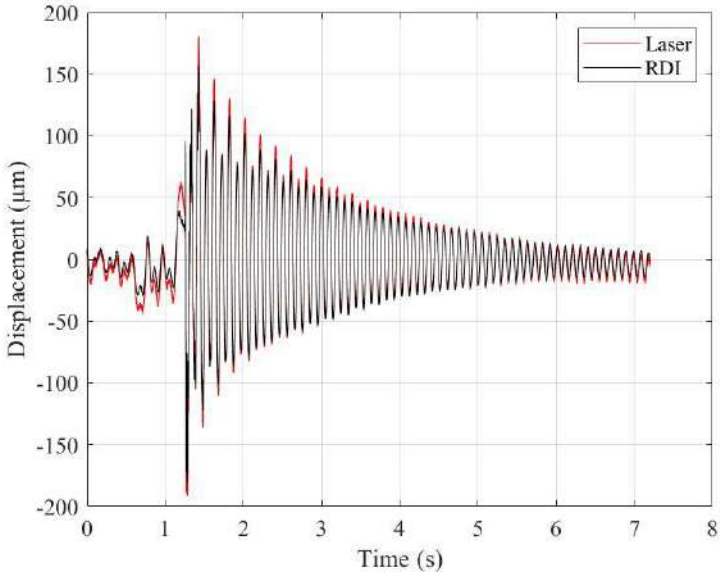

Figure 36: Time Domain Sample 2

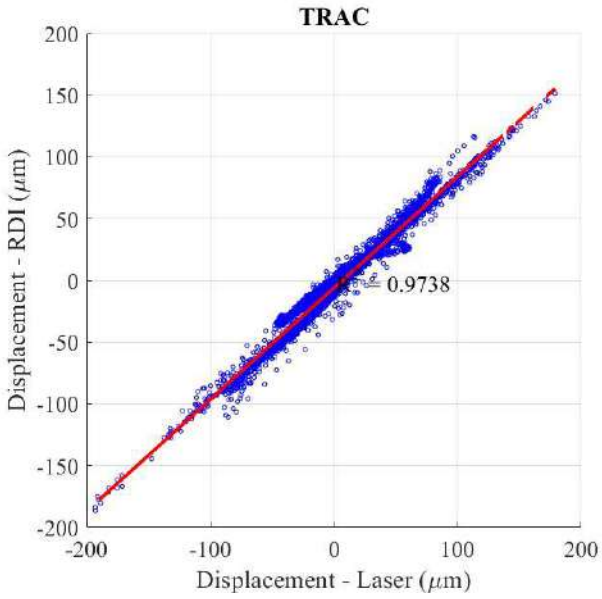

Figure 37: Time Response Amplitude Curve Sample 2

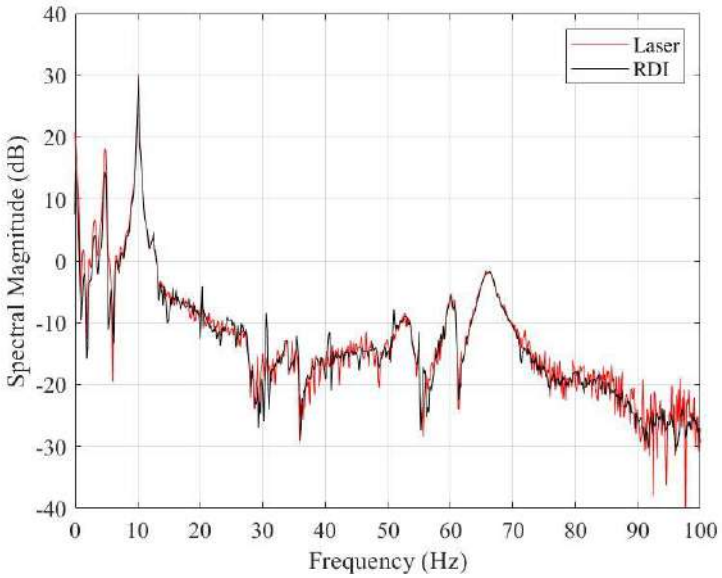

Figure 38: Frequency Domain Sample 2

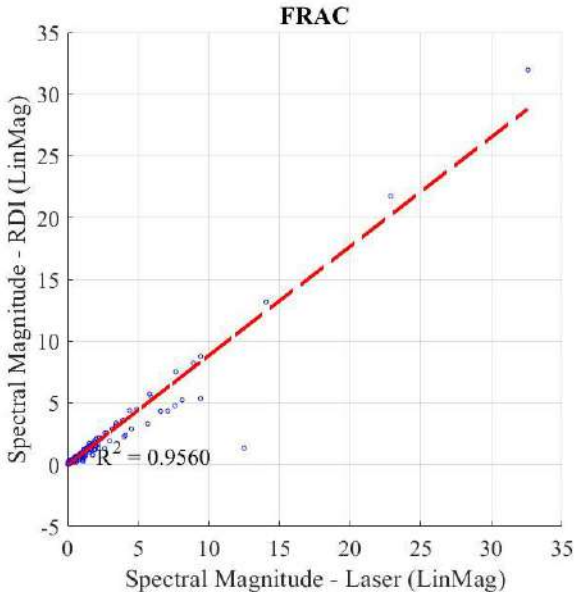

Figure 39: Frequence Response Amplitude Curve Sample 2

c) Sample 3

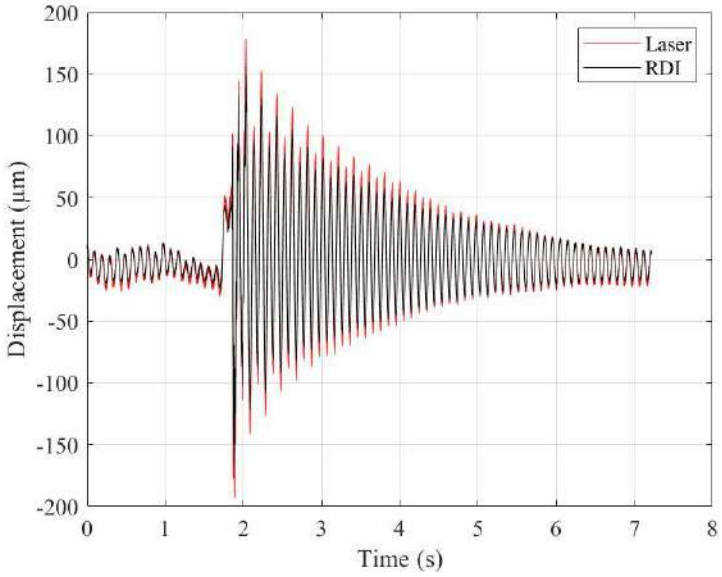

Figure 40: Time Domain Sample 3

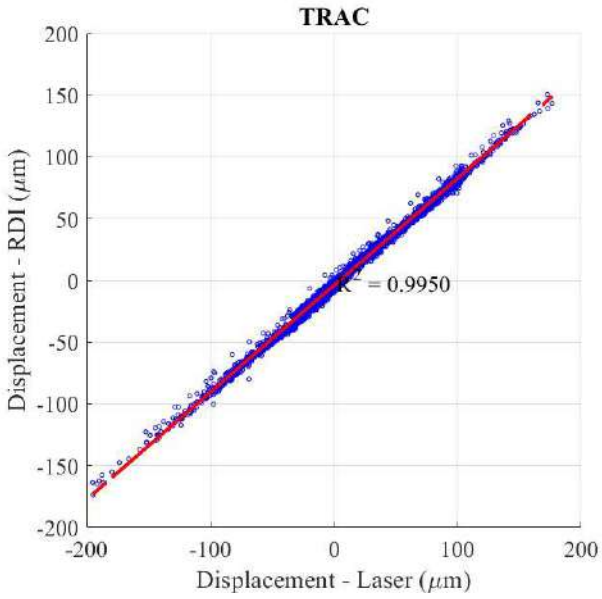

Figure 41:Time Response Amplitude Curve Sample 3

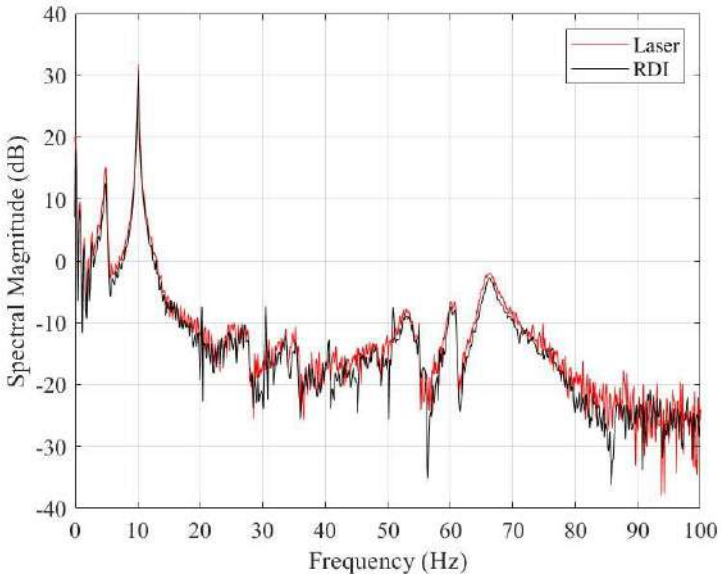

Figure 42: Frequency Domain Sample 3

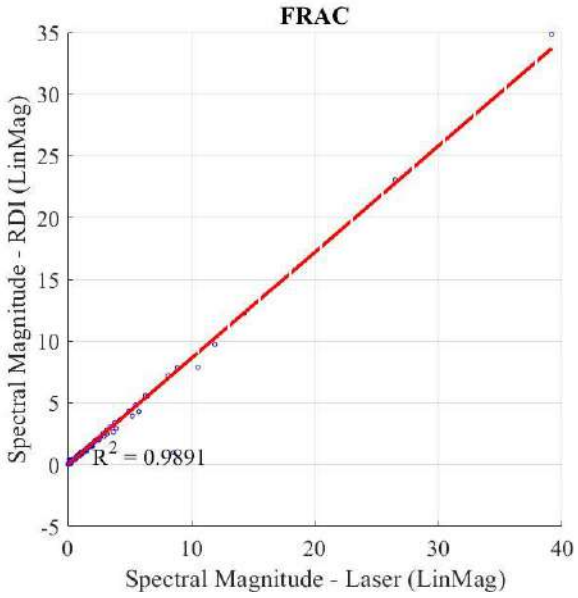

Figure 43: Frequency Response Amplitude Curve Sample 3

d) Sample 4

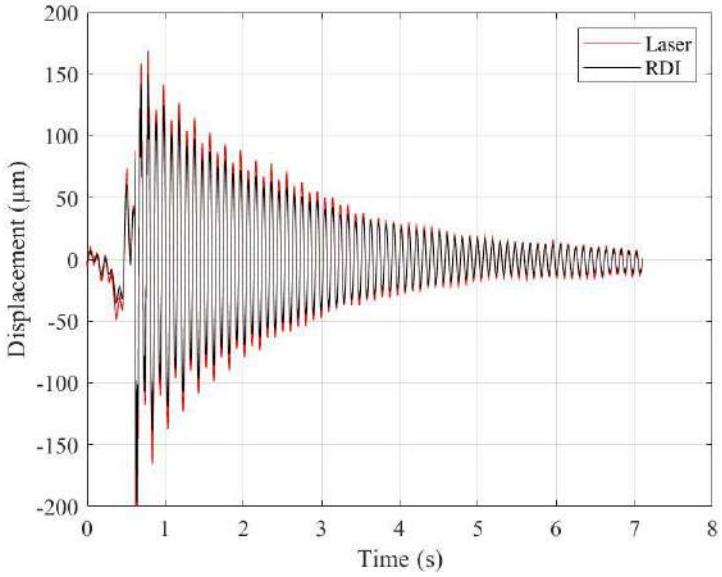

Figure 44: Time Domain Sample 4

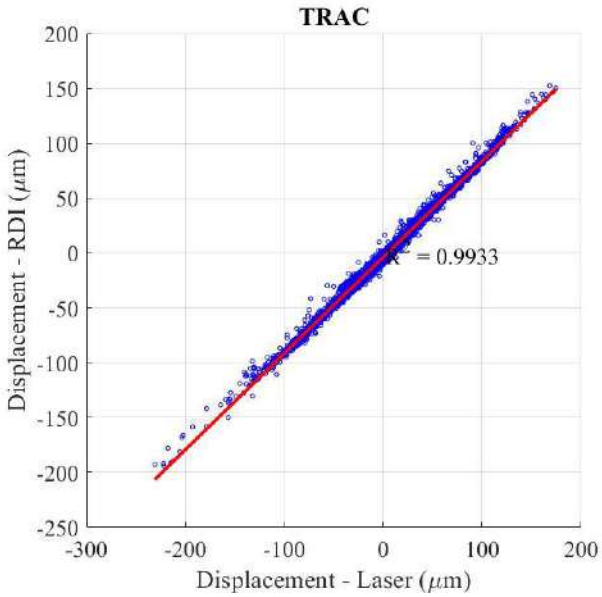

Figure 45: Time Response Amplitude Curve Sample 4

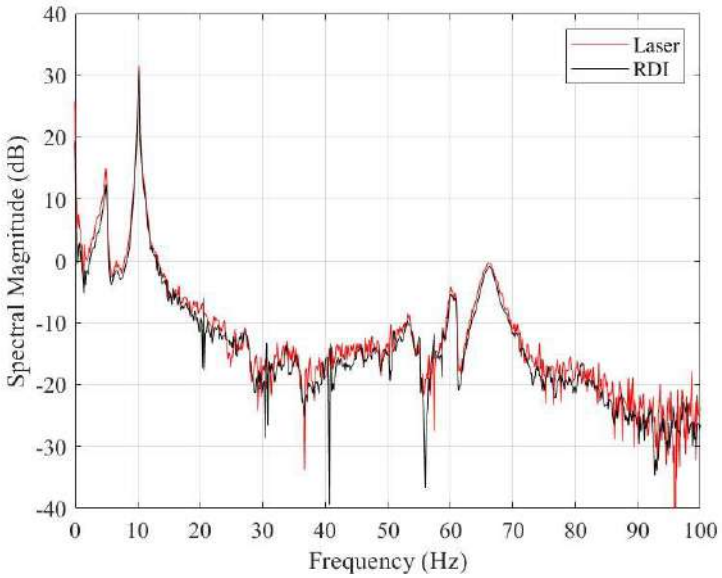

Figure 46: Frequency Domain Sample 4

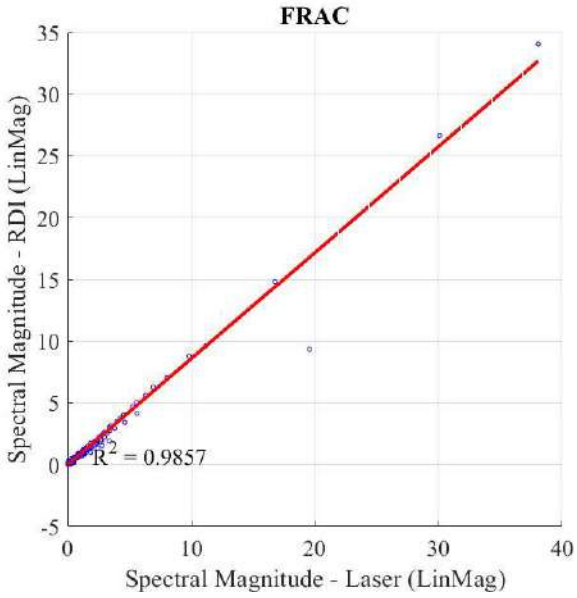

Figure 47: Frequency Response Amplitude Curve Sample 4

e) Conclusion

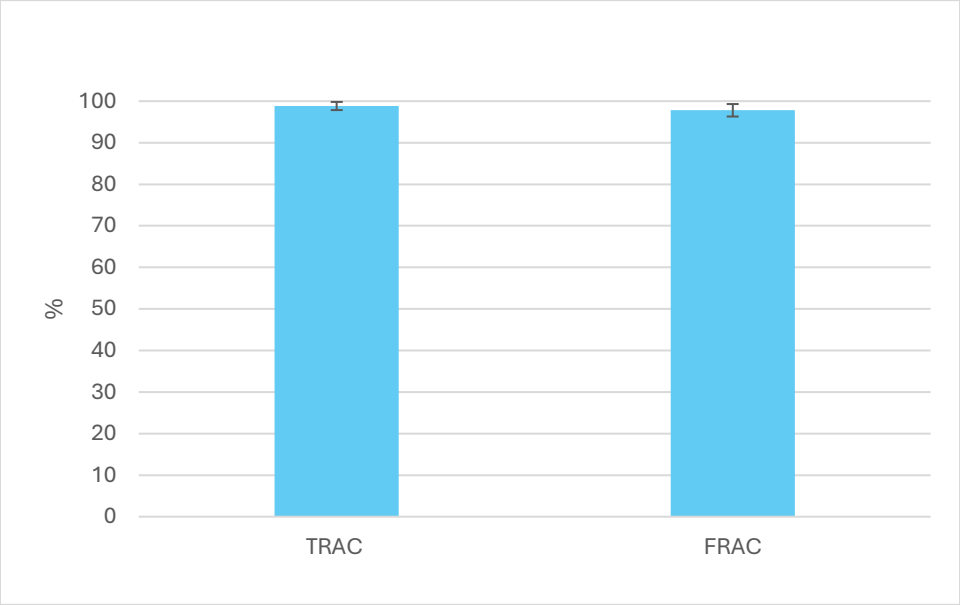

Figure 48: TRAC and FRAC Accuracy Percentage

Following these tests, I achieved around 97% accuracy in both the time and frequency domains, indicating that RDI is a reliable method.

7. Experiment 3

The study focuses on understanding the relationship between the Field of View, Working Distance, and Noise Floor in vibration analysis. To achieve this, experiments are conducted at varying working distances, ensuring that the measured vibrations exceed the noise floor. These tests help evaluate how changes in working distance influence the quality and reliability of the data. Additionally, the time-domain results obtained from the RDI software are compared with those acquired through laser-based measurement techniques, such as laser measuring device, to assess the accuracy and consistency of the two methods. This analysis aims to determine the extent to which working distance impacts measurement precision, providing insights for optimizing experimental setups in vibration studies.

a) Field of View

The Field of view depends on Camera type, focal length and working distance.

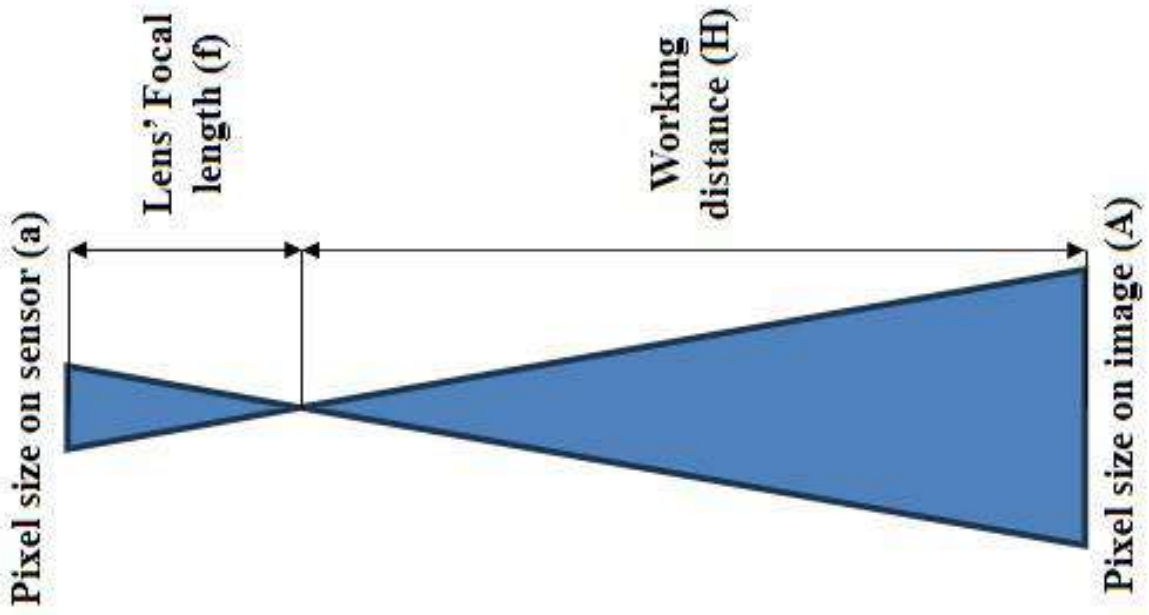

Figure 49: Optical Geometry (Pixel Scaling with Focal Length and Working Distance)

From the formula below, we can see that only the working distance changes. This change helps us understand the relationship between working distance and the Field of View. By studying this, we can see how adjusting the working distance affects the area captured.

$$FOV(m) = \frac{sensor(px) \times Pixel\ size\left(\frac{micron}{px}\right) \times Working\ Distance(m)}{1000 \times Focal\ Length\ (mm)}$$

Equation 1

Camera IRIS MX characteristics:

- Sensor Width (px) = 2560
- Sensor Height (px) = 2080
- Pixel Size Width (micron/px) = 5
- Pixel Size Height (micron/px) =5
- Focal Length (mm) = 25

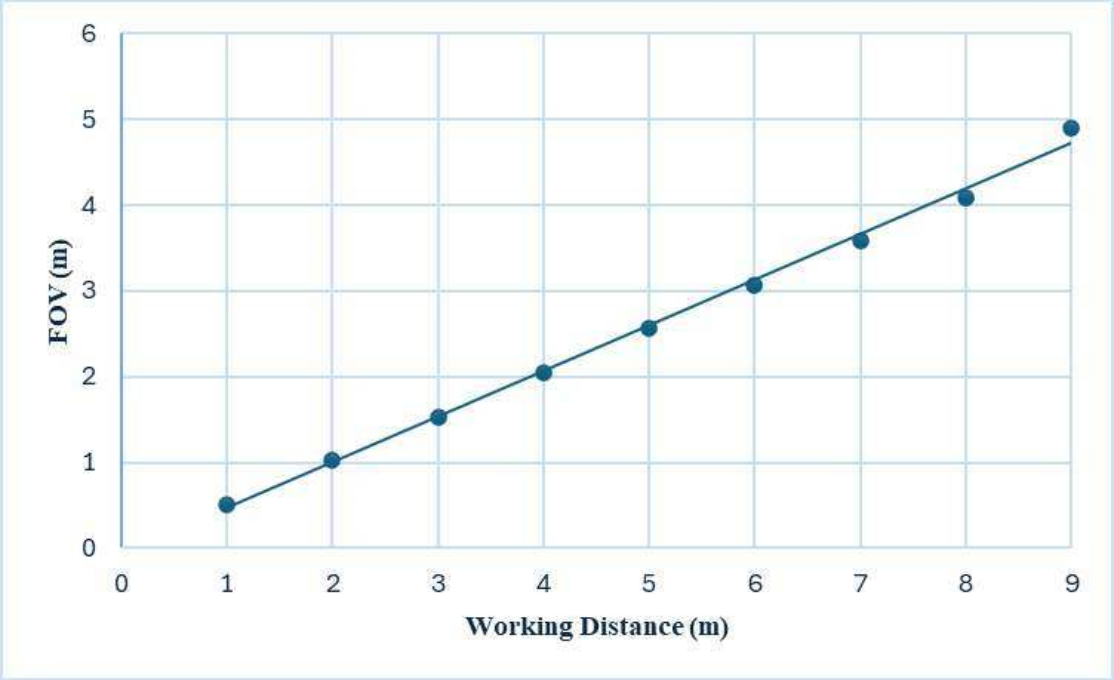

Figure 50: The Variation of Width with Respect to Working Distance

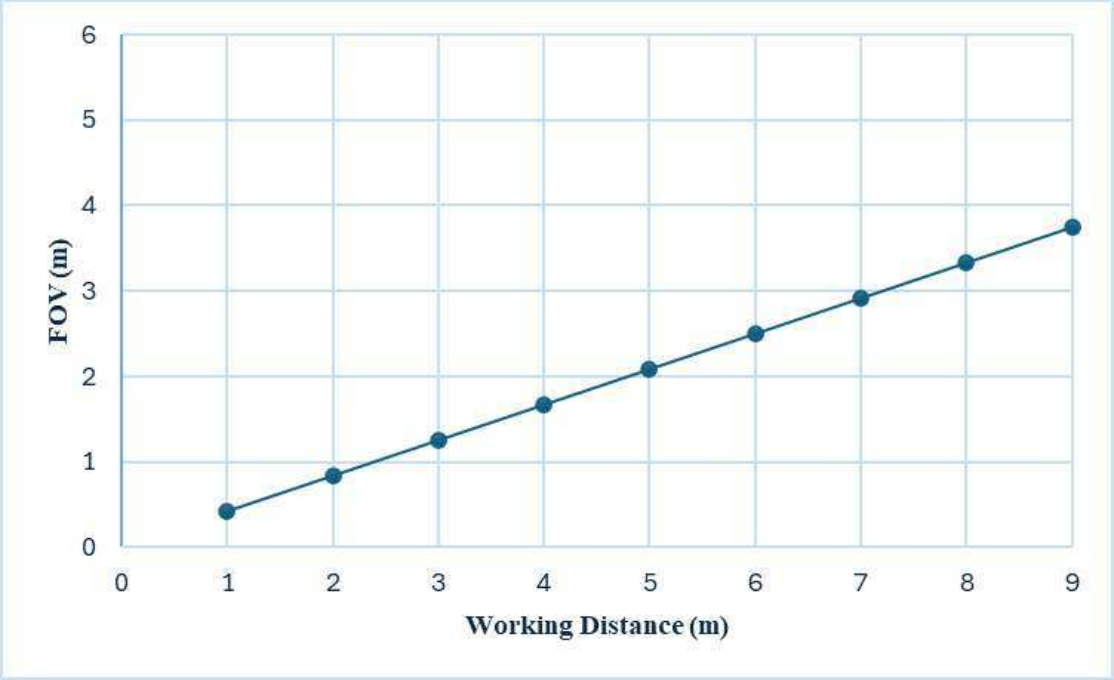

Figure 51: The Variation of Height with Respect to Working Distance

For example, once I choose the Field of View I want, I can refer to these curves to determine the working distance needed. This helps me figure out exactly where to position my tools to achieve the desired Field of View for accurate measurements.

By selecting either the width or height of the field of view, it becomes possible to determine the exact working distance for positioning the camera.

b) Noise Floor

In this experiment, the shaker remains stationary without any vibrations while the working distance is adjusted between 1 meter to 7 meters. To ensure reliable results, the data is filtered to reduce the influence of lighting conditions. The Root Mean Square (RMS) of the time-domain data is then calculated for both the width (x-axis) and the height (y-axis) to analyze the measurements accurately.

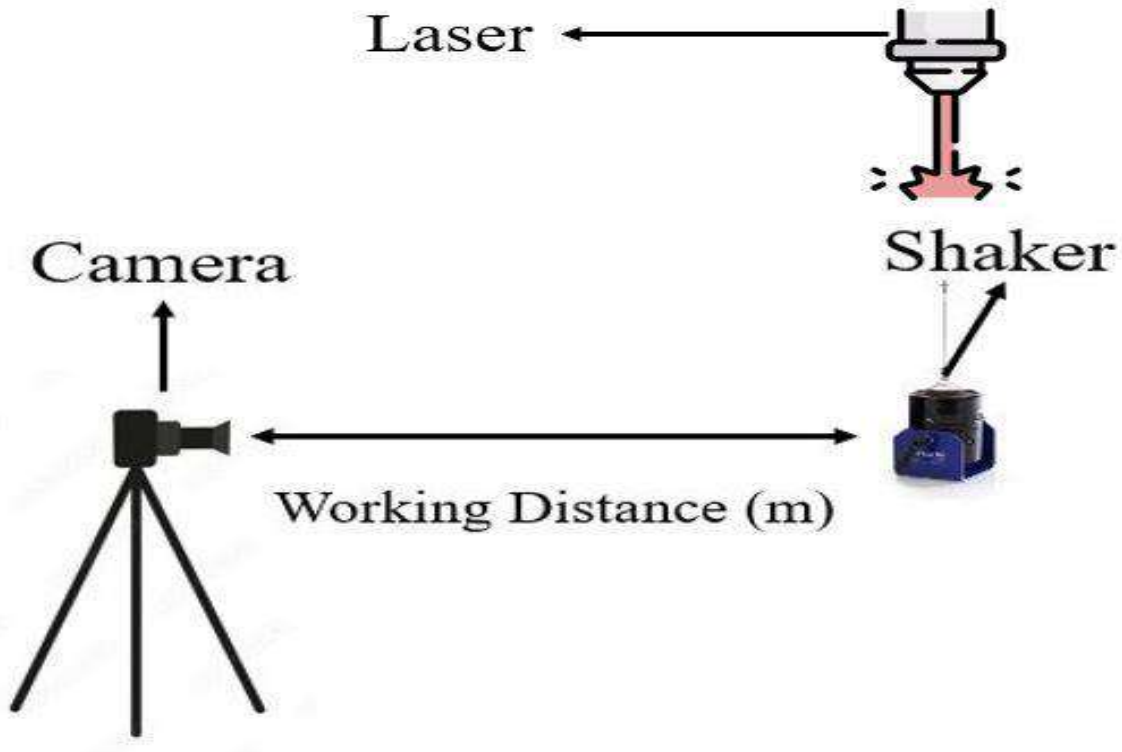

Figure 52: Setup of experiment 3

The working distance is changed from 1 to 7m.

The results have been filtered to eliminate the effect of light.

The Camera is focused on the cube placed at the top of the shaker as shown in the figure below:

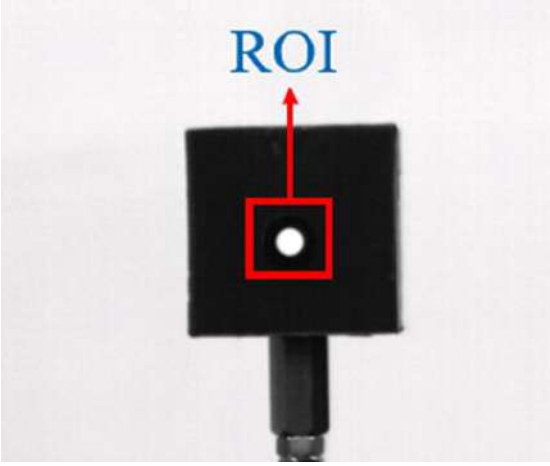

Figure 53: Region of Interest

The pictures below show the time-domain of the noise floor at 7 different working distances in 2 directions.

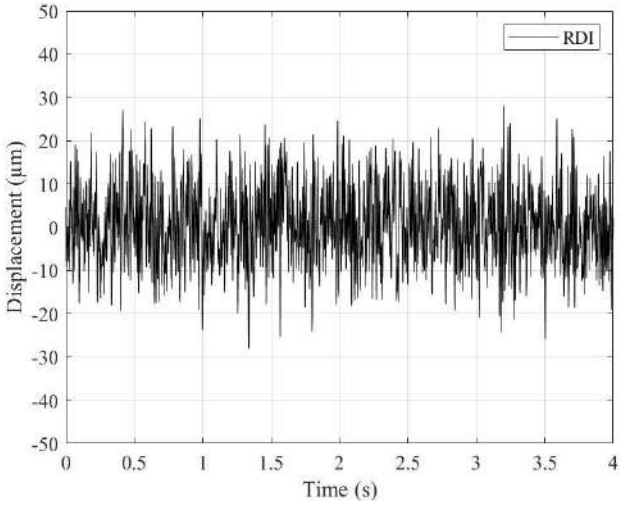

Figure 54:Time Domain for Noise Floor at Working Distance 1m in x Direction

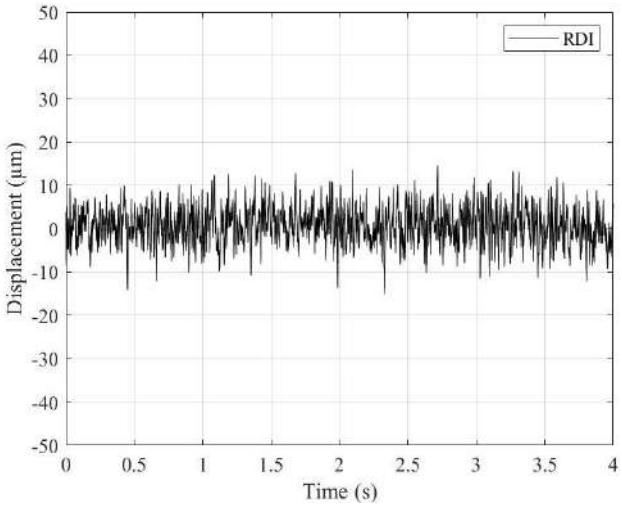

Figure 55:Time Domain for Noise Floor at Working Distance 1m in y Direction

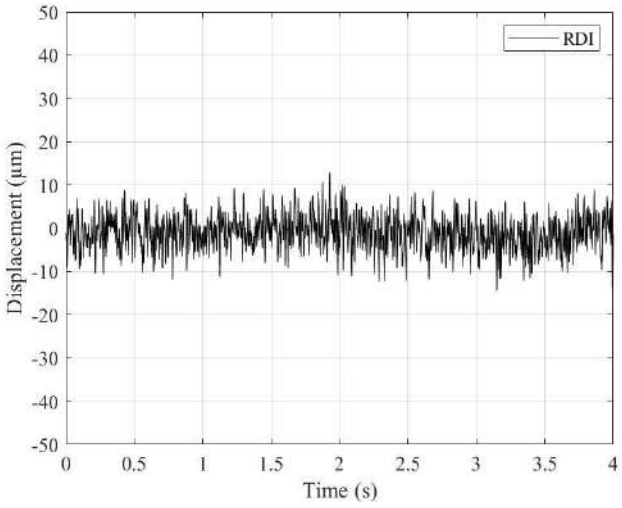

Figure 56:Time Domain for Noise Floor at Working Distance 2m in x Direction

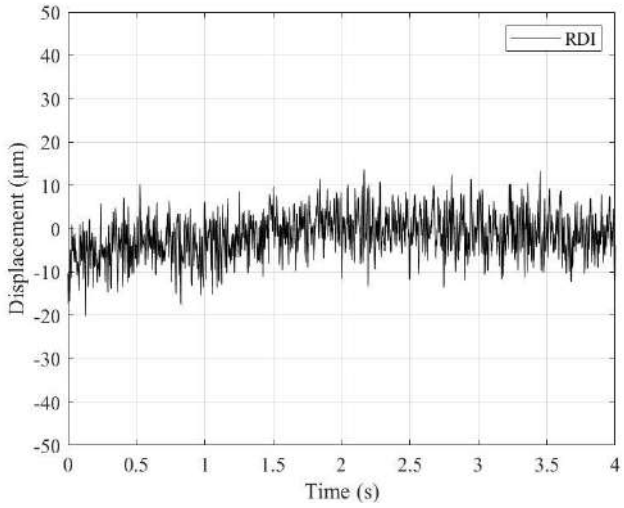

Figure 57:Time Domain for Noise Floor at Working Distance 2m in y Direction

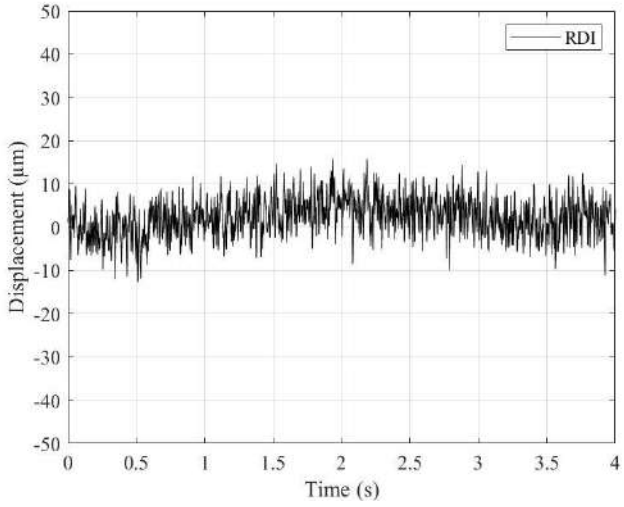

Figure 58:Time Domain for Noise Floor at Working Distance 3m in x Direction

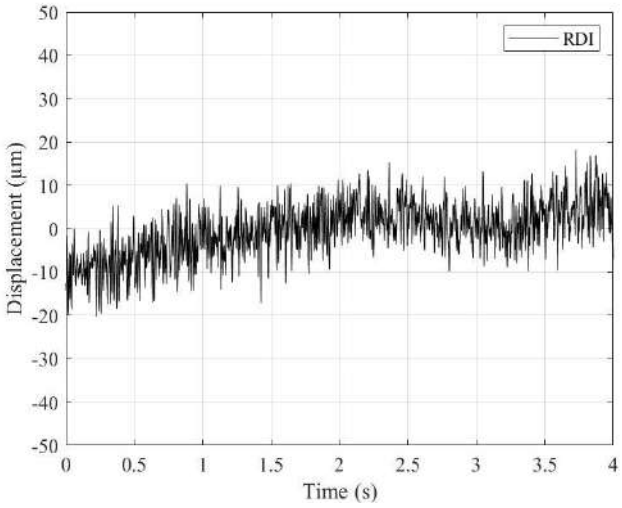

Figure 59: Time Domain for Noise Floor at Working Distance 3m in y Direction

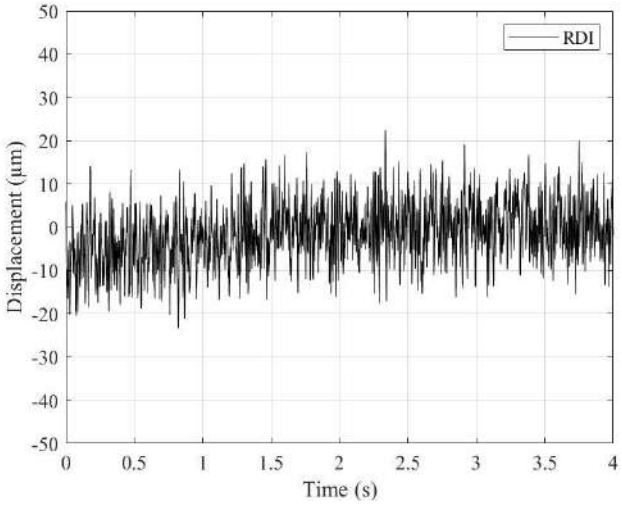

Figure 60:Time Domain for Noise Floor at Working Distance 4m in x Direction

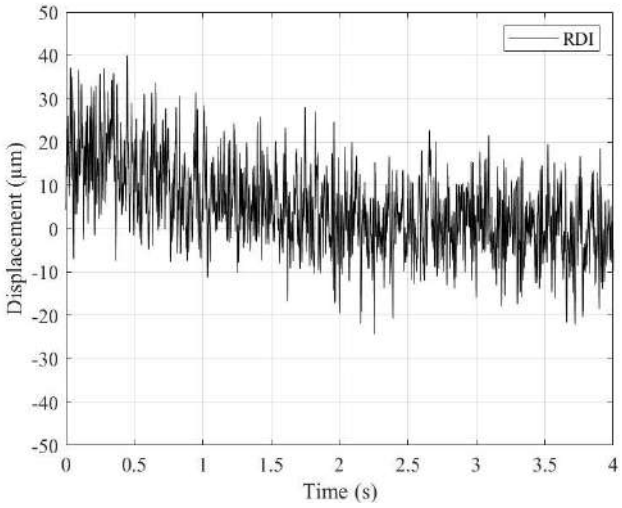

Figure 61:Time Domain for Noise Floor at Working Distance 4m in y Direction

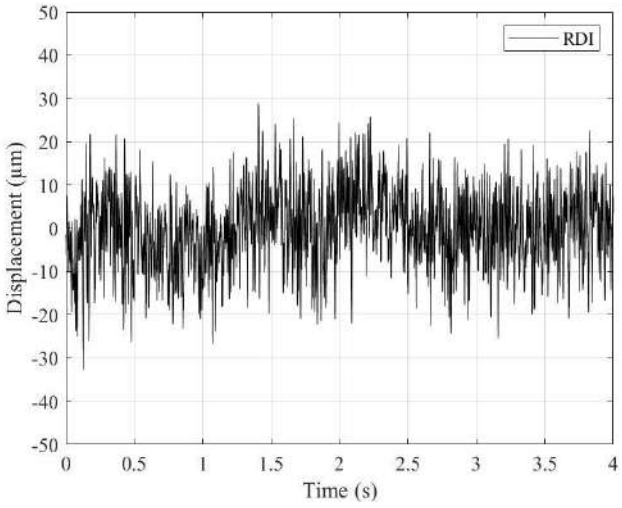

Figure 62:Time Domain for Noise Floor at Working Distance 5m in x Direction

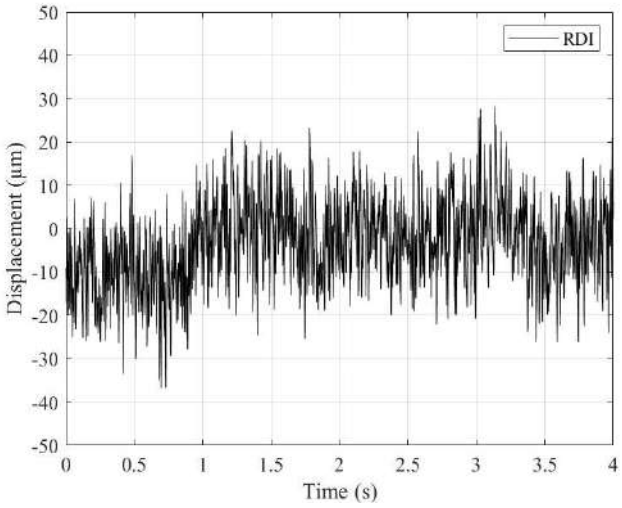

Figure 63:Time Domain for Noise Floor at Working Distance 5m in y Direction

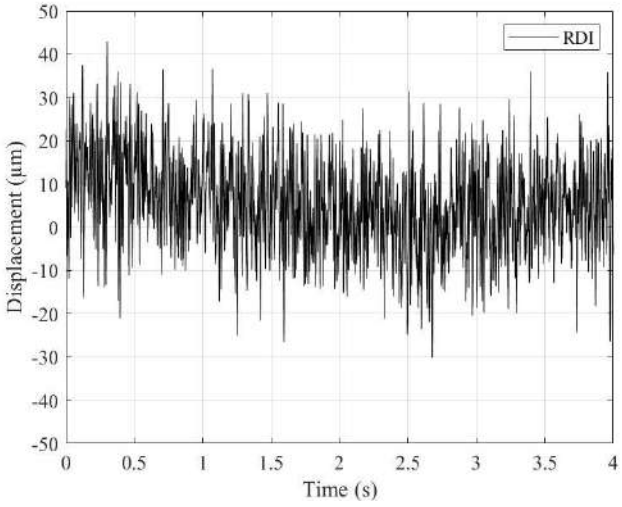

Figure 64:Time Domain for Noise Floor at Working Distance 6m in x Direction

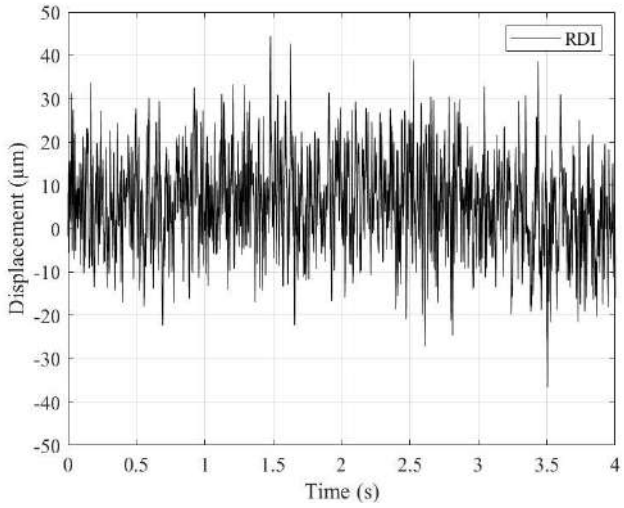

Figure 65:Time Domain for Noise Floor at Working Distance 6m in y Direction

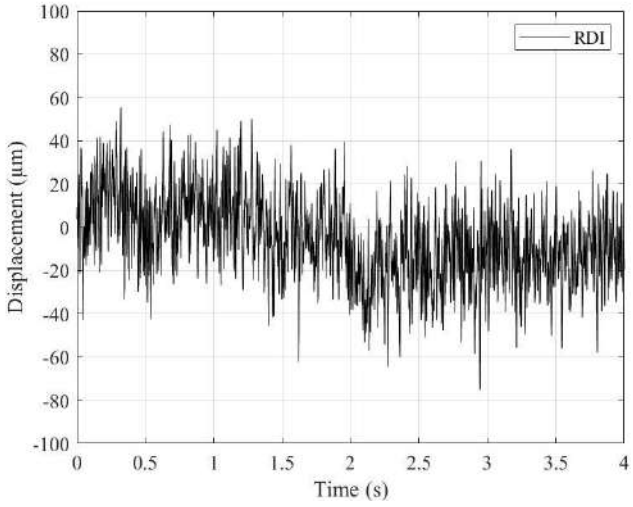

Figure 66:Time Domain for Noise Floor at Working Distance 7m in x Direction

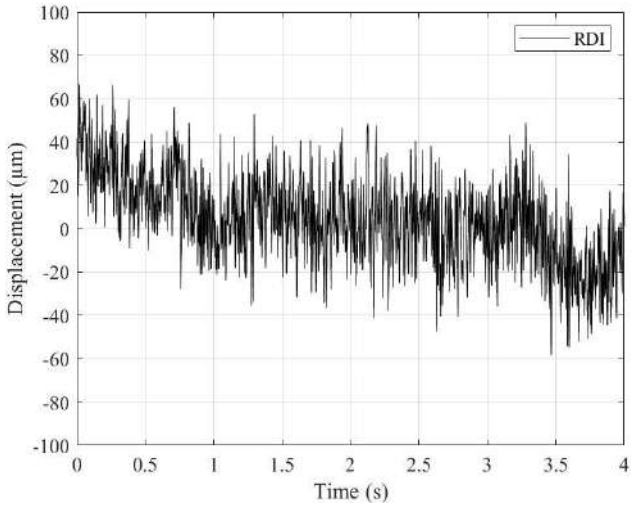

Figure 67:Time Domain for Noise Floor at Working Distance 7m in y Direction

Then, we calculate the RMS in both directions.

	Noise Floor µm	
Working Distance m	X-direction	Y-direction
1	4.20	5.23
2	4.76	11.38
3	5.22	13.74
4	7.79	15.74
5	11.58	16.01
6	13.58	23.88
7	19.17	38.39

Table 2: Results of RMS in x and y Direction

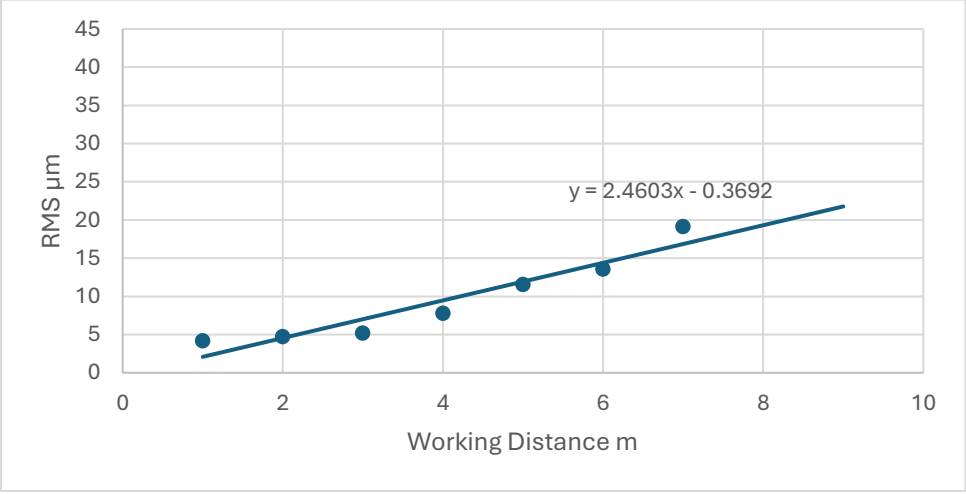

Figure 68:This Curve Shows the Relationship Between Working Distance and RMS in x Direction

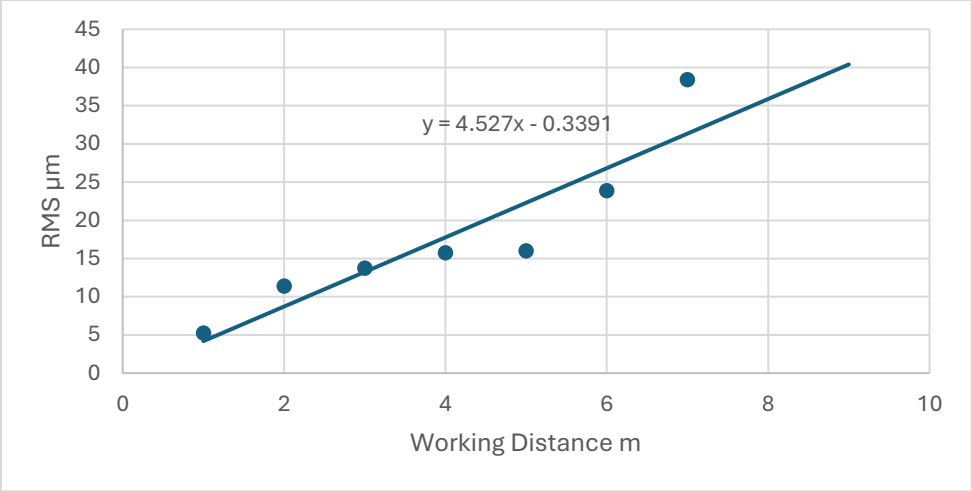

Figure 69:This Curve Shows the Relationship Between Working Distance and RMS in y Direction

As expected, the results indicate that the noise floor increases with increasing working distance.

Further tests have taken, data was collected at working distances ranging from 1 to 7 meters, with three samples taken at each distance to ensure consistency. The shaker operated at a vibration frequency of 2-3 Hz, maintaining an RMS value above the noise floor. The results were then compared with measurements obtained from a laser-based device to evaluate accuracy and reliability. To check how the increase of noise floor will affect the accuracy and consistency, the experiment's main goal was to align the signals from the two measuring devices and produce the Time Response Amplitude Curve (TRAC) and Frequency Response Amplitude Curve (FRAC).

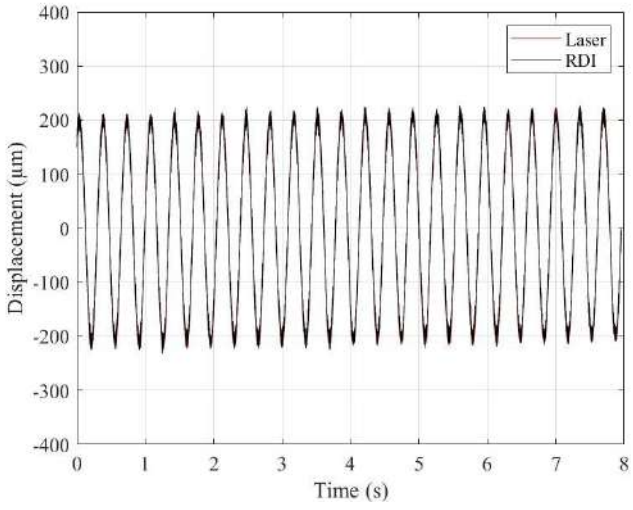

Figure 70:Time Domain at Working Distance 1m Sample 1

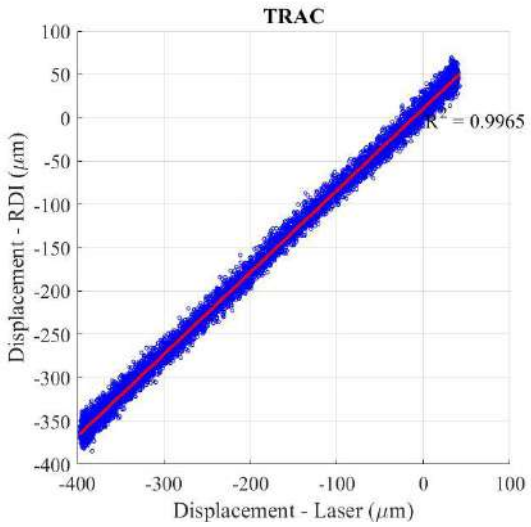

Figure 71: Time Response Amplitude Curve at Working Distance 1m Sample 1

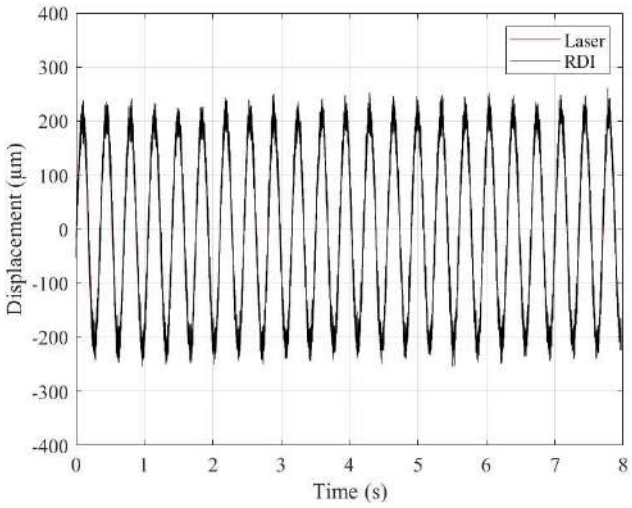

Figure 72:Time Domain at Working Distance 1m Sample 2

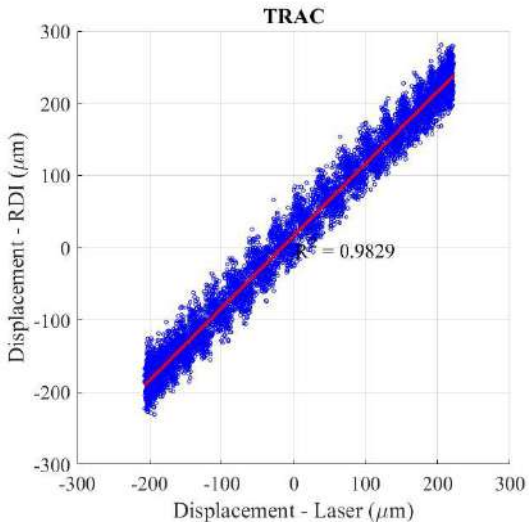

Figure 73:Time Response Amplitude Curve at Working Distance 1m Sample 2

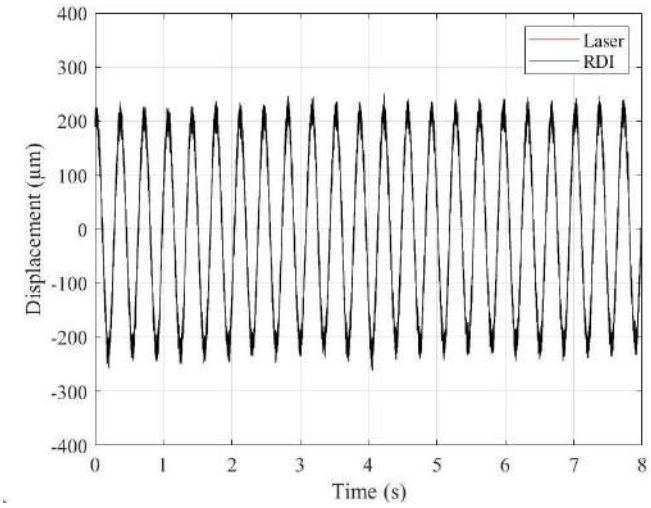

Figure 74:Time Domain at Working Distance 1m Sample 3

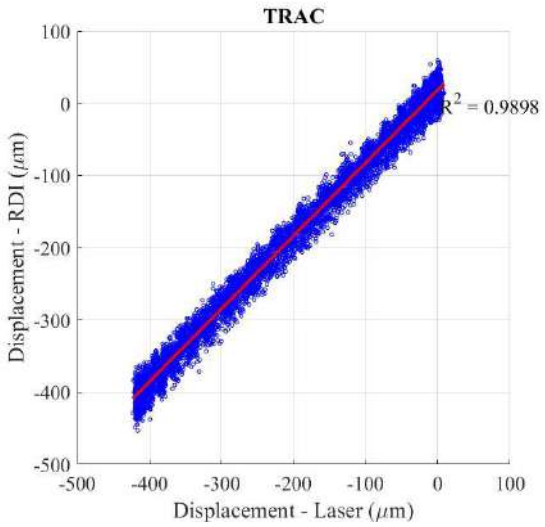

Figure 75:Time Response Amplitude Curve at Working Distance 1m Sample 3

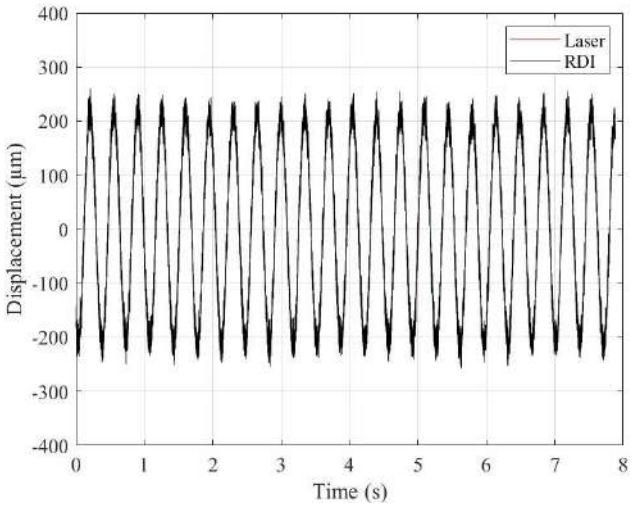

Figure 76:Time Domain at Working Distance 2m Sample 1

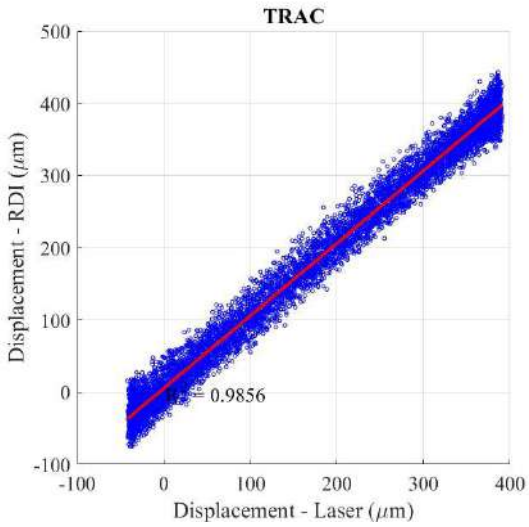

Figure 77:Time Response Amplitude Curve at Working Distance 2m Sample 1

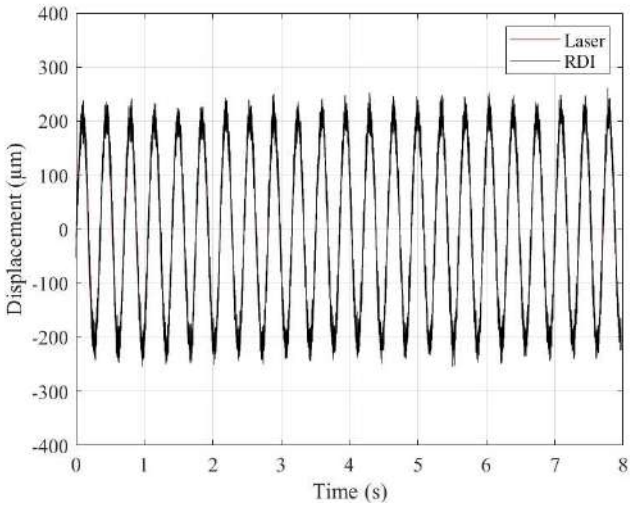

Figure 78:Time Domain at Working Distance 2m Sample 2

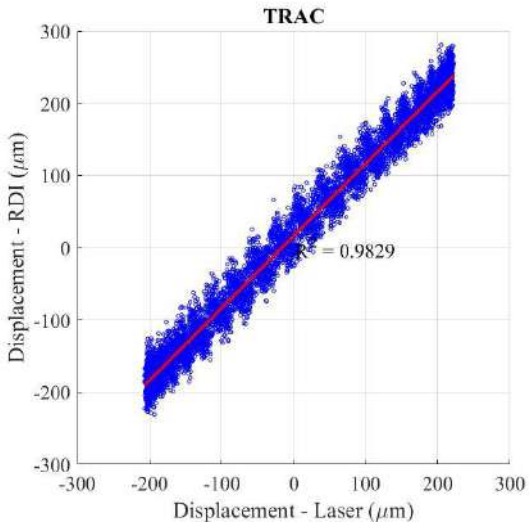

Figure 79:Time Response Amplitude Curve at Working Distance 2m Sample 2

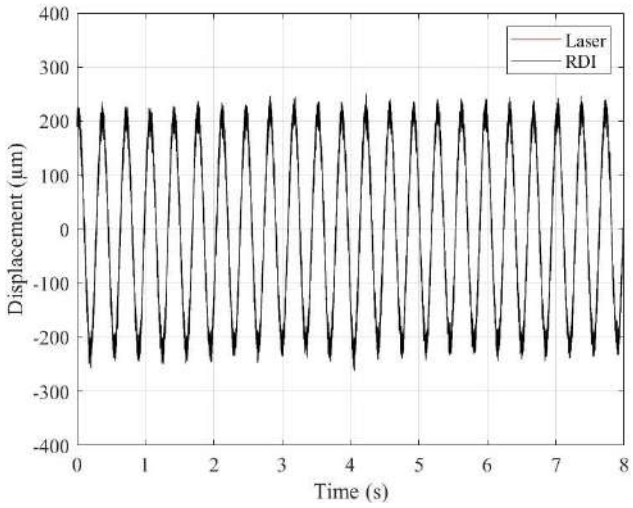

Figure 80:Time Domain at Working Distance 2m Sample 3

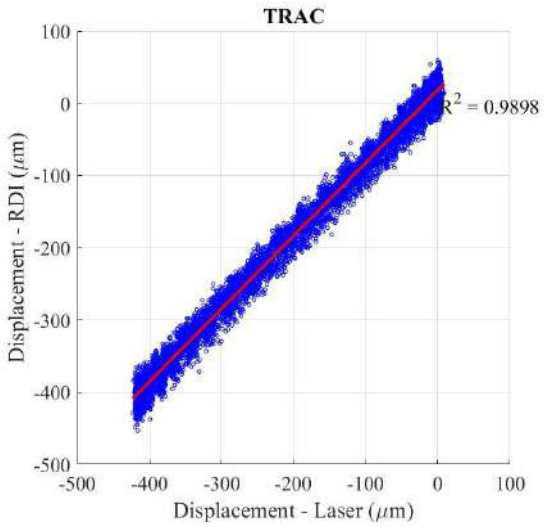

Figure 81:Time Response Amplitude Curve at Working Distance 2m Sample 3

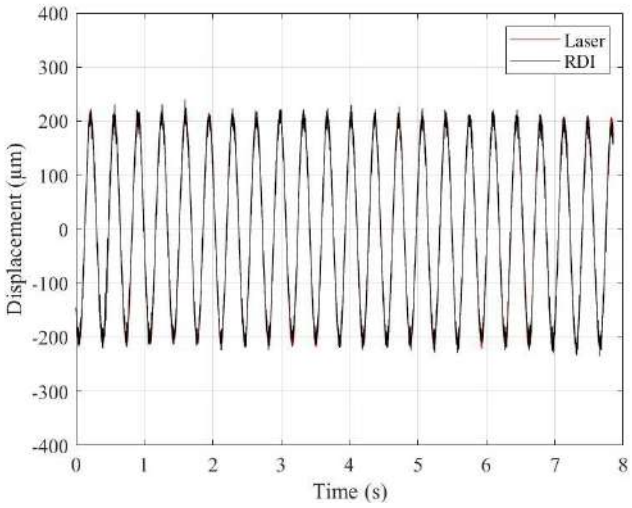

Figure 82:Time Domain at Working Distance 3m Sample 1

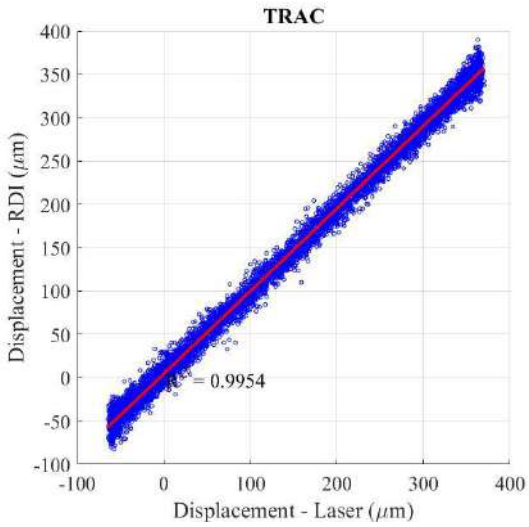

Figure 83:Time Response Amplitude Curve at Working Distance 3m Sample 1

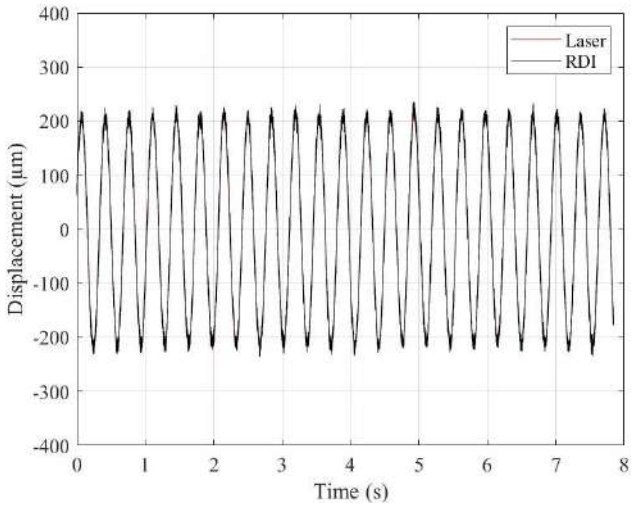

Figure 84:Time Domain at Working Distance 3m Sample 2

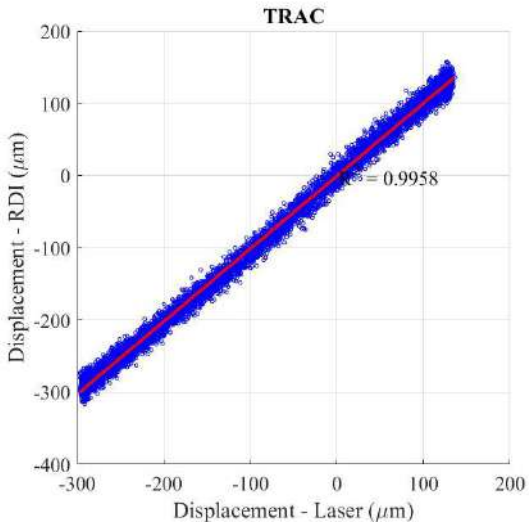

Figure 85:Time Response Amplitude Curve at Working Distance 3m Sample 2

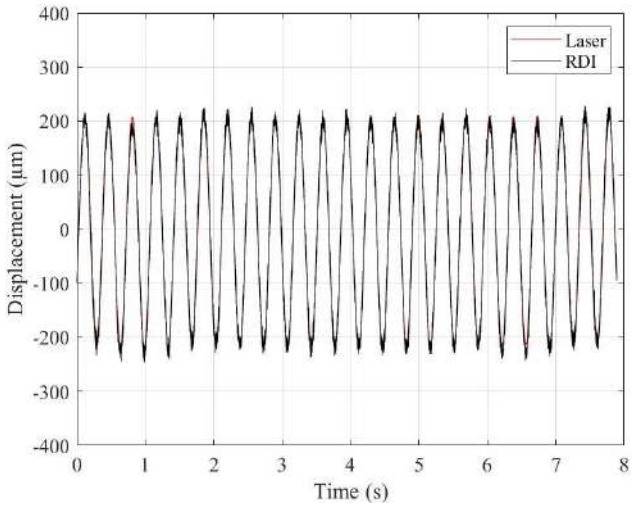

Figure 86:Time Domain at Working Distance 3m Sample 3

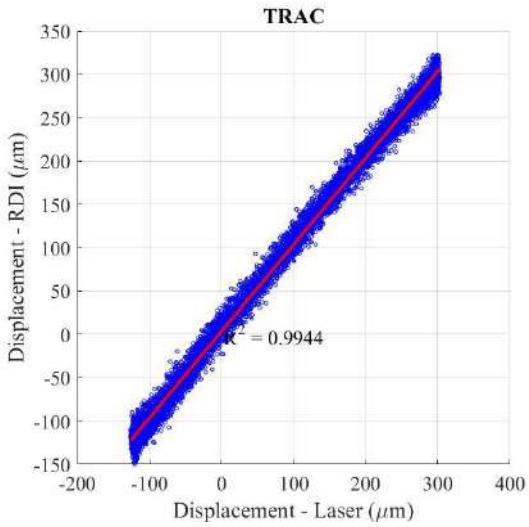

Figure 87:Time Response Amplitude Curve at Working Distance 3m Sample 3

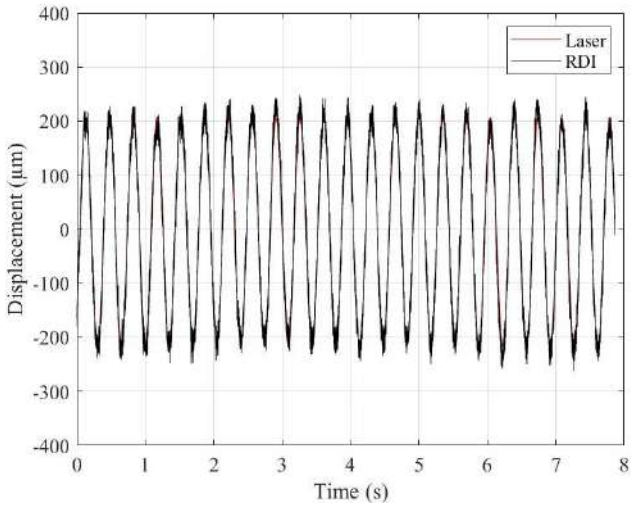

Figure 88:Time Domain at Working Distance 4m Sample 1

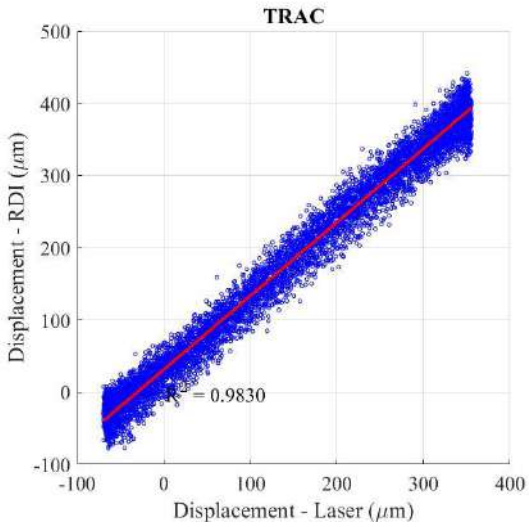

Figure 89:Time Response Amplitude Curve at Working Distance 4m Sample 1

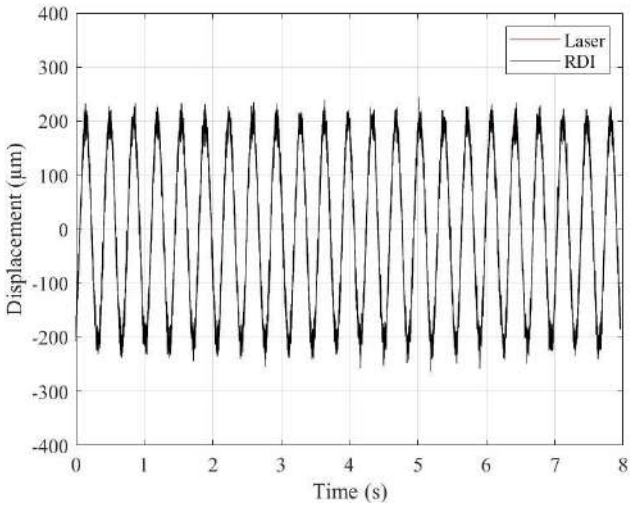

Figure 90:Time Domain at Working Distance 4m Sample 2

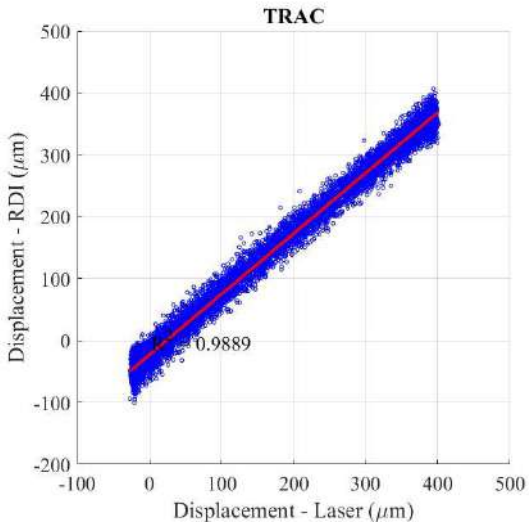

Figure 91:Time Response Amplitude Curve at Working Distance 4m Sample 2

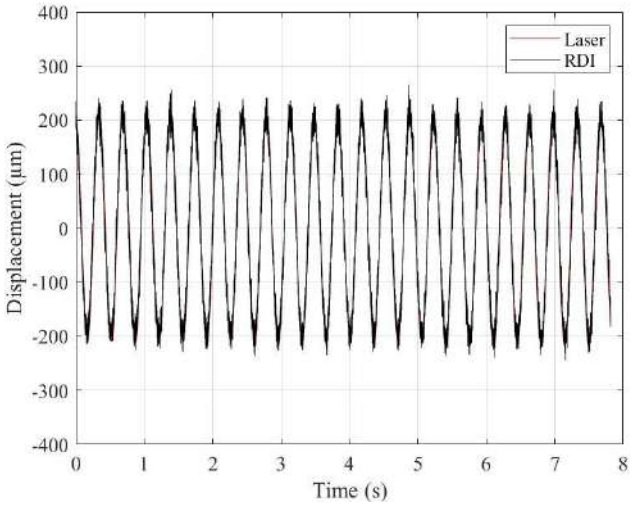

Figure 92:Time Domain at Working Distance 4m Sample 3

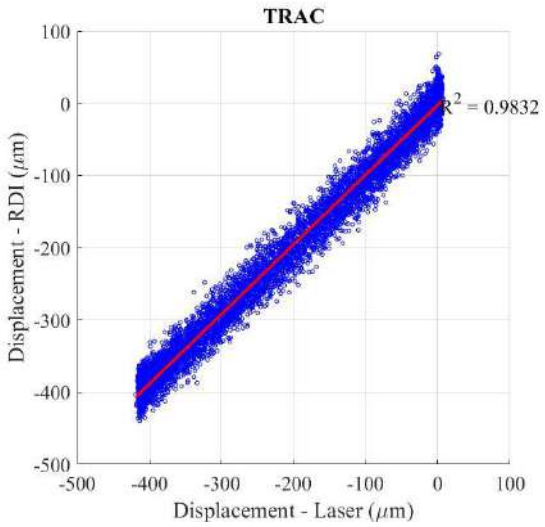

Figure 93:Time Response Amplitude Curve at Working Distance 4m Sample 3

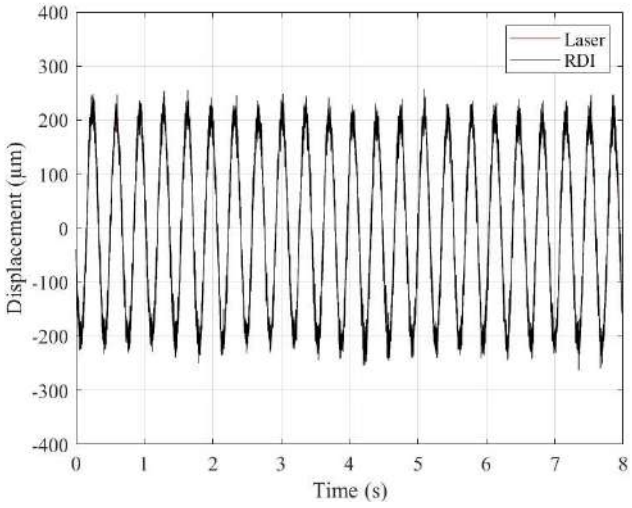

Figure 94:Time Domain at Working Distance 5m Sample 1

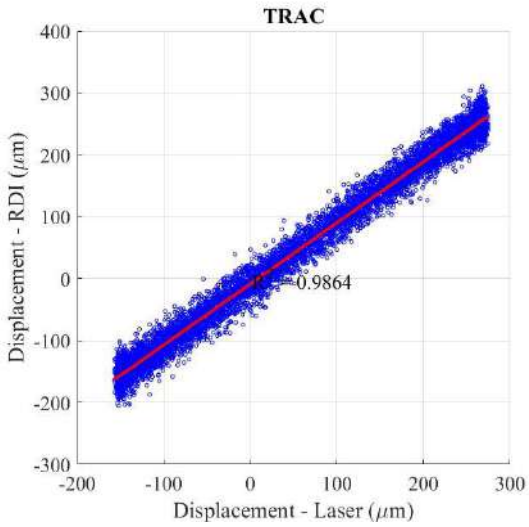

Figure 95:Time Response Amplitude Curve at Working Distance 5m Sample 1

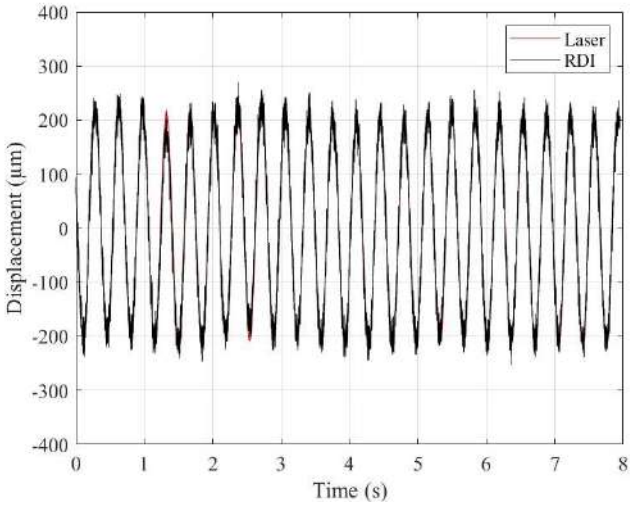

Figure 96:Time Domain at Working Distance 5m Sample 2

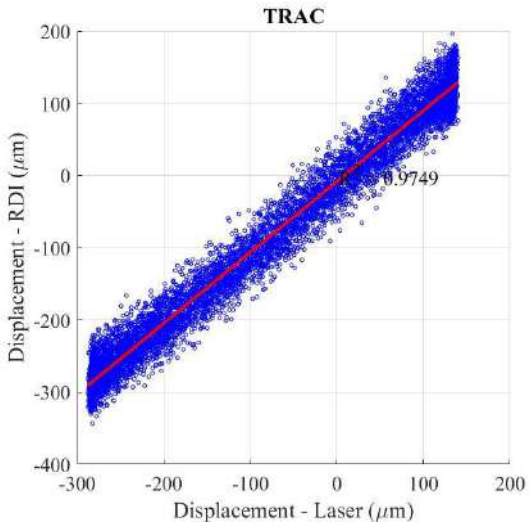

Figure 97:Time Response Amplitude Curve at Working Distance 5m Sample 2

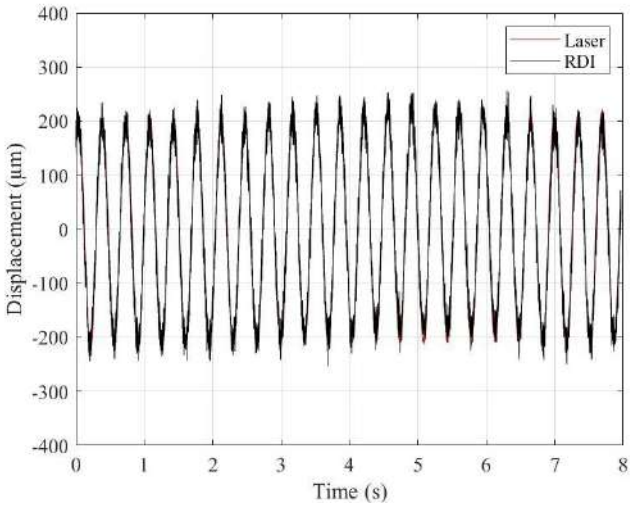

Figure 98:Time Domain at Working Distance 5m Sample 3

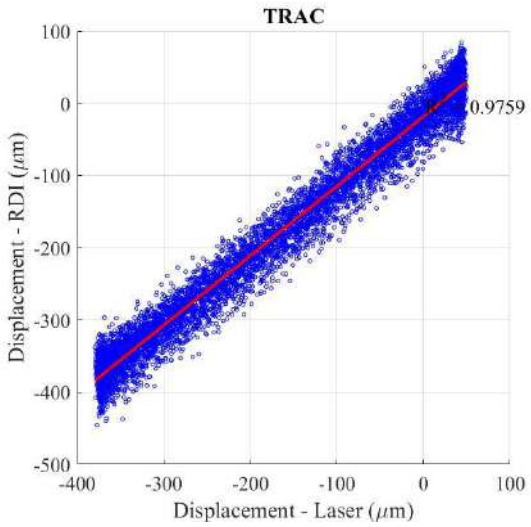

Figure 99:Time Response Amplitude Curve at Working Distance 5m Sample 3

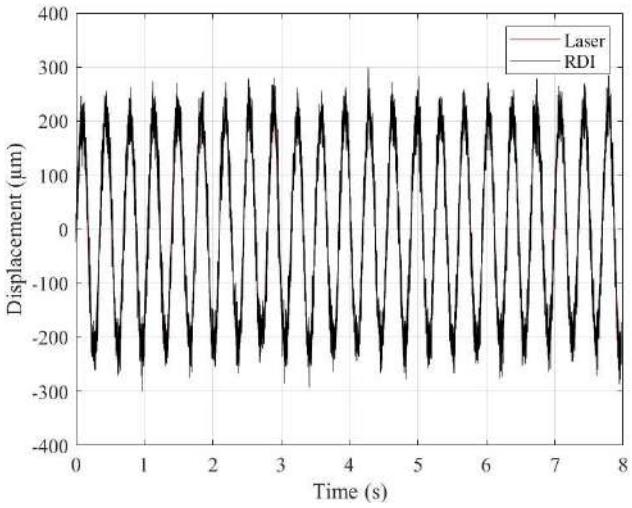

Figure 100:Time Domain at Working Distance 6m Sample 1

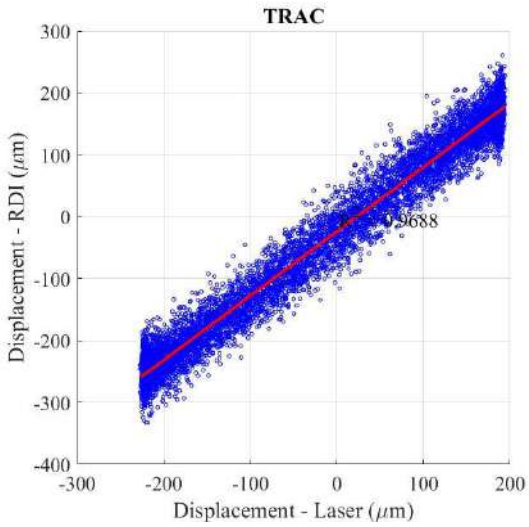

Figure 101:Time Response Amplitude Curve at Working Distance 6m Sample 1

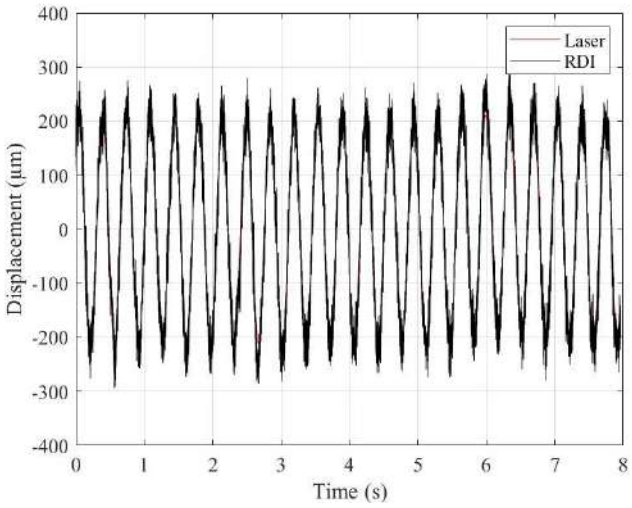

Figure 102:Time Domain at Working Distance 6m Sample 2

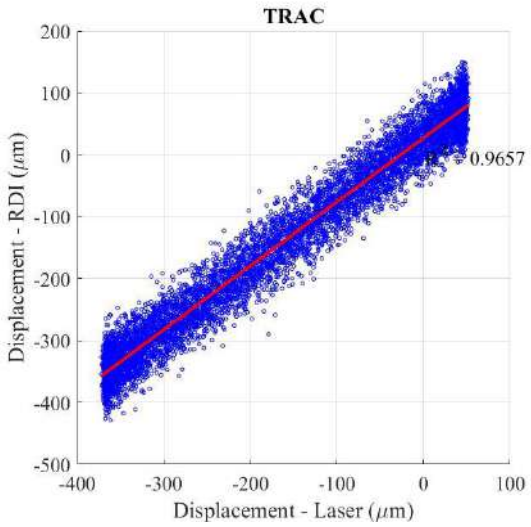

Figure 103:Time Response Amplitude Curve at Working Distance 6m Sample 2

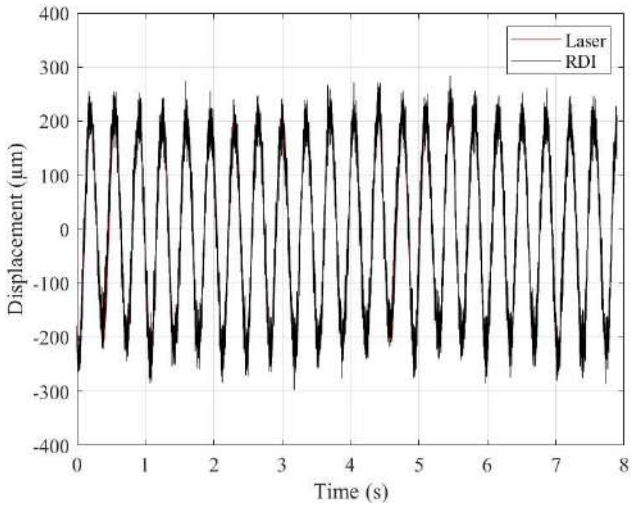

Figure 104:Time Domain at Working Distance 6m Sample 3

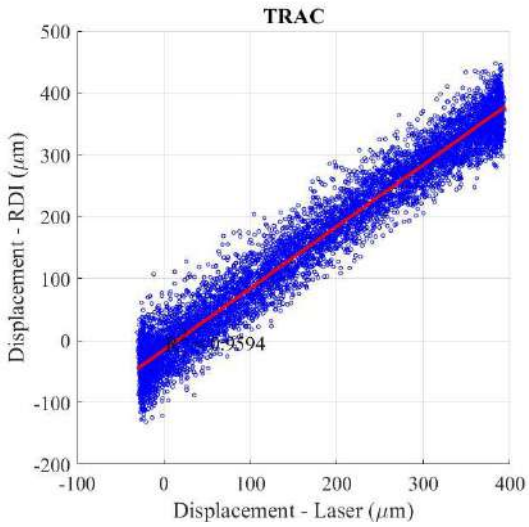

Figure 105:Time Response Amplitude Curve at Working Distance 6m Sample 3

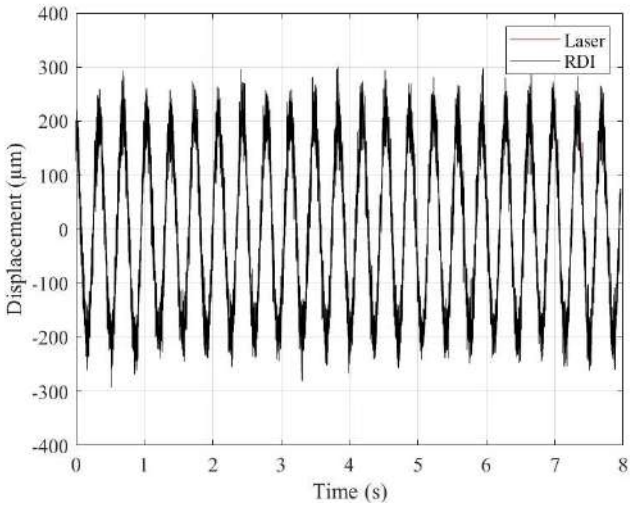

Figure 106:Time Domain at Working Distance 7m Sample 1

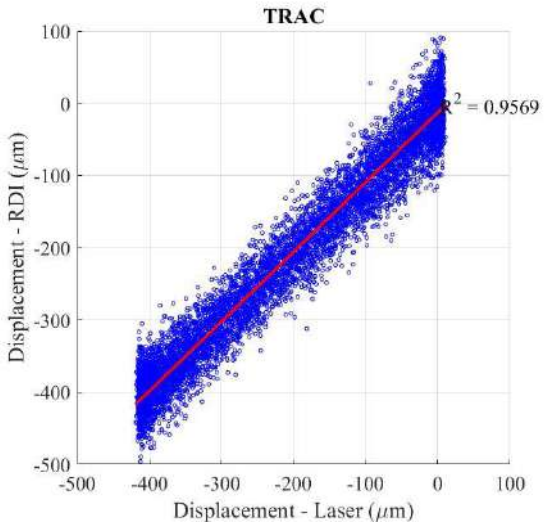

Figure 107:Time Response Amplitude Curve at Working Distance 7m Sample 1

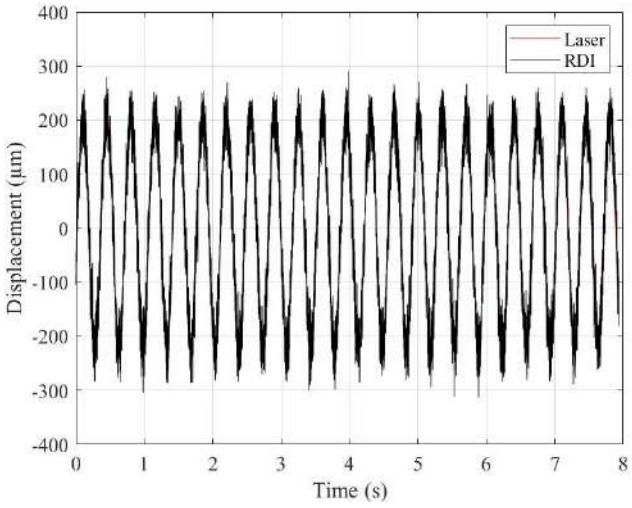

Figure 108:Time Domain at Working Distance 7m Sample 2

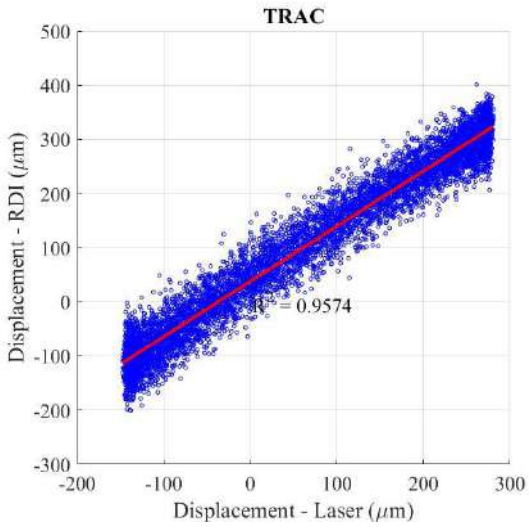

Figure 109:Time Response Amplitude Curve at Working Distance 7m Sample 2

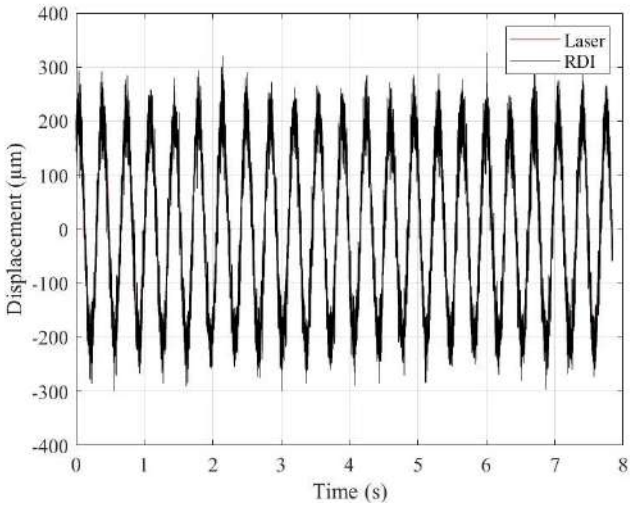

Figure 110:Time Domain at Working Distance 7m Sample 3

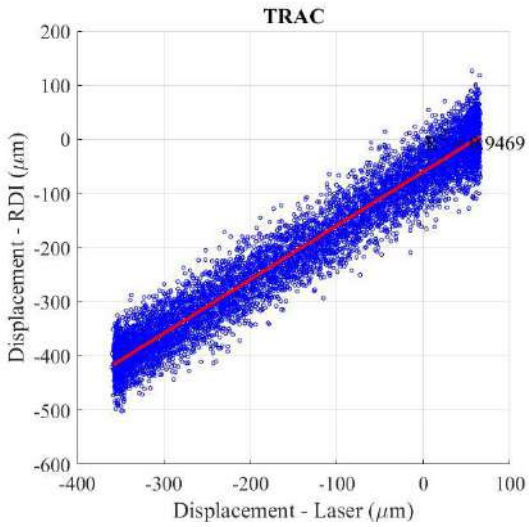

Figure 111:Time Response Amplitude Curve at Working Distance 7m Sample 3

The results shown above demonstrate that the spread of the blue data points increases with greater working distances, indicating a decline in measurement accuracy.

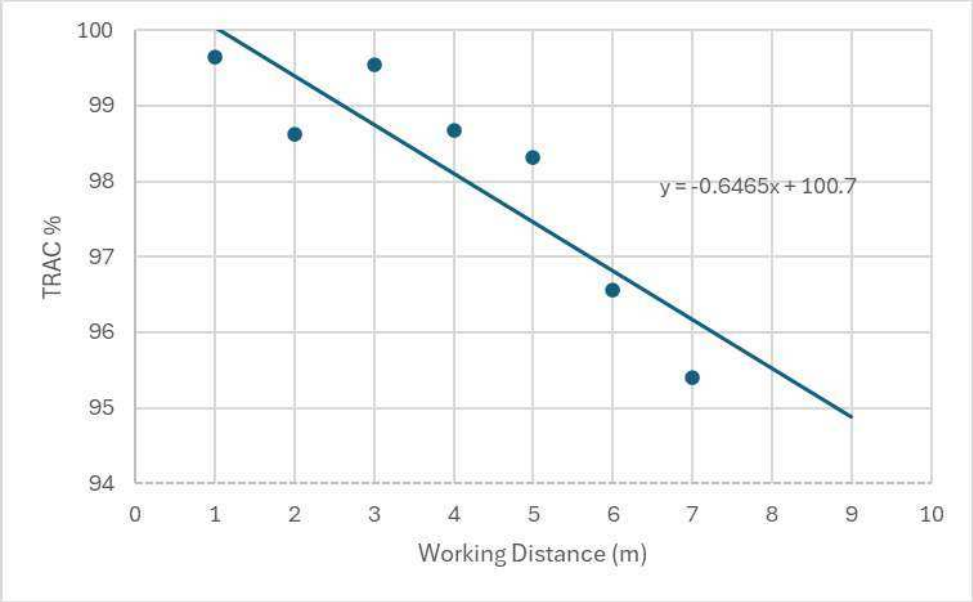

Figure 112: This Curve Show the Variation of TRAC% with Respect to Working Distance

c) Conclusion

If the intended field of view is known, Figure 60 and 61 can be used to calculate the necessary working distance for camera placement. Then, figures 78 and 79 can be used to calculate the relevant noise floor, and figure 101 is used to determine the percentage of accuracy.

VI. Field Test

The test has been taking place on an 8.65 MW Francis turbine in the Boott Hydropower plant in Lowell town, Massachusetts state, United state of America.

Figure 113: Location of the Hydropower Plant

Characteristics of the turbine:

- Head = 11.89 m (39ft)
- Speed = 120rpm (2 Hz)
- Manufacture = Fuji Electric

Figure 114: Top View of the Hydropower Turbine

Figure 115: Side View of the Hydropower Turbine

Our examination centers on two primary components: Shaft 1 and Shaft 2.

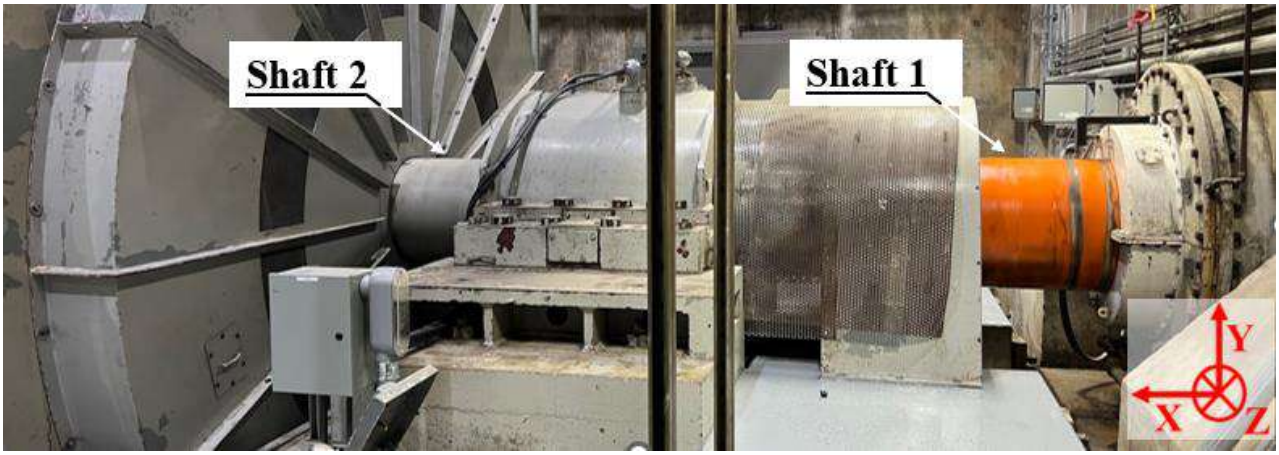

Figure 116:Identification of the two analyzed regions and reference system.

In this test, we compared the performance of a preinstalled proximity on the shafts with both RDI software and laser displacement sensor.

For shaft 1, the comparison between proximity probe and RDI was conducted in Y-direction, while the comparison between proximity probe and the laser displacement sensor was carried out in Z-direction.

For shaft 2, the comparison between proximity probe and RDI was conducted in Y-direction, while there is no comparison in Z-direction for impossibility to place the laser displacement sensor.

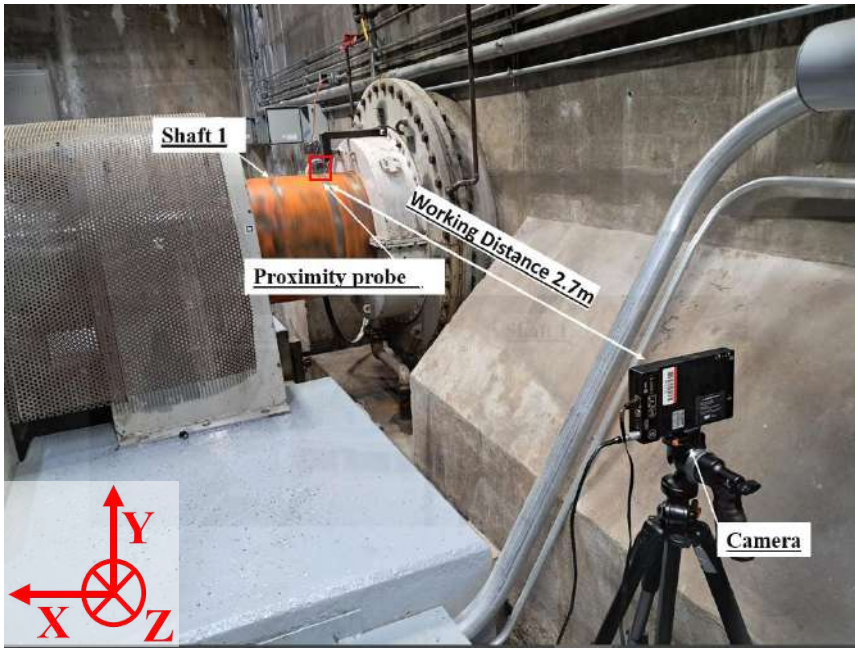

Figure 117: Experiment Setup for Shaft 1 in Y-Direction

Working distance is 2.7m so the noise floor in Y-direction for shaft 1 is 11.88µm we can capture any movement above this value.

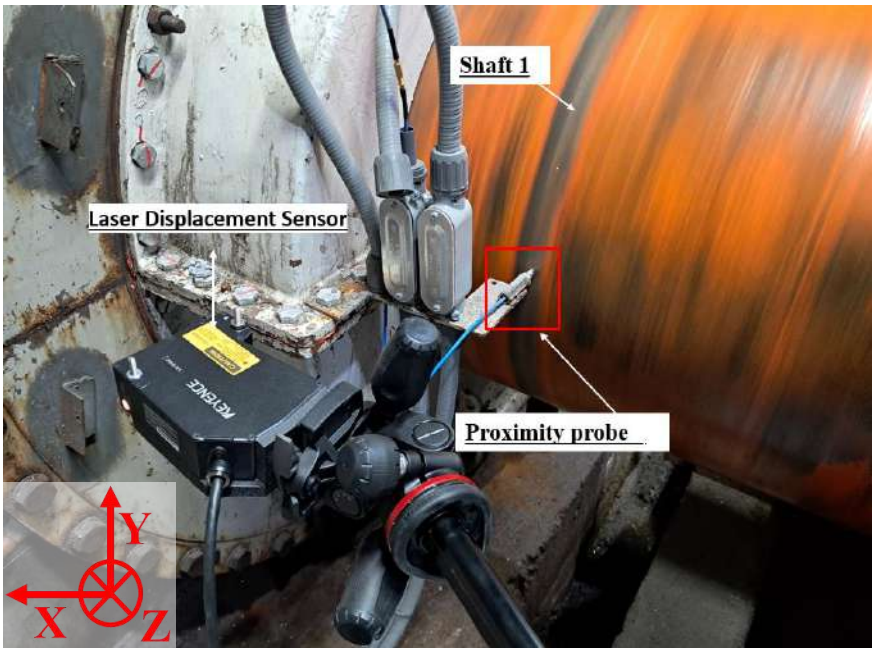

Figure 118: Experiment Setup for shaft 1 in Z-Direction

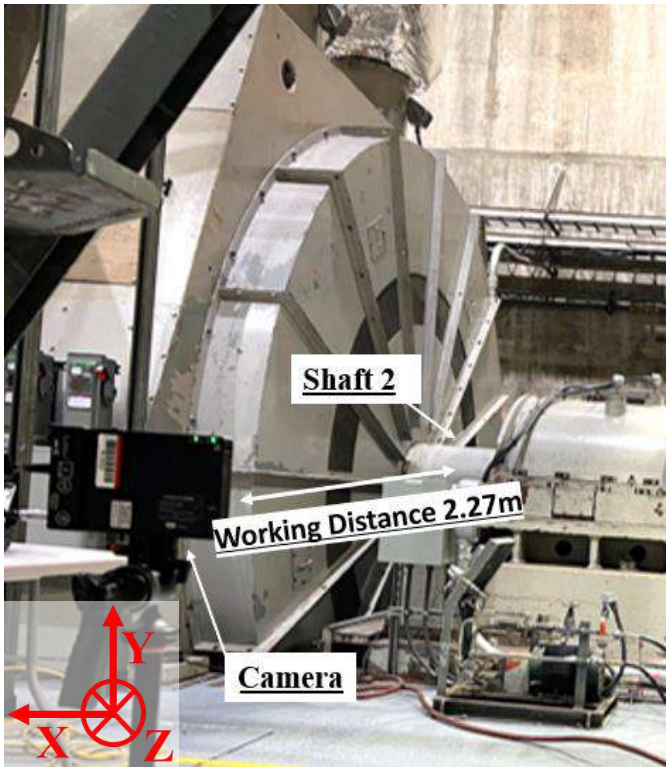

Figure 119: Experiment Setup for Shaft 2 in Y-Direction

Working distance is 2.27m so the noise floor in Y-direction for shaft 1 is 9.94µm we can capture any movement above this value.

Sensor characteristics:

- 5mega pixel Iris MX camera operating at 125 fps.
- Keyence LK-G402 laser displacement sensor operates at 1,000 Hz.

We plotted the time-domain data from the laser and the RDI, computed the peak-to-peak values for each cycle, and then calculated the average and standard deviation because the proximity probe delivers peak-to-peak values. These outcomes were compared with the proximity probe's readings. Two measurements were made to allow statistical analysis.

1. Shaft 1

In shaft 1 we examined the shaft in two directions Y-direction and Z-direction.

a) Y-direction

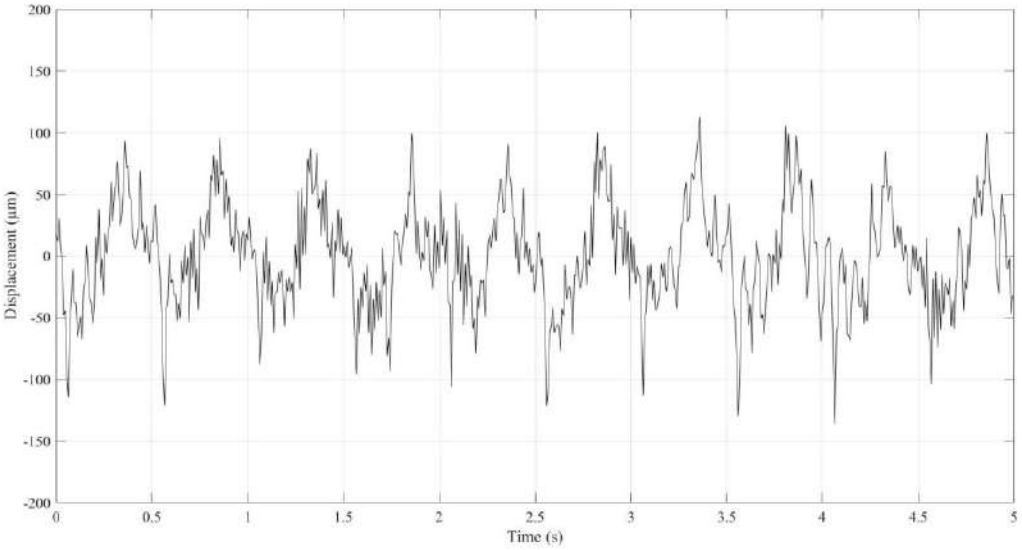

Figure 120: Time Domain Sample 1

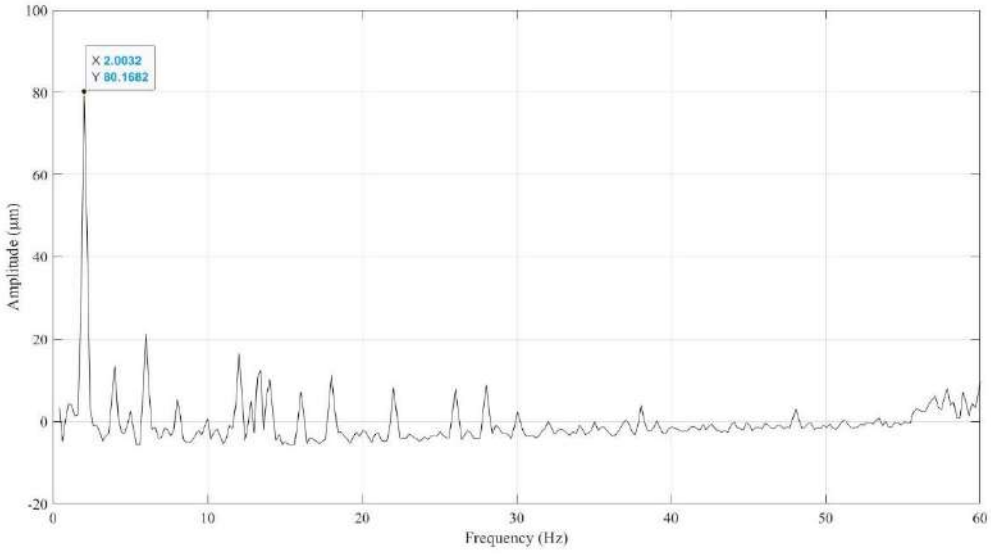

Figure 121:Frequency Domain Sample 1

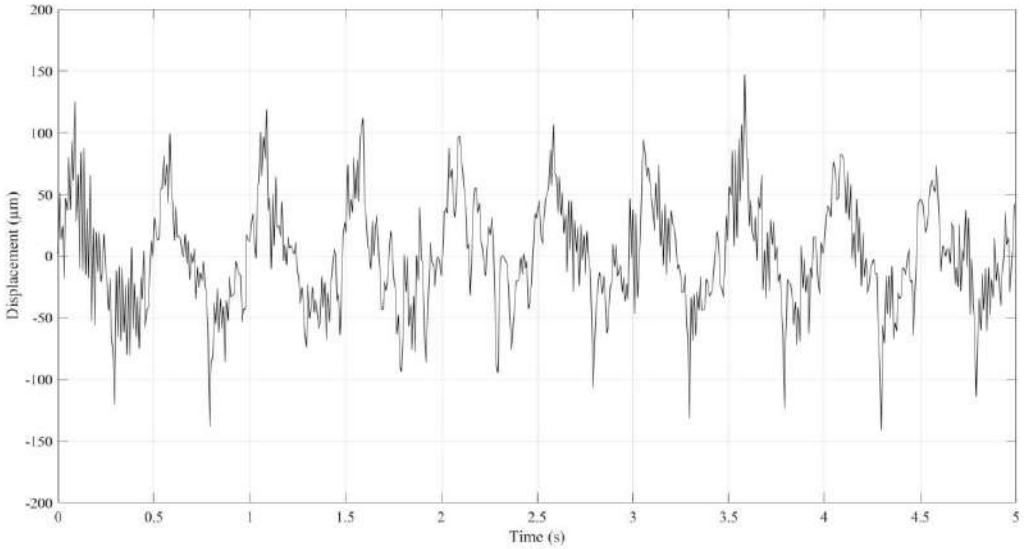

Figure 122:Time Domain Sample 2

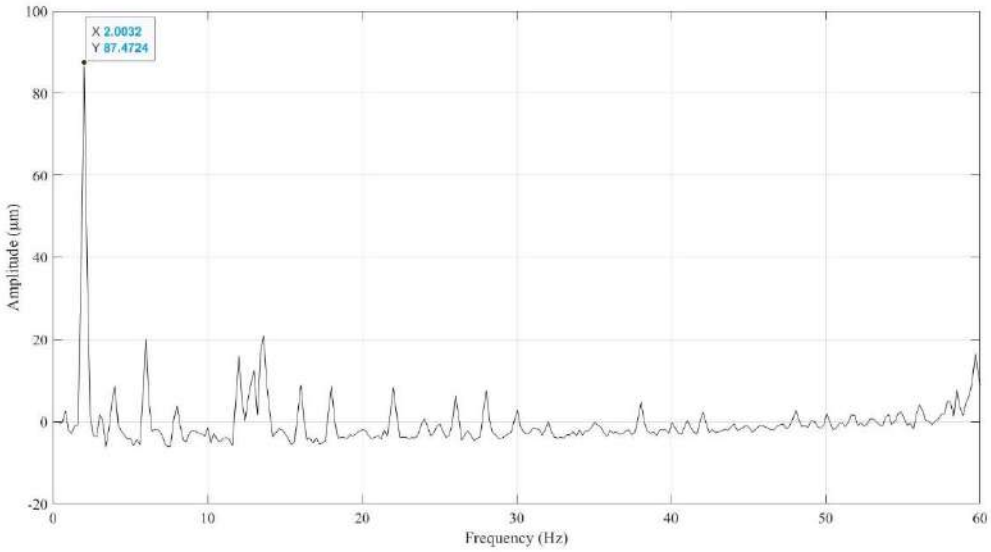

Figure 123: Frequency Domain Sample 2

Then we calculate Peak-to-Peak from the time domain for each cycle, then get the average and the standard deviation. Then compared the results with proximity probe.

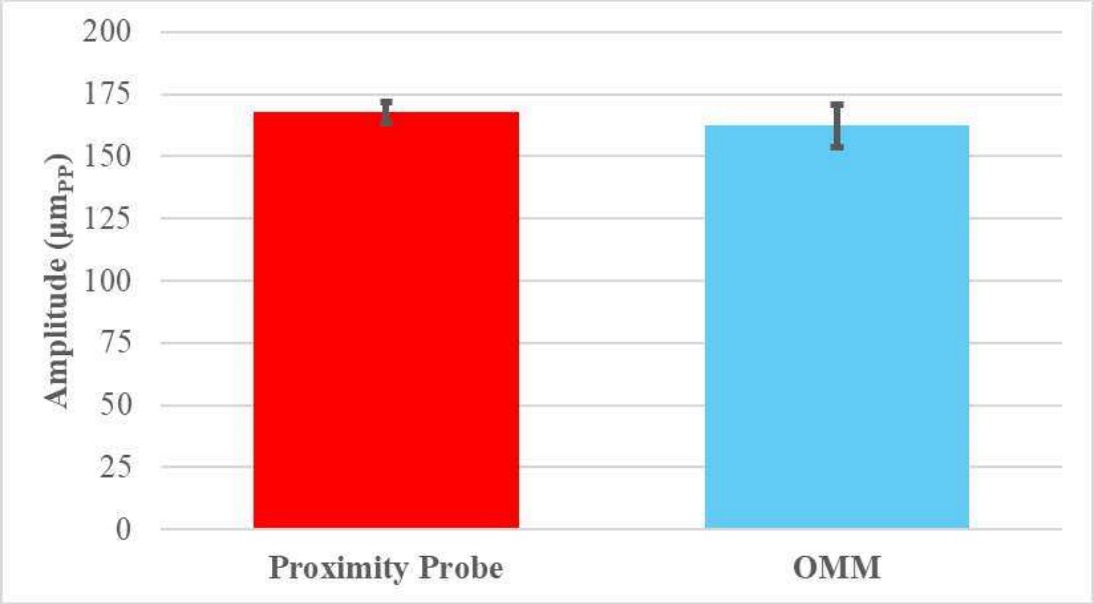

Figure 124:Results Comparison for shaft 1 in Y-Direction.

b) Z-direction

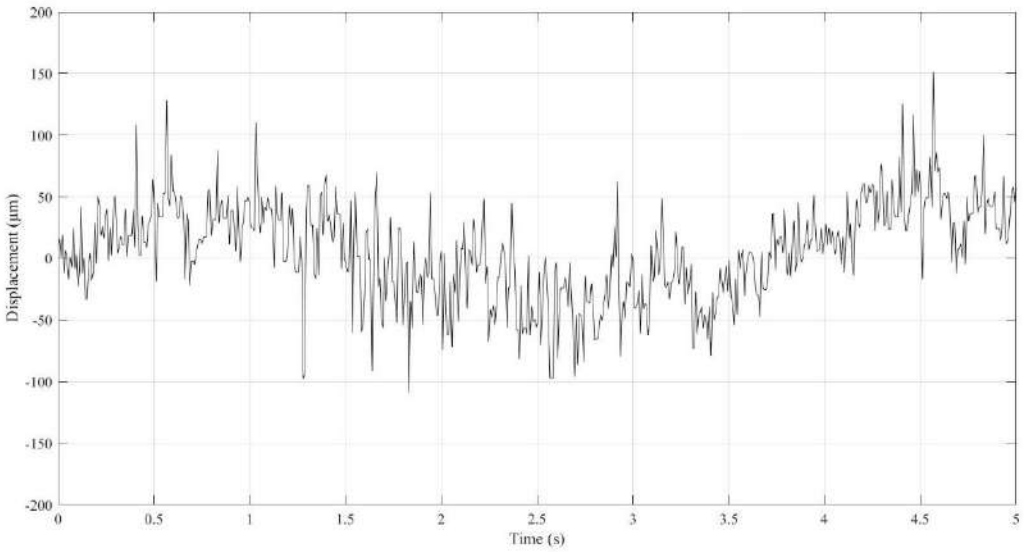

Figure 125: Time Domain Sample 1.

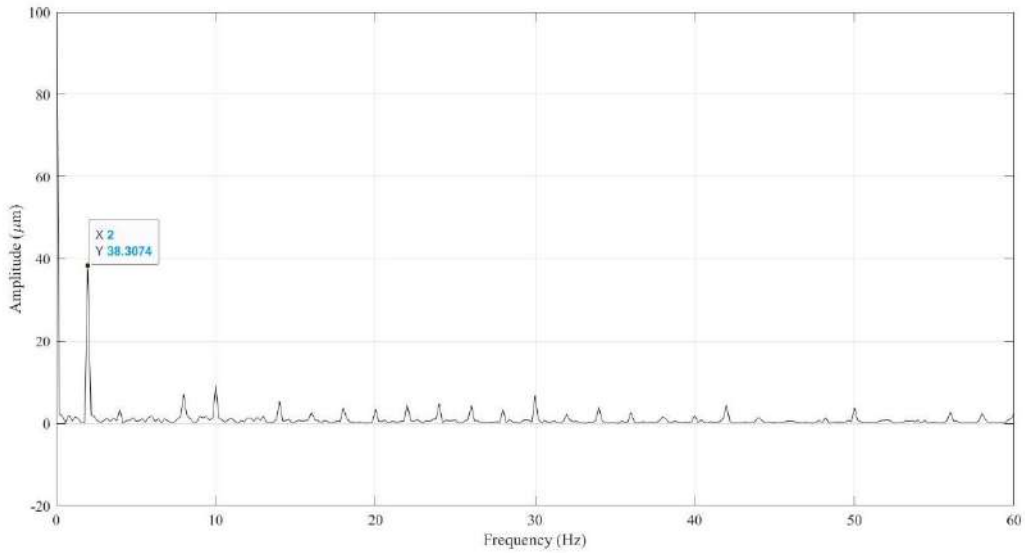

Figure 126: Frequency Domain Sample 1.

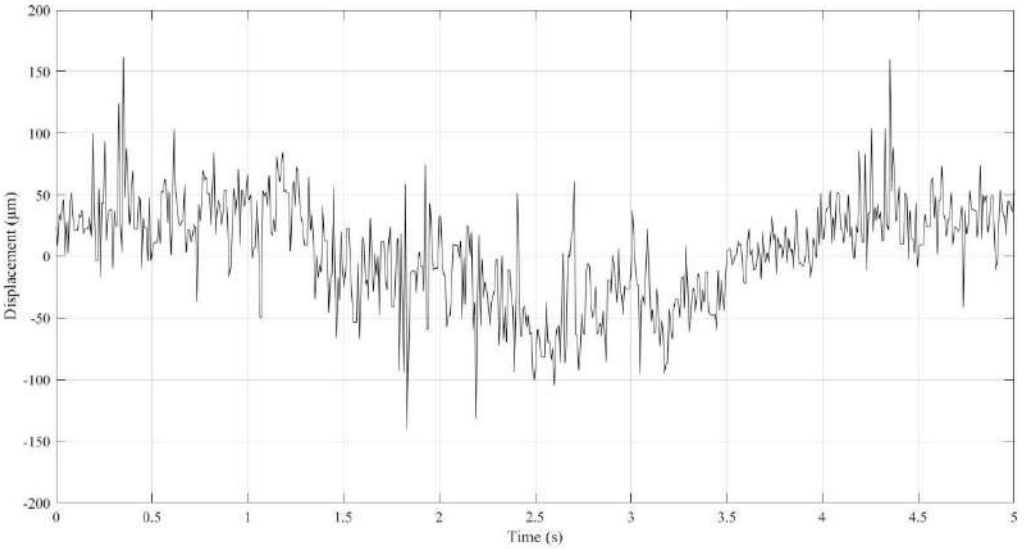

Figure 127: Time Domain Sample 2

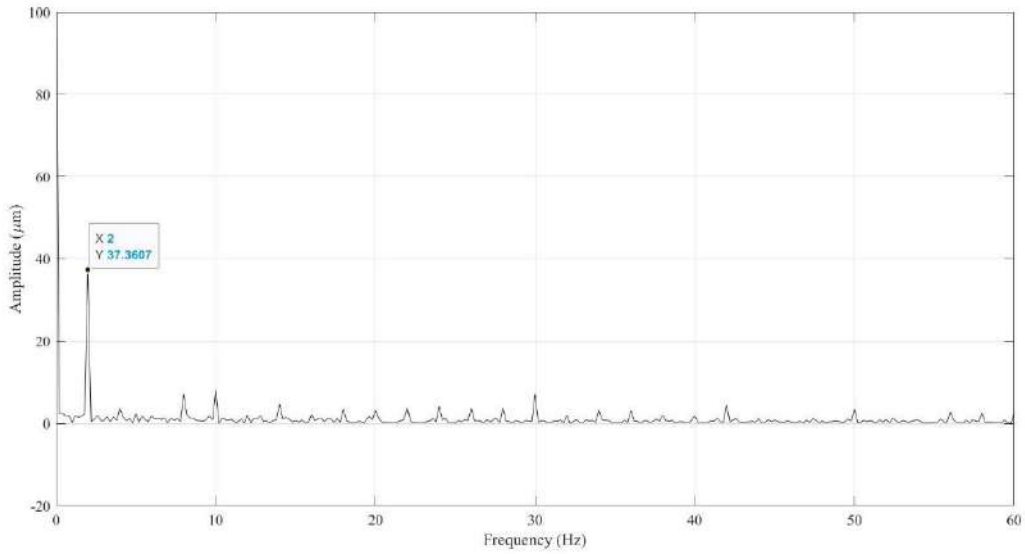

Figure 128: Frequency Domain Sample 2

Then we calculate Peak-to-Peak from the time domain for each cycle, then get the average and the standard deviation. Then compared the results with proximity probe.

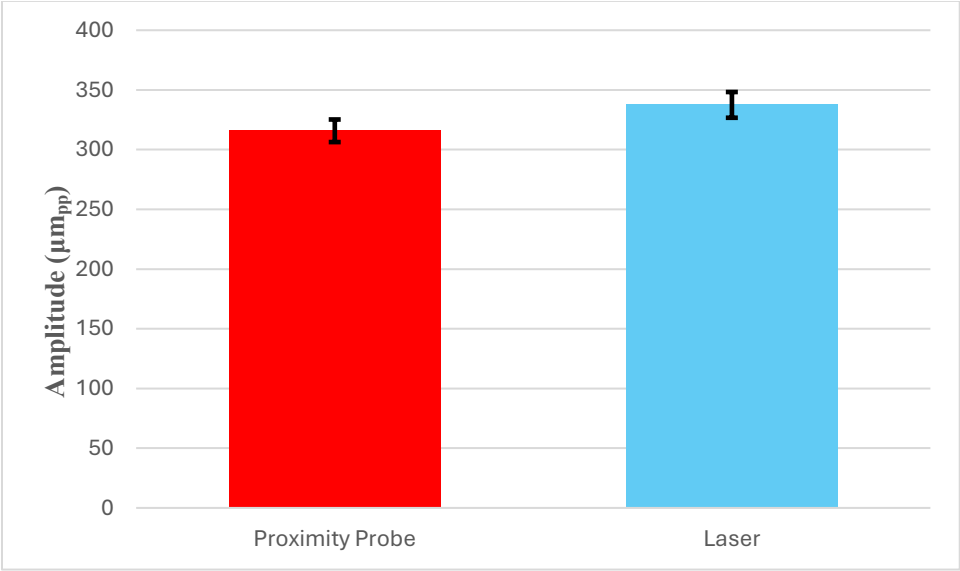

Figure 129:Results Comparison for shaft 1 in Z-Direction.

2. Shaft 2

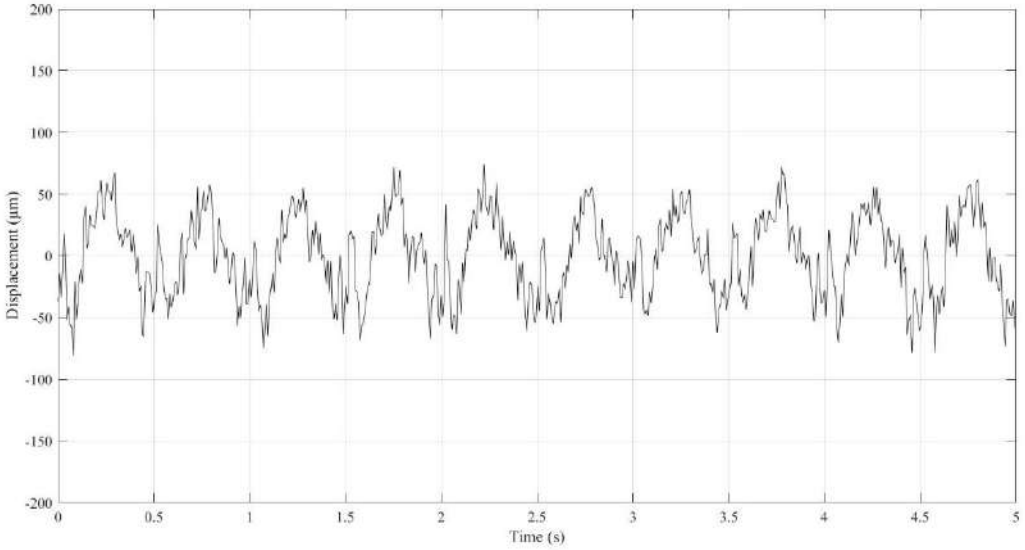

Figure 130: Time Domain Sample 1

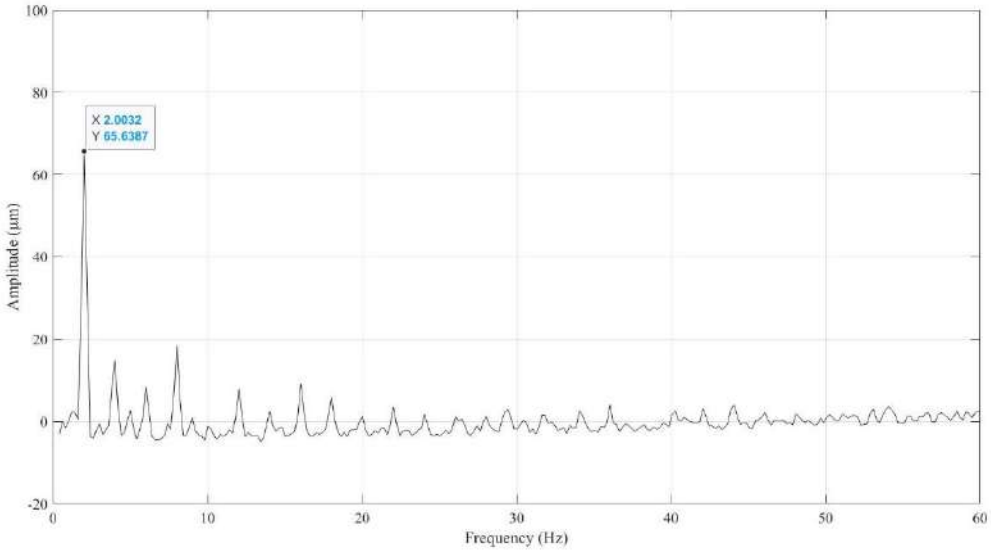

Figure 131: Frequency Domain Sample 1

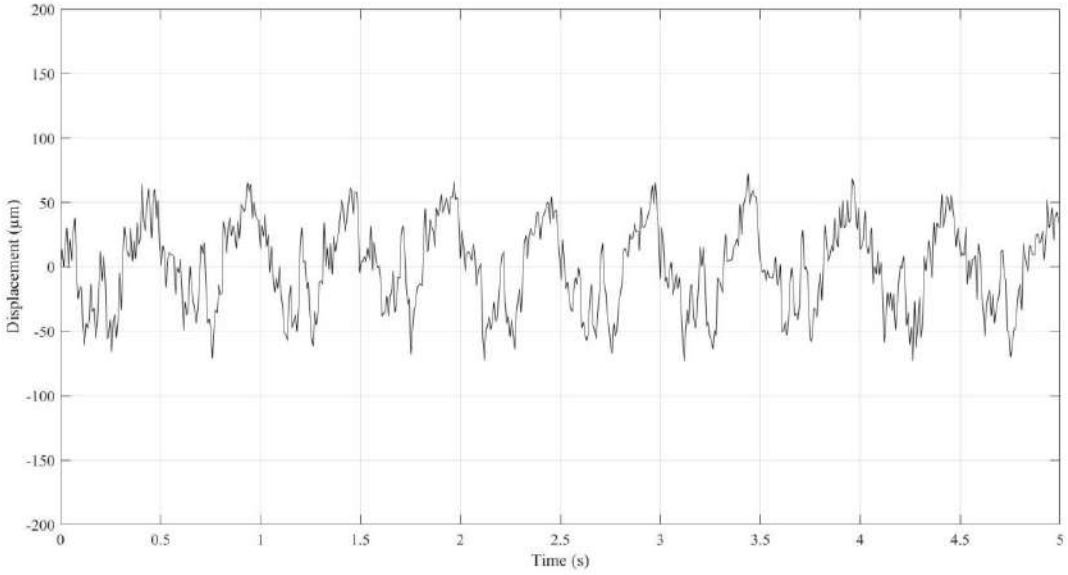

Figure 132: Time Domain Sample 2

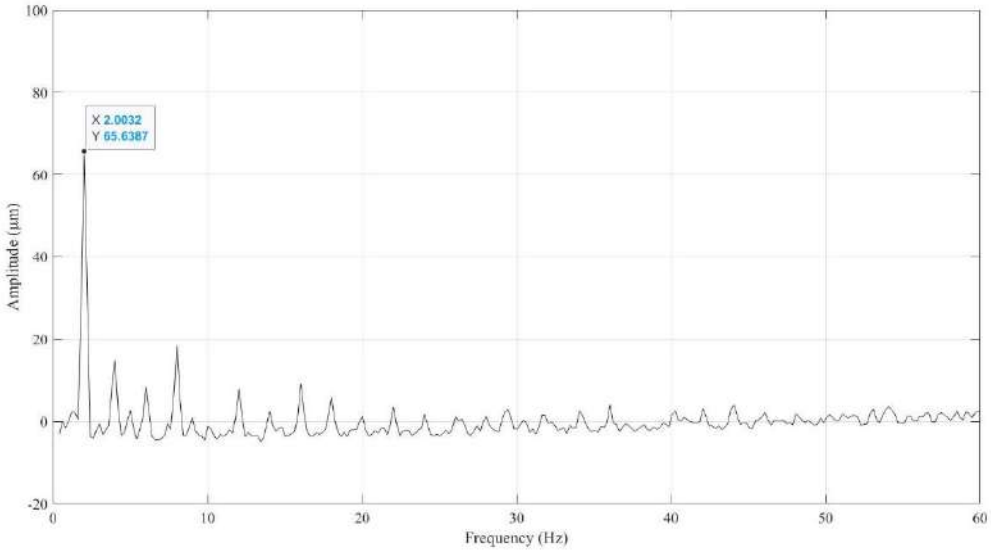

Figure 133: Frequency Domain Sample 2

Then we calculate Peak-to-Peak from the time domain for each cycle, then get the average and the standard deviation. Then compared the results with proximity probe.

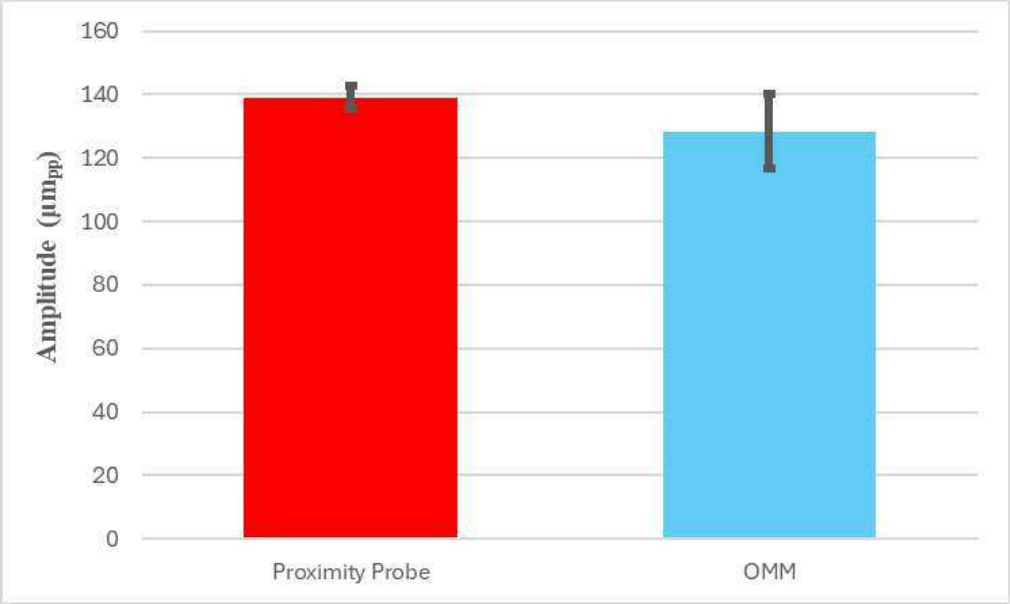

Figure 134:Results Comparison for shaft 2.

3. Conclusion

Tests were carried out on a working 8.65 MW Francis turbine to check how well OMM can detect movements of the machine's shaft. The results showed that OMM can detect very small displacements, around 100 micrometers, with accuracy like the proximity probes already installed on the turbine. The measurement errors ranged between 3% and 19%. Although more testing is still required, OMM has proven to be a dependable method for this kind of task.

4. Miter Gate

a) Gate Rotation Bearing

Every rotating gate needs some kind of support to rotate. Because they sustain the gate and enable appropriate opening and closing, hinges, bearings, or bushings are crucial components of hydraulic gates. Both a top hinge (called a gudgeon) and a bottom hinge (called a pintle) are used in common lock gates, such as miter gates. The design of sector gates is similar. A trunnion pin, which sustains water pressure and permits movement, is encircled by radial and visor gates. Similarly, horizontal hinge is used by hinge crest gates and flap gates to transmit water forces to the concrete structure.

The ease of maintenance must be considered by engineers when constructing bushings, hinges, or bearings. A system may wear out before it reaches the end of its anticipated life if it is difficult to maintain. As a result, the design needs to include the loads on the structure, the frequency and distance of part movement, and the system's expected lifespan.[14]

b) Electromechanically Driven Gate

An electric motor, a gearbox, a sector gear, and a linkage that attaches to the gate are frequently used in electromechanical miter gate systems. Mechanical systems require frequent lubrication since they contain more moving components than hydraulic ones, which can wear out more quickly. Parts are frequently more difficult to replace, and maintenance is more rigorous. The system may deteriorate more quickly if alignment is not done correctly. While hydraulic systems may experience comparable problems, mechanical systems may also be more susceptible to abrupt forces or impacts from boats.

The longevity and reputation for dependability of mechanical systems are two advantages. They also lessen the possibility of significant oil spills into the lake. They can still pollute the environment, though, by leaking oil and grease, particularly from springs, bearings, and open gears. According to contemporary environmental guidelines, these materials have the potential to pollute the environment by washing into the water. Gearboxes should be positioned above flood levels or appropriately sealed to minimize leaks.

Another problem is that it's not always easy to find spare parts, like gears. Because many parts are custom-made, replacing them could take a while. For maintenance, they frequently need to be sent back to the manufacturer. Components like screw rods and gearboxes are scarce, and the original manufacturer is typically required to do repairs.

Shock absorbers, like strut springs, are advised to lessen the effect of abrupt forces on electromechanical systems. These can shield the system from light collisions, abrupt stops or starts, and wave motion. Since hydraulic systems frequently incorporate integrated shock control, this is particularly crucial for electric systems.

The gates can be moved more smoothly by using hydraulic pumps or motors with multiple speeds, particularly at the beginning or conclusion of the action. The size of the gates determines how long it takes to open or close them.

Finally, miter gates are often constructed to withstand one side of water pressure. To prevent the gates from opening in the wrong direction, additional safety measures or locks might be required in locations where water levels can rise on either side.[15]

c) Mechanical Linear Actuator

A sealed electro-mechanical device including a motor, a bearing-equipped screw drive, a housing, and a piston rod that moves in and out to transfer power is called a linear mechanical electric actuator. These actuators are an updated form of mechanical drive systems from the past.
Long extension distances and tremendous force are within their capabilities. The two primary components are an electric motor and a screwdriver, which, depending on the direction of the motor, drives the piston rod forward or backward.

Linear actuators are less complicated and require less maintenance than earlier mechanical systems. Many providers offer them as regular items, which eliminates the need for intricate maintenance and specially built parts. Their design necessitates less frequent maintenance and reduces the possibility of oil leaks.

These actuators are comparable to self-contained hydraulic systems due to their complete enclosure. Their primary benefit is that they don't require fluid lines or external systems. This lessens the chance of environmental leaks.

Other benefits include:

- No oil leakage due to sealed design and quality seals.
- Electro-mechanical force instead of hydraulic pressure.
- Built in controls to adjust movement and force for smooth and accurate gate operation.
- Long lasting components that reduce maintenance.
- Standard design makes spare parts easier to find.
- Energy is only during movement, which saves power.
- Low noise levels.

These actuators may not have the same power as conventional hydraulic systems, despite their ability to deliver a powerful force.

The actuator should have a spring system to lessen impact damage. There are several ways to build the screw mechanism (such as ball or trapezoid threads), and the piston rod needs to be completely shielded from ice, water, and dirt. A frequency converter controls torque and speed, while a hand wheel enables manual operation in an emergency.

The motor works in both directions, moving the piston in or out, like how hydraulic systems connect directly to gates. A spring assembly helps protect the system from minor collisions.[15]

d) Miter Gate

Our job is to keep an eye on the motor that runs one side of the miter gate. In addition to the motor itself, we are also examining the motor shaft and the surrounding buildings, among other related components. Our objective is to comprehend the behavior of each of these components when in use, particularly regarding vibration.

We are employing a camera to simultaneously monitor vibration in several locations. This enables us to investigate the responses of each component to various vibration frequencies. Our goal is to determine which component is aroused at which frequency and the intensity of the vibration in each instance. This is crucial because excessive vibration in specific frequency ranges may cause wear, damage, or decreased functionality.

We can get a better understanding of the system's overall behavior by simultaneously concentrating on multiple areas of interest. This aids in the early detection of possible issues and improves our comprehension of the motor's and its associated structure's dynamic functioning. Future designs or maintenance schedules can be enhanced with the help of the data we gather.

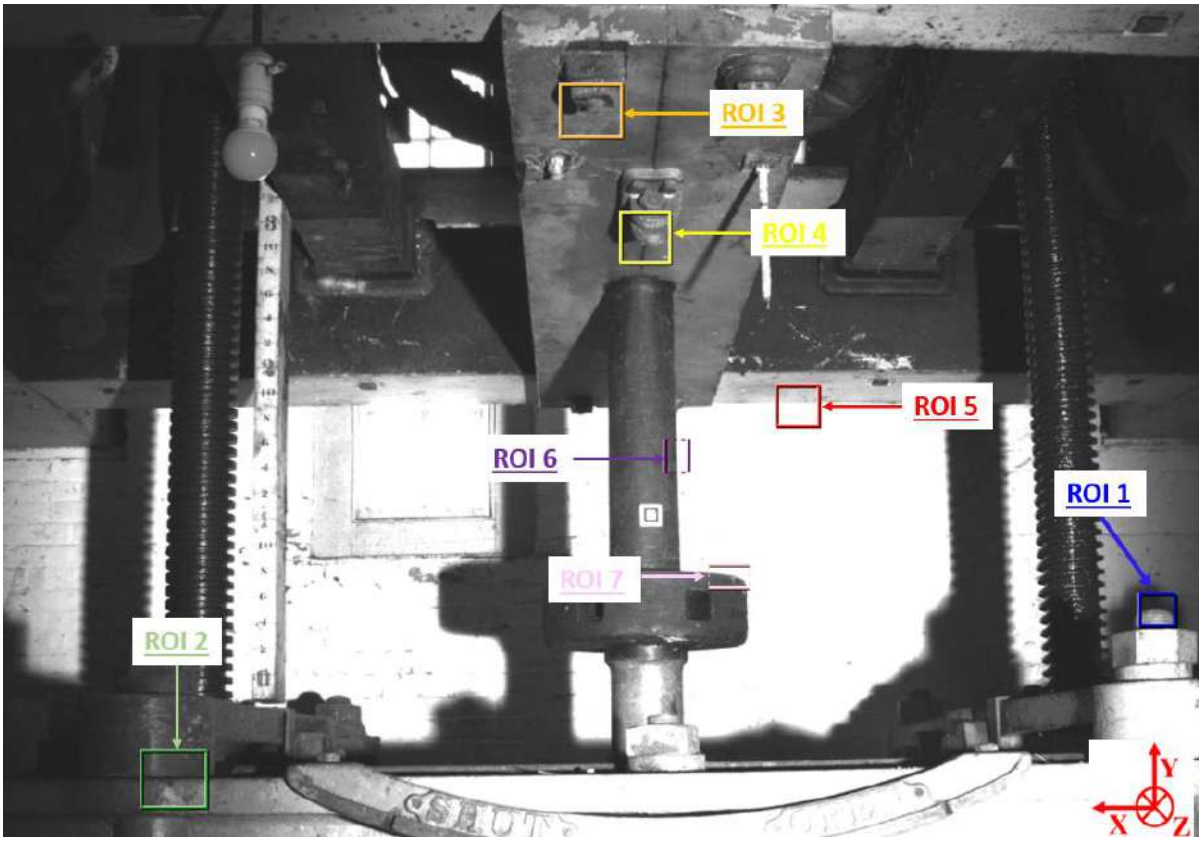

Figure 135: Regions of Interest

(1) Region of Interest 1

In X-Direction:

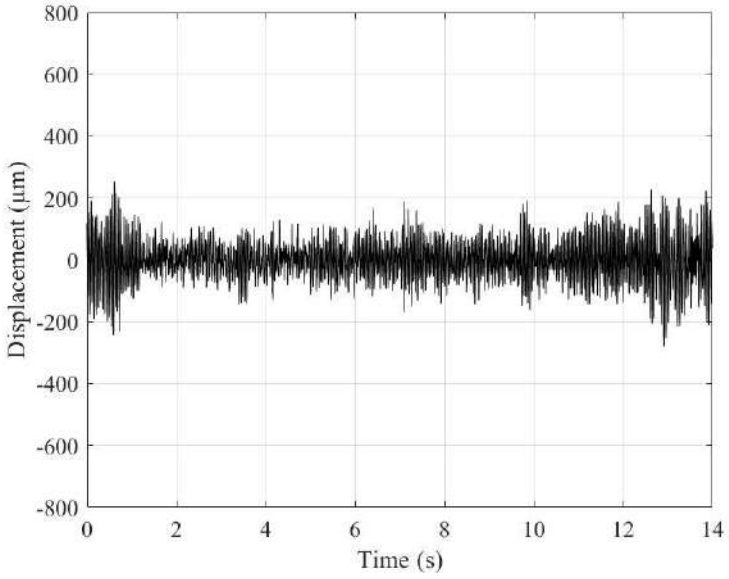

Figure 136: Time Domain in X-Direction

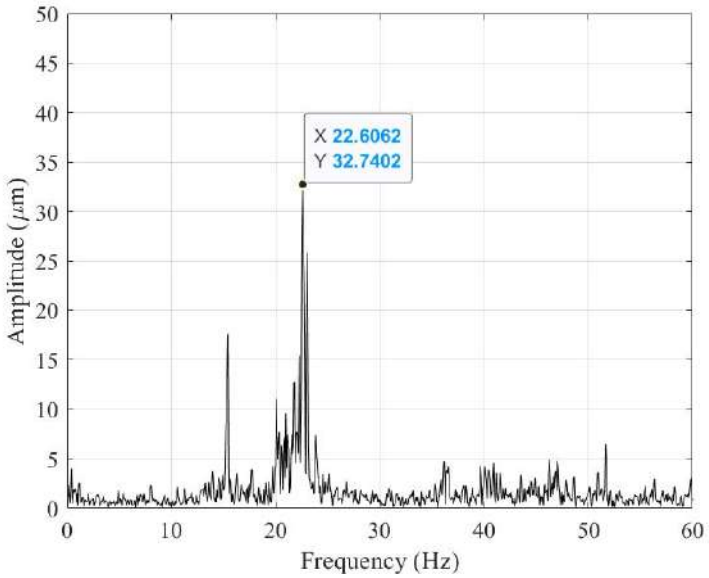

Figure 137: Frequency Domain in X-Direction

In Y- Direction:

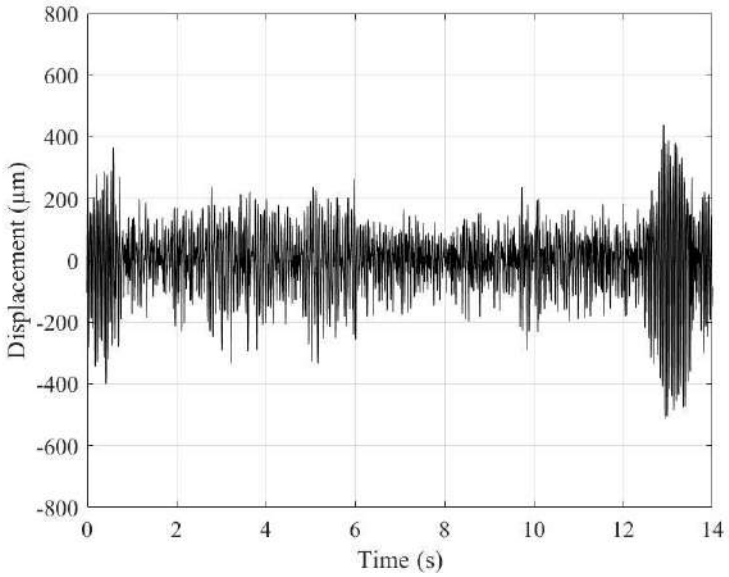

Figure 138: Time Domain in Y-Direction

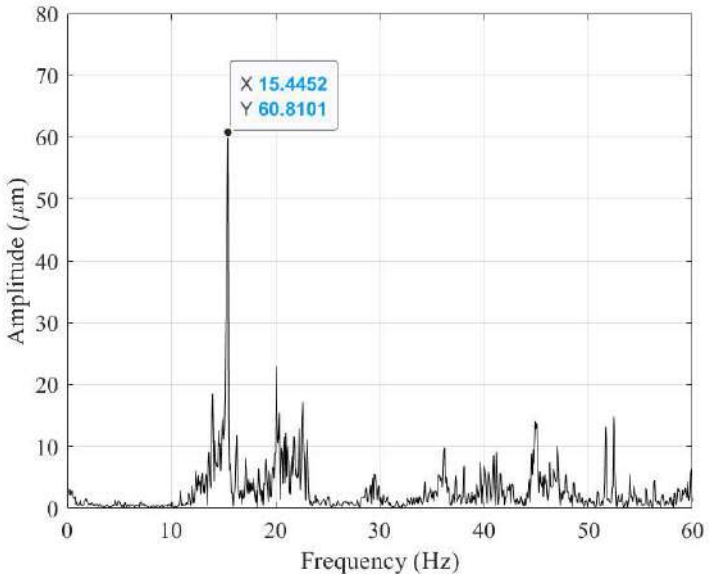

Figure 139: Frequency Domain in Y-Direction

(2) Region of Interest 2

In X-Direction:

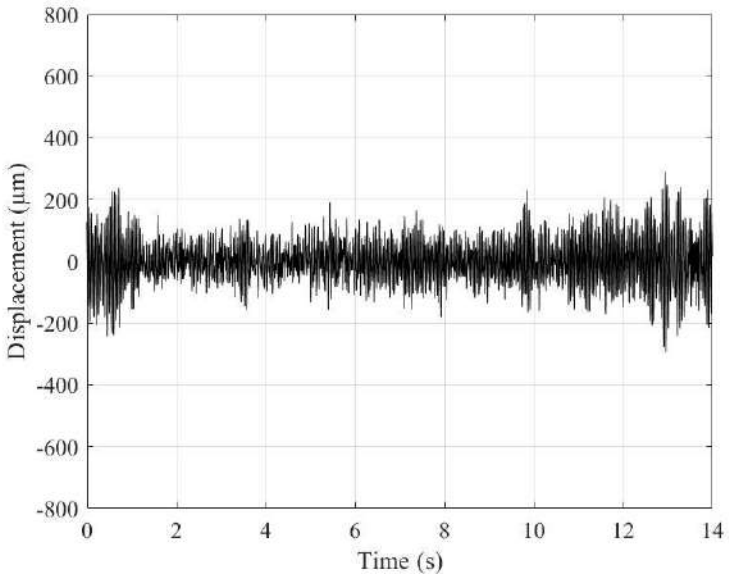

Figure 140: Time Domain in X-Direction

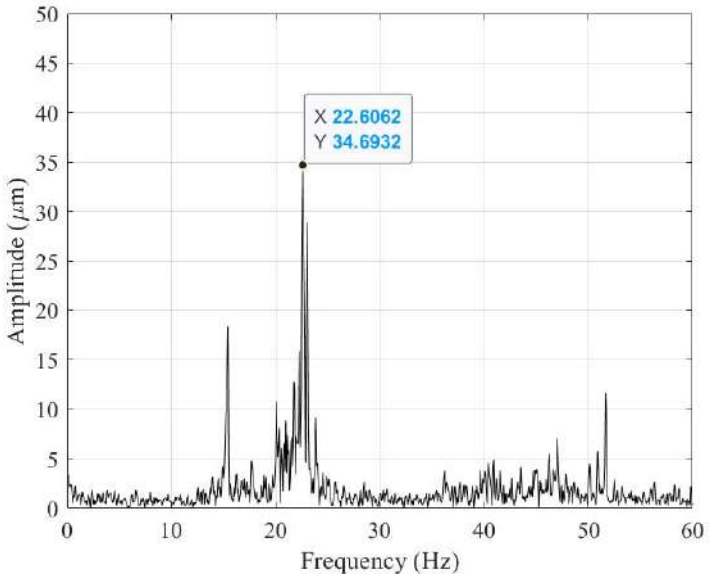

Figure 141: Frequency Domain in X-Direction

In Y-Direction:

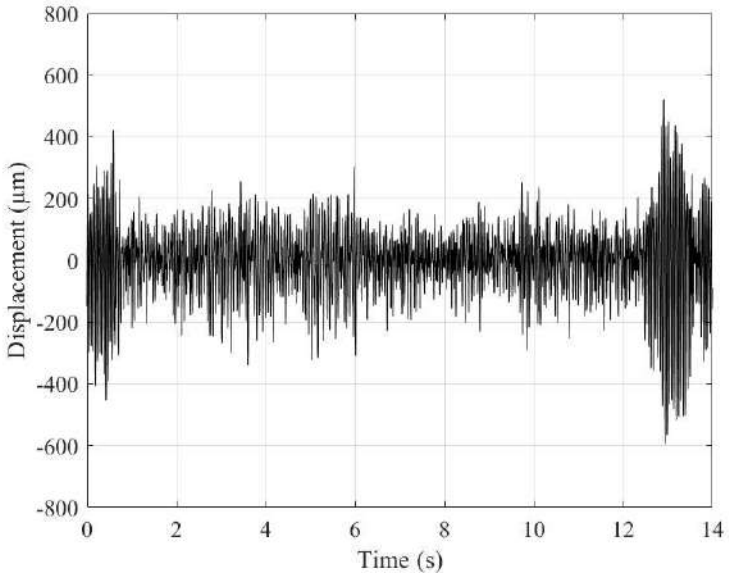

Figure 142: Time Domain in X-Direction

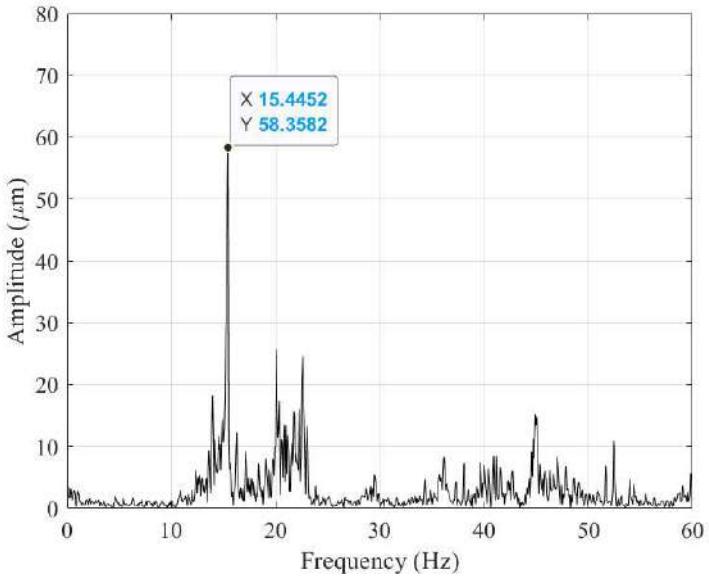

Figure 143: Frequency Domain in Y-Direction

(3) Region of Interest 3

In X-Direction:

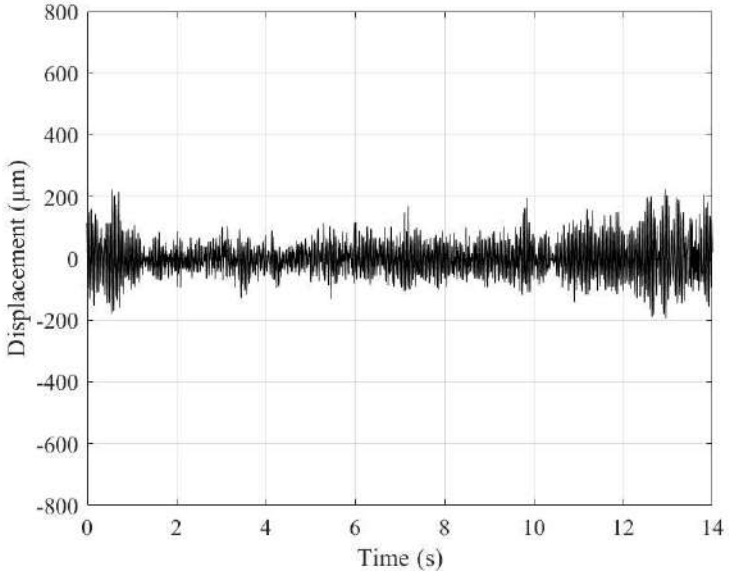

Figure 144: Time Domain in X-Direction

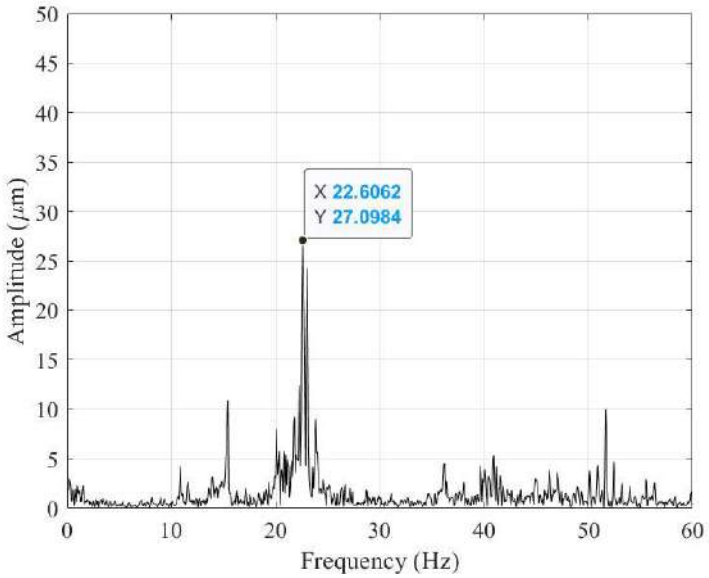

Figure 145:Frequency Domain in X-Direction

In Y-Direction:

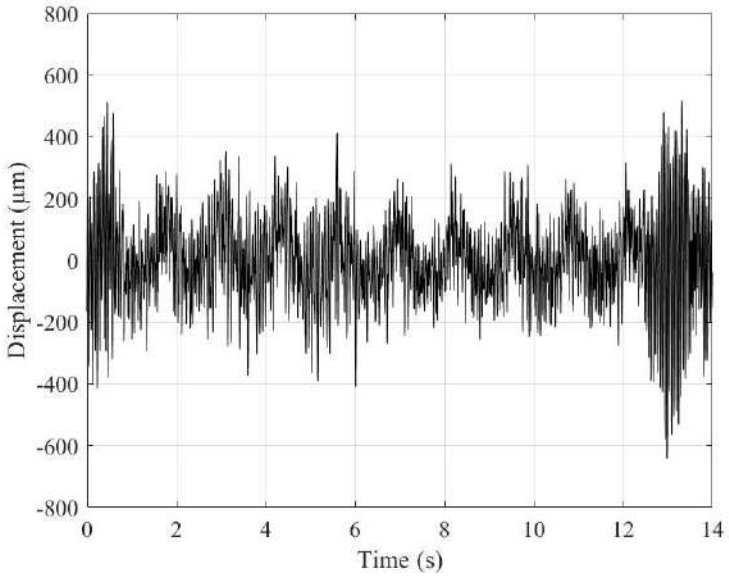

Figure 146: Time Domain in Y-Direction

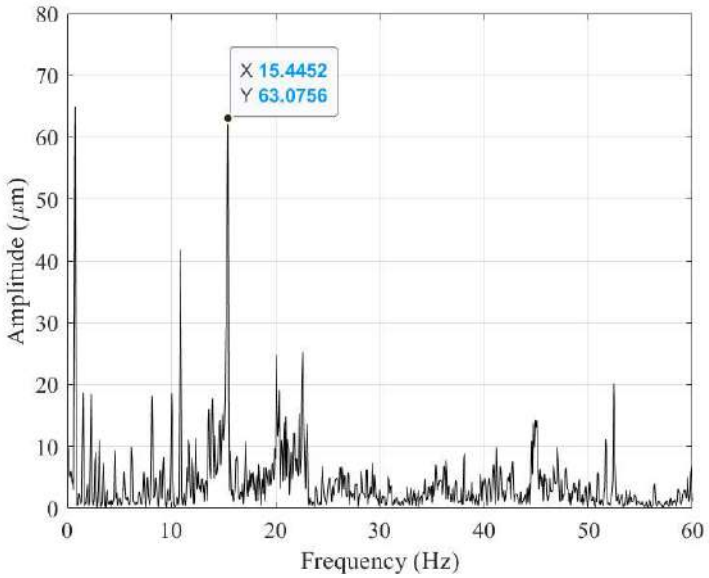

Figure 147: Frequency Domain in Y-Direction

(4) Region of Interest 4

In X-Direction:

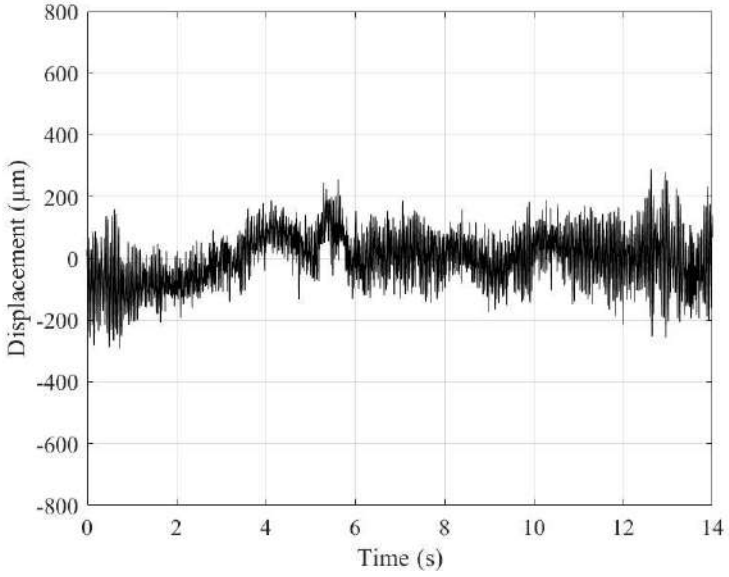

Figure 148: Time Domain in X-Direction

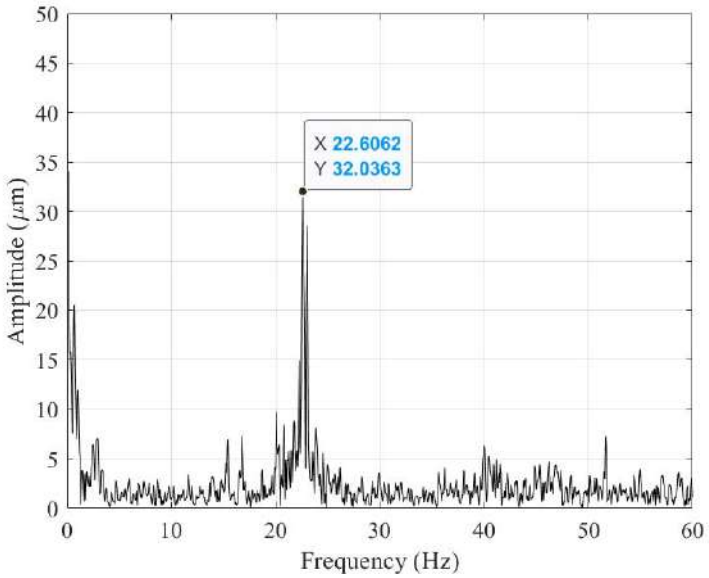

Figure 149: Frequency Domain in X-Direction

In Y-Direction:

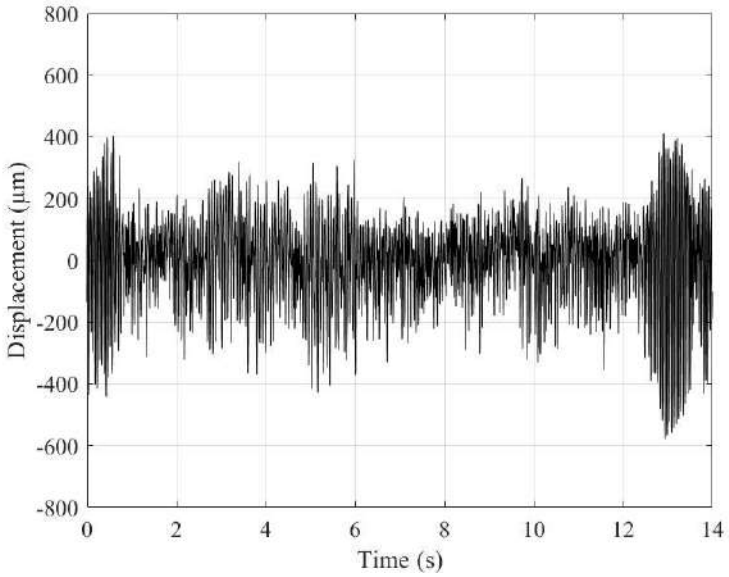

Figure 150: Time Domain in Y-Direction

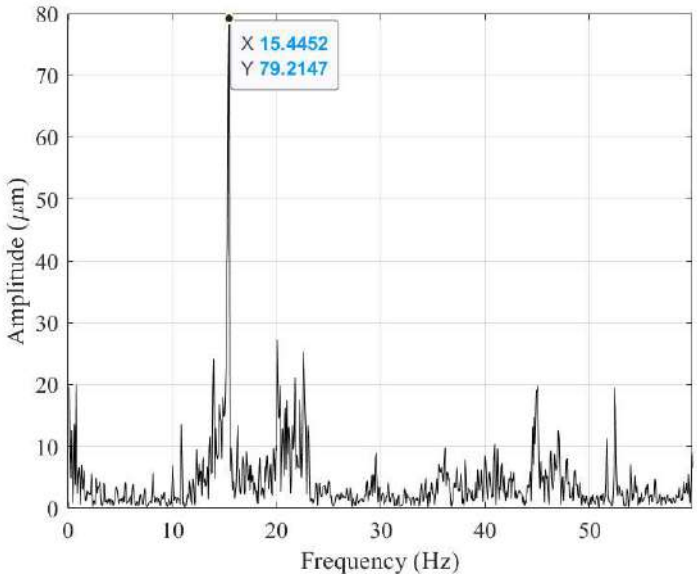

Figure 151: Frequency Domain in Y-Direction

(5) Region of Interest 5

In X-Direction:

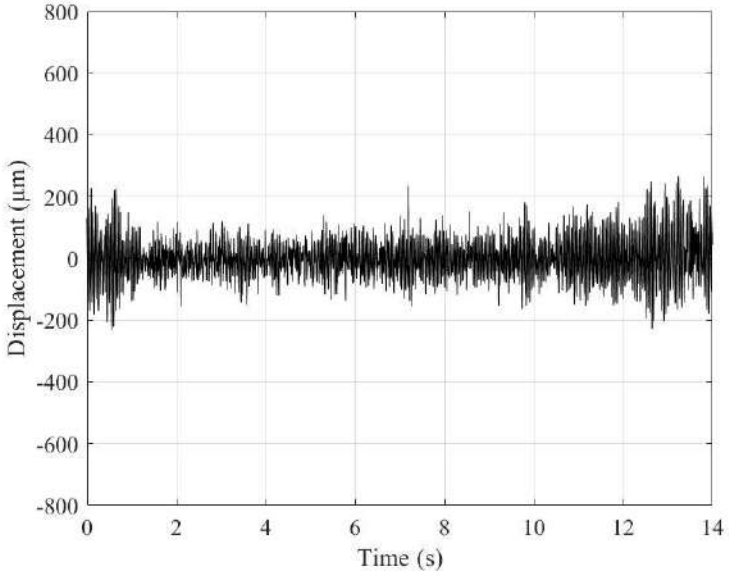

Figure 152: Time Domain in X-Direction

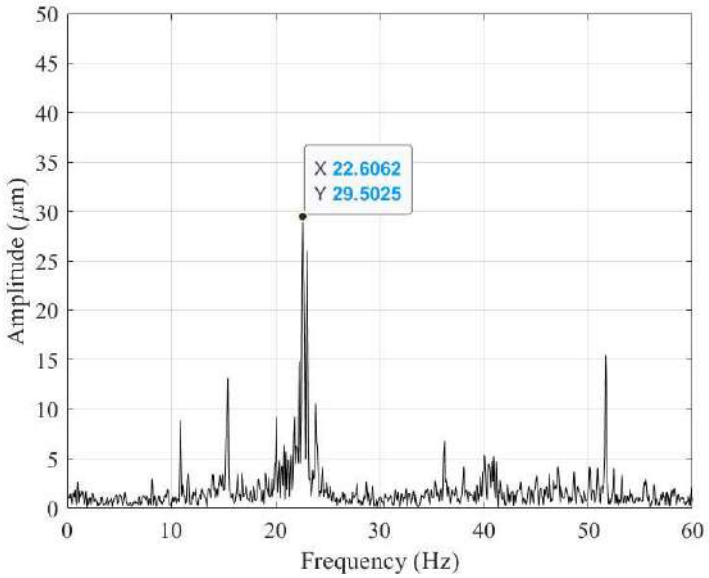

Figure 153: Frequency Domain in X-Direction

In Y-Direction:

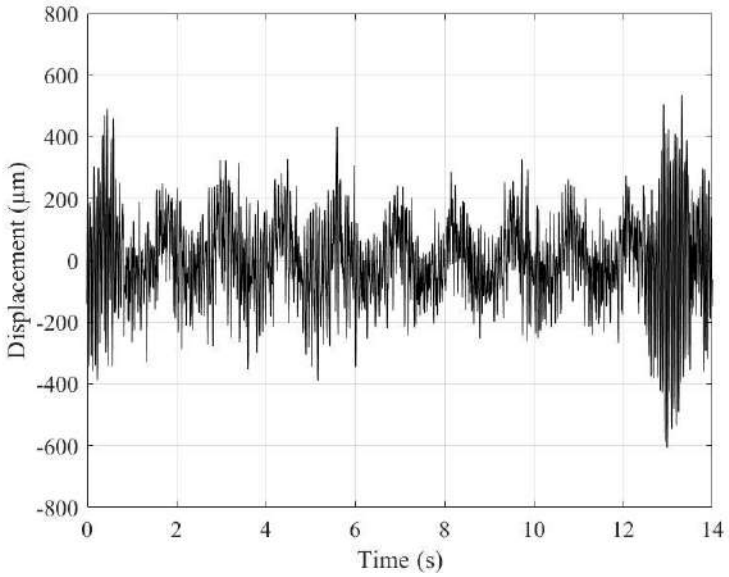

Figure 154: Time Domain in Y-Direction

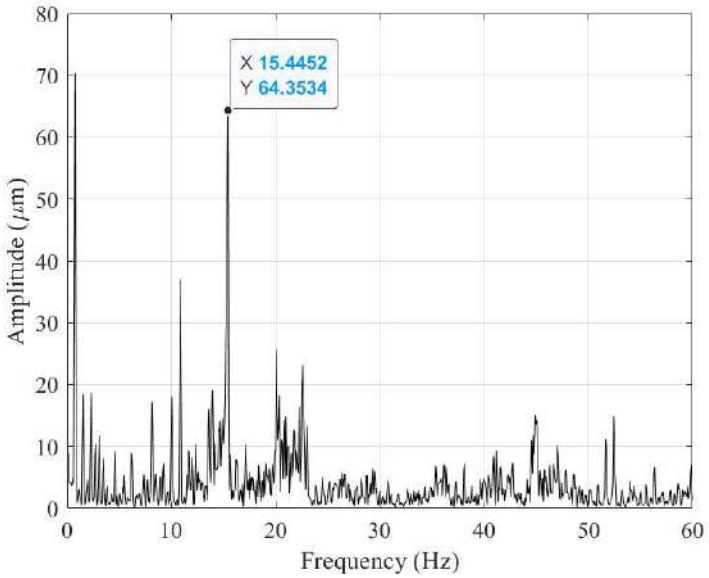

Figure 155: Frequency Domain in Y-Direction

(6) Region of Interest 6

In X-Direction:

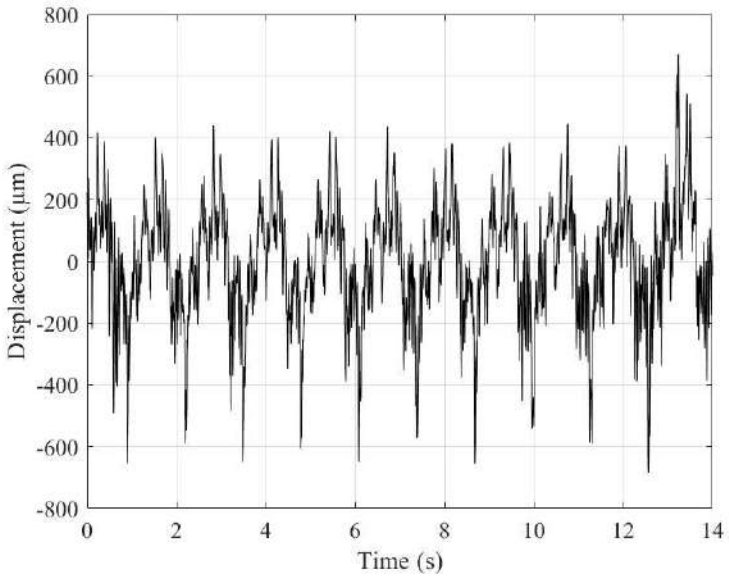

Figure 156: Time Domain in X-Direction

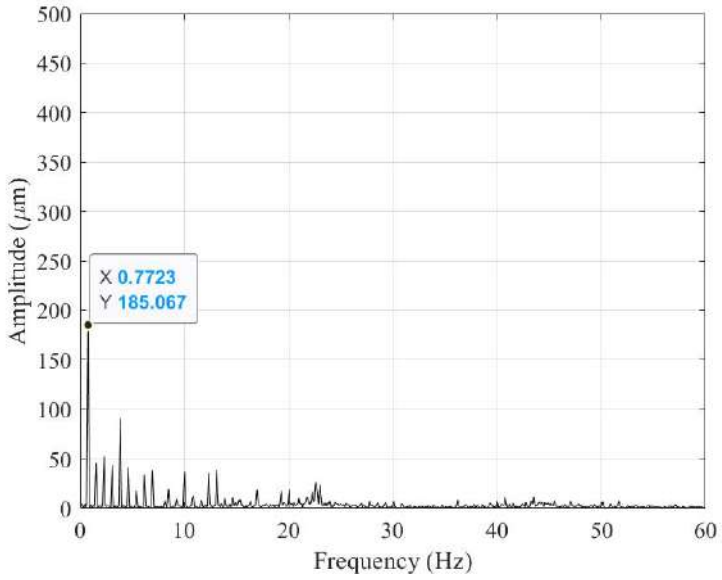

Figure 157: Frequency Domain in X-Direction

(7) Region of Interest 7

In X-Direction:

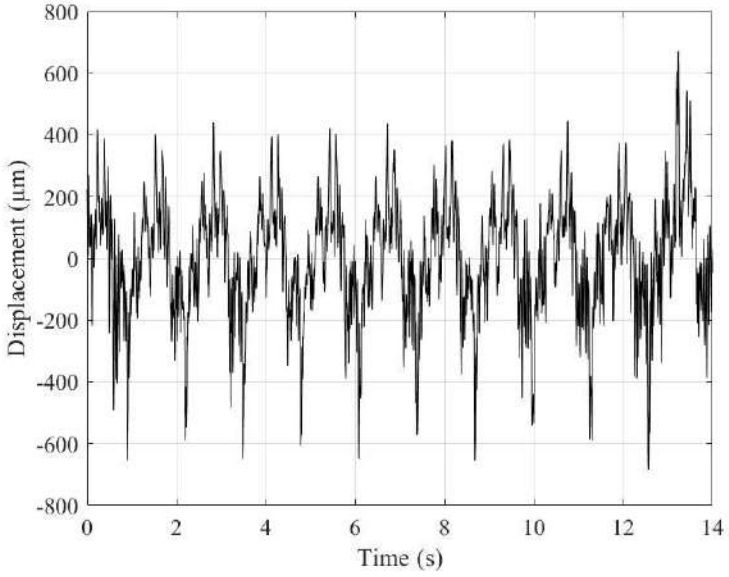

Figure 158: Time Domain in X-Direction

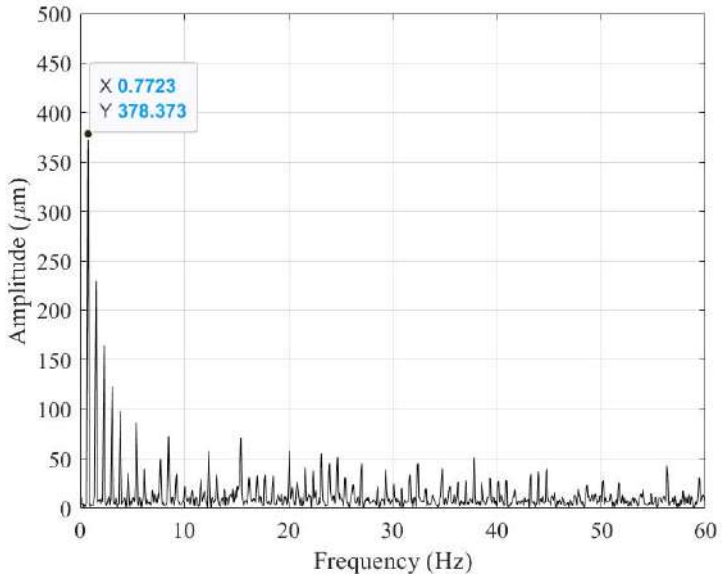

Figure 159: Frequency Domain in X-Direction

(8) Conclusion

The shaft of this motor vibrates between 180 and 380 microns in the X-direction at a frequency of 0.78 Hz. The nearby structures also exhibit vibrations at the same time, albeit with varying amplitudes and frequencies.

The structures vibrate at 22.5 Hz in the X-direction, with amplitudes ranging from 25 to 35 microns. The structures vibrate at 15.5 Hz in the Y-direction, with amplitudes ranging from 55 to 65 microns

We can better comprehend how each component of the system reacts to movement thanks to these variations in vibration frequencies and amplitudes. Additionally, it demonstrates that certain parts are activated at various frequencies, which is useful for identifying possible problems or enhancing the design.

VII. Expanding OMM Utility in Operational Hydropower Environments

1. Flow-Rate Variation Tests

Evaluate how changing hydraulic impacts OMM's ability to detect shaft and blade vibration.

Methodology:

- Operate turbine at low, medium, and high flow.
- Simultaneously capture video and conventional sensor data under each flow.
- Apply band-pass temporal filters tuned to known blade-pass frequencies.

2. Multi-View 3D Displacement Mapping

Extend OMM from 2D plane measurements to full 3D displacement mapping of rotating components.

Methodology:

- Deploy two or more synchronized high-speed cameras at orthogonal vantage points.
- Calibrate a 3D coordinate system.
- Fuse 2D OMM results into 3D trajectories of critical.

3. Long-Term Health Monitoring and Fatigue Detection

Demonstrate OMM's capability for continuous, long-term monitoring and early detection of fatigue-induced changes.

Methodology:

- Install a fixed OMM rig on a non-critical turbine during routine operation for several months.
- Schedule periodic recordings under consistent load.

- Track statistical trends in vibration amplitude, frequency drift, and phase coherence over time.

4. Cavitation and Erosion Detection on Runner Blade

Use OMM to visualize and quantify blade surface oscillations associated with cavitation inception and progression.

Methodology:

- Apply a speckle or high-contrast pattern on blade surfaces under laboratory or scaled model conditions.
- Vary cavitation number to induce incipient and full cavitation.
- Perform high-fps OMM to reveal localized high-frequency and low-frequency envelope modulations.

5. Comparative Study with Other Non-Contact Techniques

Benchmark OMM against alternative vision-based methods such as digital image correlation, laser vibrometry.

Methodology:

- Select a common test rig.
- Simultaneously apply OMM, digital image correlation (DIC), and single-point laser Doppler vibrometry (LDV).
- Compare spatial resolution, sensitivity, setup complexity, and cost.

VIII. References

[1]: Motion magnification for video-based vibration measurement of civil structures.

[2]: Measurements for Condition Monitoring of Hydropower

[3]: Review of rotating machinery elements condition monitoring using acoustic emission signal.

[4]: Condition monitoring and predictive maintenance methodologies for hydropower plants equipment.

[5]: Infrared thermography for condition monitoring.

[6]: Analysis of High Frequency Component of Ultrasound Signal for Fault Evaluation and Condition Monitoring of Ball Bearing in Induction Machine.

[7]: Importance of condition monitoring in mechanical domain.

[8]: Motion Magnification of Vibration Image in Estimation of Technical Object Condition-Review.

[9]: Eulerian Video Magnification for Revealing Subtle Changes in the World

[10]: Enhancing Rotary Machine Reliability Through Condition-Based Maintenance Optimization

[11]: Eulerian Video Magnification for Revealing Subtle Changes in the World

[12]: Advancement for motion magnification technics

[13]: sensors-18-02312

[14]: Vision Based Diagonal Monitoring Preprint

[15]: Miter Gate Machinery, Design Options and State of the Art

[16]: Learning-based Axial Motion Magnification

[17]: Motion Magnification Analysis for City Monitoring

[18]: On the usability of phase-based video motion magnification for defective detection in vibrating panels

[19]: Motion Magnification of Vibration Image in Estimation of Technical Object Condition-Review

[20]: Vision-Based Structural Modal Identification Using Hybrid Motion Magnification

[21]: Video Magnification for Structural Analysis Testing

[22]: Frequency Decoupling for Motion Magnification via Multi-Level Isomorphic Architecture

[23]: Experimental Modal Damping Identification of a Mechanical Structure Using Video Magnification Technique

[24]: Revisiting Learning-based Video Motion Magnification for Real-time Processing